Applicability of Using Physical Stability Data and Advanced Visualization Methods in Protein Comparability Studies

By

Mohammad A. Alsenaidy

Submitted to the graduate degree program in Pharmaceutical Chemistry and the Graduate Faculty of the University of Kansas in partial fulfillment of the requirements for the degree of Doctor of Philosophy.

_____

Chairperson David Volkin Ph.D.

_____

C. Russell Middaugh Ph.D.

_____

Thomas Tolbert, Ph.D.

_____

Teruna Siahaan Ph.D.

_____

Heather Desaire Ph.D.

Date Defended: Dec 9th, 2013

The Dissertation Committee for Mohammad A. Alsenaidy
certifies that this is the approved version of the following dissertation:

Applicability of Using Physical Stability Data and Advanced Visualization Methods in Protein Comparability Studies

_____

Chairperson David Volkin Ph.D.

Date approved: Dec 9th, 2013

Abstract

Comparability assessments are frequently performed during biopharmaceutical drug development to evaluate the effects of manufacturing process changes on the structural integrity, safety and efficacy of candidate protein drug products. Physiochemical analytical evaluations (an essential element of any comparability exercise) involve multiple assessment techniques mapping the different aspects of protein structural integrity (primary and higher-order structures). Although significant advances in regards to primary structure evaluations have been made including peptide and oligosaccharide mapping techniques combined with mass spectrometry, the need for more sensitive approaches for the evaluation of higher order structures of proteins, especially in their final pharmaceutical dosage forms, remains an important challenge. In this dissertation, the ability of using multiple protein conformational stability studies (combined with novel data visualization approaches) as surrogates for evaluating and comparing different proteins's higher-order structure are explored in the context of comparability. Empirical phase diagrams (EPDs) and radar charts, constructed using large data sets from high throughput, lower-resolution biophysical techniques, are used to detect major (point mutations of FGF-1) and minor (different glycosylation patterns of an IgG1 mAb and Fc molecules) structural differences between proteins. In addition, for the IgG1 Fc glycoforms expressed in yeast, the effect of N-linked glycosylation site occupancy, as well as

the effect of different charge states in various nonglycosylated forms, within the C_H2 domain was examined. Using this approach, differences in conformational stability were detected under stress conditions that did not necessarily detect structural integrity differences in these proteins in the absence of these stresses. Thus, an evaluation of conformational stability differences may serve as an effective surrogate to monitor more subtle differences in higher-order structure between protein samples as part comparability assessments.

Dedicated to:

My

Mom
(Hessa Altowaiher)

Dad
(Prof. Abdulrahman Alsenaidy)

Wife
(Khaloud Alsaid)

and

Children
(Abdulrahman and Noor)

Acknowledgements

Completing this dissertation is an accomplishment that I could not have realized if not for the help and support of my family, colleagues, and friends. I would specifically like to recognize the following people:

To my advisor, Dr. David Volkin, I am thankful for your guidance, support, and friendship. The time and energy you committed to me has been an invaluable part of my scientific development. Thank you for allowing me to pursue mutual and individual scientific interests. I truly admire your knowledge base, passion for science and dedication to both applied and basic research.

To my committee members Dr. C. Russell Middaugh, Dr. Thomas Tolbert, Dr. Teruna Siahaan and Dr. Heather Desaire, I would like to say thank you for taking the time out of your full schedules to serve on my dissertation defense committee. I specially would like to thank Dr. C. Russell Middaugh for his constant guidance and support during my stay in KU. I also would like to thank Dr. Siahaan and Dr. Tolbert for reading my thesis.

To the past and present members of the Volkin/Middaugh group, Thank you for your friendship and valuable scientific discussions. I would especially like to thank Dr. Sangeeta Joshi for her outstanding lab manager, a great scientific resource, and a good friend during my stay in KU. I would like as well to thank Dr. Tingting Wang for training me to use various laboratory instruments at the start of my graduate school career. I also would like to acknowledge both Drs.

Justin Thomas and Santoshanand Thakkar for all the valuable scientific discussions we had that helped me throughout my graduate study years.

To King Saud University and Saudi Arabian Cultural Mission, Thank you for your generous financial and logistic support of my graduate research.

To my family, Mom, Dad, brothers and sister. Thank you for your unending love and support! Without all of you, I would not have accomplished this feat, I would not be the man I have grown to be. Thank you all for believing in me and providing me with the opportunity to accomplish all that is imaginable. I love you all.

To my wife Khaloud Alsaid. Your love and support has guided me through a tough path. I am ever so grateful to have someone like you in my life. Because of you I am a much better person, friend and father. I can not express in words my appreciation for everything that you have done. I love you!

Table of Contents

Chapter 1

Introduction

1.1 Overview

Protein based drugs (also known as protein therapeutics or biopharmaceuticals) are structurally complex, highly specific macromolecules used therapeutically to compensate for body deficiencies (e.g., hormones and clotting factors), as medical treatments (e.g., cytokines and monoclonal antibodies) as well as to prevent diseases (e.g., polyclonal antiserum and certain vaccines).[1] A protein molecule's structural complexity makes it quite challenging to preserve biological activity and stability throughout manufacturing, storage (shelf-life) and administration. The primary structure of a protein is defined by the sequence of twenty different amino acid residues covalently linked to each other through peptide bonds, in addition to any enzymatic, post-translational covalent modifications of certain amino acid residues such as N-linked glycosylation of asparagine, phosphorylation of serine and sulfation of tyrosine. The local folding into secondary structures is the first step in for the formation of higher-order structures in proteins: for example, α-helices and β-sheets formed through hydrogen bonding between the main chain NH and C=O groups. The packing of such secondary structural elements into a three dimensional folded, globular unit, called a domain; a folded, protein molecule may contain one or multiple domains. This, formation of the overall three dimensional shape of protein is referred to as the tertiary structure of a protein. Lastly, the arrangement of multiple polypeptide

chains, that each form independent tertiary structures, into an oligomeric complex is termed as a protein's quaternary structure.

Protein drug molecules are prone to different degradation mechanisms (chemical or physical) during manufacturing and storage, which ultimately can lead to the loss of structural integrity and potency (through structural alterations) as well as potentially increases in immunogenicity reactions upon administration.[2-5] Chemical degradation pathways involve covalent bond modifications, as in Asn deamidation, Asp isomerization, Met oxidation, polypeptide chain proteolysis and disulfide bond shuffling.[2] Physical degradation, on the other hand, includes distinct pathways such as protein structural alterations,[6] surface adsorption,[7] aggregation [8] and precipitation.[9] There are many causes leading to the physical and chemical degradation of proteins including exposure to different environmental stresses (e.g., agitation,[10] UV light [11]and temperature [12]) as well as changes in solution and formulation conditions (e.g., pH [13], ionic strength [14] and additives [15]). A better understanding of the possible degradation mechanism of a protein therapeutic is key step in the formulation development of safe and effective product candidates to be evaluated in clinical trials.

In 1982, the first biotechnology derived protein product (Humulin®) based on recombinant DNA technology was approved in the U.S. to be used for insulin-dependent diabetes mellitus patients. The doors were then opened for

development of more biotechnology based pharmaceutical products, and in 1986, the first monoclonal antibody (mAb), Muromonab (Orthoclone, OKT3), came to the market as an immune suppressant for patients subjected to organ transplant. Currently there are more than 150 protein-based drugs approved by the FDA and EMEA, 35 of those are mAbs, and more than 900 medicines and vaccines are being developed, with 30 mAbs in late-stage development. [1, 16, 101]

In the mid-1980s and early-1990's, the demand for production capacity to make larger amounts of protein drugs increased substantially, causing manufacturers to develop new technologies and scale-up their manufacturing process to meet up higher demands. The need for an efficient and scientifically based protocols to evaluate the effect of process changes and production scale-up on the structural integrity and clinical safety and efficacy of protein drug candidates was realized then by the biopharmaceutical industry and government regulators, which gave birth to the terms such as "well characterized biotechnology products" and "comparability" in FDA guidance in April, 1996. [17] The general concepts of comparability were then further defined and expanded by additional regulatory guidances from the European Medicines Agency (EMEA) in 2003, [18] the International Conference on Harmonization (ICH) (Q5E) in 2003 [19] and by the World Health Organization (WHO) in 2009. [20]

1.2 Comparability study definition, concept, and goals.

The primary and higher order structure of protein drug molecules are delicate in nature, especially compared to small molecule drugs, and are highly sensitive to environmental changes and stresses in general. Changes in the manufacturing process for a protein therapeutic may occur during clinical development or after commercialization. These changes are frequently applied in either the manufacturing steps of the active drug substance (e.g., facility, equipment or process changes) or in the finished drug product (e.g., formulation excipients, container-closure system, dosage form changes). [21, 22] A manufacturer may apply changes in their manufacturing processes for variety of reasons such as improving yields and purity, ensuring better patient convenience, or facilitating compliance with new regulations. Comparability studies are performed to assess the effect of these process and product changes on the "critical quality attributes" (CQAs) by comparing the pre and post-change protein products through a series of tests performed in a head-to-head fashion. Critical quality attributes are defined as the collective product qualities defining the identity, purity, potency, safety and stability of the protein drug product.[19]

Changes in critical quality attributes of a biological drug due to manufacturing process changes were historically anticipated since, as was commonly said, "the process is the product", a phrase used to summarize the potential sensitivity of a biological product towards manufacturing changes. Given numerous advances in analytical technologies to characterize proteins

along with a greatly improved understanding of protein structure and stability, the ability to better assess whether a given process and product change affected the structural integrity, efficacy or safety profile of a given protein drug became possible. These advances in our scientific understanding therefore allowed for the implementation of comparability studies in the biopharmaceutical industry. The scientifically based assessment of comparability between the pre and post-change product relies on the ability to show experimentally using "appropriate assays" that the pre and post-change products are "highly similar" in terms of physiochemical and biological characteristics, degradation profile, pharmacokinetics and immunogenicity.[19] Physiochemical characterizations, biological assays and stability degradation profiles of the drug product are considered the corner stone of any comparability exercise. The ability to establish highly similar analytical profiles removes the need for additional clinical evaluations such as pharmacokinetic, efficacy and/or immunogenicity studies. The ICH Q5E regulatory guideline describes comparability exercises and some of elements to consider in order to determine physiochemical similarity between a drug product made by two different manufacturing processes.[19]

1.3 Elements of a protein comparability study

1.3.1 Physiochemical characterization

Extensive physiochemical analytical characterization of the pre- vs. post-change active pharmaceutical ingredient (protein itself) and the final drug product (final dosage form with protein and excipients in the primary container) are typically the first steps of a comparability evaluation. In these studies, the effect of manufacturing process changes on the integrity of a protein's sequence in the polypeptide chain, as well as the integrity of the secondary, tertiary and quaternary structures are evaluated.

For protein primary structure evaluations, peptide mapping is frequently used to assess the integrity of the amino acid residues and sequence within a specific protein molecule. This technique involves the chemical or enzymatic treatment of the protein to generate a specific set of peptide fragments, which in turn are then separated using Reversed Phase High Performance Liquid Chromatography (RP-HPLC) method equipped with diode-array ultraviolet (UV) for detection. Isolated peptide fragments are then mass characterized using online mass spectrometry (MS) methods. Peptide mapping has proven to be a valuable technique in comparability studies, since each protein upon using specific proteolytic enzymes would give specific peptide fragments that are used as a fingerprint for the protein under evaluation. [23-26] Comparing the peptide map profiles for the pre and post-change proteins can show alterations in the protein

polypeptide backbone such as fragmentation or changes in individual amino acid residues (e.g., mutation, oxidation, deamidation, or post-translational modifications). The correct disulfide pairing can also be evaluated using the same technique by comparing peptides under reduced and non-reduced conditions. Alterations in a protein molecule's primary structure can have multiple possible outcomes ranging from modifications in safety (immunogenicity), efficacy (binding or enzymatic activity) or stability (folding/aggregation) profiles. In contrast, however, sometimes these changes have no significant biological effects. The nature and extent of the physicochemical changes (if they occurred during the process change) must then be fully evaluated in comparison with the "pre-change" protein (i.e., protein made from the original manufacturing process). Based on the outcomes from these types of evaluation studies, additional analytical characterization studies might be recommended to more thoroughly understand the nature of any structural changes and rule out any hidden effects on the protein's critical quality attributes.

Various post-translational modifications (PTMs) such as N-glycosylation, O-glycosylation and/or C-terminal Lysine clipping, are frequently observed upon changing cell culture manufacturing process, which is partially responsible for the heterogeneous nature of proteins since they are produced by cells.[27] The risk of having a change in the PTM of a protein depends on the nature of changes in the manufacturing process (e.g., cell line and cell culture media component changes

have higher risk of leading to PTM compared to changes in purification during downstream processing).[25] Additionally, the type of the glycoprotein under evaluation and the extent (percent by mass) of glycosylation (erythropoietin is 40% N-glycosylated vs. 2% N-glycosylation in an IgG1 monoclonal antibody) [28] plays a crucial role on the effect of process changes on PTMs as well. Mass spectrometry based techniques are frequently used to obtain insight into a glycoprotein's glycosylation composition and distribution. Mass spectrometric ionization based techniques such as matrix-assisted laser desorption/ionization (MALDI-MS) and electrospray ionization (ESI-MS) are frequently used for this purpose. [28-32] A more detailed picture about the glycan structure and composition can be achieved using oligosaccharide mapping were the glycan residues are enzymatically cleaved from the protein and then labeled with a fluorescent molecule (e.g., 2-Aminobenzamide is frequently used) for detection. [33, 34] The different fluorescently-labeled glycans are then passed through an normal phase HPLC system equipped with a fluorescence detector for separation and analysis. Using such a method, extent of similarity between the pre- and post-change protein in terms of the correct glycosylation site, branching, sequence and sugar types is feasible. This is an important result given that glycosylation plays a critical role in defining protein conformation, clearance, functionality, folding and stability.

Ensuring native-like higher order structures (secondary, tertiary and quaternary structures) in a protein produced from both the pre- and post-change manufacturing process is essential since the overall three dimensional configuration not only defines a protein's stability and functionality, but also its efficacy and safety when being used a drug candidate. Differences in higher order structures could stem from physical changes in structural integrity (i.e., partial unfolding, conformation changes and aggregation) as well as from modifications in either the back-bone structure (mutation, deamidation) and/or PTMs such as glycosylation. These differences in higher order structure (HOS) sometimes are only detected during long term storage or during accelerate storage which involve changes to the surrounding environment (e.g., temperature shifts or agitation). In addition to the properties of the protein molecule itself, pharmaceutical additives (i.e., excipients such as salts, surfactants, sugars), solution conditions (such as pH and ionic strength) as well as the nature of the final dosage form (liquid vs. lyophilized) can also impact the HOS of a protein.

The assessment of higher order structural integrity and conformation stability of proteins in comparability studies can be performed using multiple biophysical and calorimetric techniques. Far-ultraviolet Circular Dichroism (CD) and Fourier Transform Infrared Spectroscopy (FT-IR) have been widely used in studying the overall secondary structure content of proteins where this method gives distinctive signals that corresponding to the different secondary structural

folds (i.e., α-helices and β-sheets). Detailed studies regarding the use of CD spectra for structural comparisons in comparability studies have been published recently.[99, 100] Common techniques for the evaluation of the overall tertiary structure of proteins are fluorescence spectroscopy and near-UV CD. Owing to the unique fluorescence properties of aromatic amino acid residues (Tryptophan, Tyrosine and Phenylalanine) and their sensitivity toward polarity of its surrounding environment, changes in a protein's structural integrity and conformational stability upon partial or full unfolding can be monitored. Furthermore, extrinsic fluorescence dyes (e.g., 1-anilino-8-naphthalenesulfonate, ANS, as well as Sypro orange) have been employed successfully in monitoring partially unfolded intermediates (molten globular states) which have been shown to play a role in initiating protein aggregation process. [13, 86] Such dyes have the unique property of being relatively nonfluorescent in polar environments and with greatly enhanced fluorescence in less polar, more hydrophobic milieu. These features allow scientists to examine the onset of structural unfolding of a protein as more hydrophobic patches within the protein are exposed to the solution/dye when the protein solution is stressed (e.g., during heating or agitation). Differential Scanning Calorimetry (DSC), another powerful analytical technique to monitor protein conformational stability, measures heat capacity difference between the protein solution and a reference buffer as a function of temperature. As a protein starts unfolding, heat capacity increases resulting in an endothermic

peak centered at the thermal melting temperature (Tm), or the midpoint of the protein unfolding event(s). As part of a comparability study, DSC can provide information about the overall conformation stability of the proteins under evaluation. Structural alterations in a protein as a result of manufacturing process changes could be detected in the form of a Tm shift or a change in the shape of the endothermic peak. Multi-domain proteins (such as a monoclonal antibody) show multiple endothermic peaks in a given DSC thermogram. Structural changes in one of these domains can be reflected in corresponding changes to the associated DSC peak.

Other emerging analytical techniques for use in comparability studies to evaluate higher order structure of proteins are Nuclear Magnetic Resonance (NMR) spectroscopy and Hydrogen/Deuterium Exchange Mass Spectrometry (H/DX-MS). Although these techniques are very powerful in terms of obtaining detailed information about the folded protein structure, their use has been limited due to some drawbacks including protein size and formulation restrictions in addition to being technically challenging and time consuming techniques. Research is currently being done to overcome these drawbacks. For example, the effect of different anions and excipients on an IgG1 mAb local flexibility was evaluated using H/DX-MS.[35, 36] An increase in the local flexibility of a certain peptide fragment in the C_H2 domain of the mAb was seen upon using thiocyanate (as anion) and arginine (as an excipient) that was correlated with decreased

thermal stability of the C_H2 domain and increase in aggregation propensity. These results demonstrate the intricate interrelationships between different excipients and their effect on protein dynamics and physiochemical stability of a monoclonal antibody.

Only a limited number of case studies evaluating the effect of changes in the manufacturing processes on protein structure and function from a comparability point of view have been published. In one study, the effects of changing the final dosage form a lyophilized formulation to a liquid dosage form, in addition to the impact of transferring the bulk drug substance to the commercial site, was evaluated for two monoclonal antibodies. [25]An increase in a specific Asn deamidation for one of these mAbs was observed which did not have any effect on the structural integrity, biological potency or the pharmacokinetic profile in animal models. This Asn deamidation was attributed to the transfer of the bulk process to the commercial site at an increased scale which required longer hold times in solution. Additional analytical evaluations of the mAb's conformational stability as well as functionality using newer analytical methods was carried out, with no differences being observed between the two dosage forms of the two mAbs. The impact of changing formulation composition on protein conformational stability has been addressed in a comparability study.[37] In this work, the effect of formulation exchange on a human growth hormone protein was evaluated. The authors concluded that the formulation change affected the

structural integrity of the protein and additional considerations needed to be given regarding the choice of final excipients. Selecting an appropriate formulation conditions for insulin was emphasized in another study as they reported that changes observed on the physical and chemical stability of insulin (due to changes in its crystallization process) were dependent on the raw materials and excipients used in formulation.[38]

Alterations in glycosylation patterns of proteins as a result of manufacturing method changes have been reported. [25] The effect of such changes on the conformational stability of protein varied depending on specific conditions. For example, the role of glycosylation on the conformational stability of erythropoietin was investigated in one study.[39] Glycosylated erythropoietin was found to be more resistant to guanidine hydrochloride (GndHCl) and acidic pH induced unfolding compared to the nonglycosylated form of the protein. Glycosylation profiles have been found to affect the structural integrity and conformational stability of mAbs as well. In one study, three intact IgG1 mAbs were compared before and after glycan residue removal using a variety of analytical techniques.[40] An increase in fluorescence signal upon deglycosylation was observed indicating structural perturbations, a conclusion that was further reinforced by DSC results indicating a structural change in the C_H2 region of all three IgG1 mAbs. A similar study looked at the influence of a series of differentially glycosylated IgG1-Fc mAbs with varying glycan length generated

through an enzymatic reaction on the conformational stability.[41] Using DSC, glycosylation length was found to play a role in IgG1 conformational stability specifically at the C_H2 domain where glycosylation resides. In addition to influencing conformation, glycosylation was found to have an effect on the protein susceptibility for proteolysis. The existence of the glycan and the type of the terminal sugar in the glycan residue were reported to influence the susceptibility of an IgG to papain digestion.[42, 43]

1.3.2 Biological activity characterization

Biological activity of a protein, an equally important critical quality attribute as physiochemical properties, defines the ability of a drug product to achieve a specifically defined biological function, ideally through an understood mechanism of action that leads to a desired clinical effect. Techniques used to characterize the biological activity of a protein serve as complement physiochemical assays in confirming the correct higher order structure of the protein. Determining bioactivity for monoclonal antibody based protein drugs is usually done using a variety of *in vitro* binding assays such as Enzyme-linked immunosorbent assay (ELISA) and Surface Plasmon Response Spectroscopy (SPR). Another group of bioassays, that directly measures biological functionality, are often also used with mAbs including *in vitro* cell proliferation and *in vitro* animal models. Using functionality bioassays (if feasible) in

comparability studies is sometimes preferred over simple antigen binding assays because some degraded, aggregated and chemically modified product could still bind nonspecifically to the target molecule in a simple binding assay. Protein molecules containing multiple regions with different functionalities should have multiple functionality and/or binding bioassays reflecting each and every structural region. For example, monoclonal antibodies are composed of two antigen binding regions (Fab), responsible for antigen binding, and one crystallizable region (Fc), responsible for immune effector function. Each one of these regions may need to be tested for its ability to bind to its specified target to perform its desirable function.

Case studies examining protein functional activity changes due to changes in manufacturing process have been reported. An oxidized form of the protein filgratism (a human granulocyte-colony stimulating factor used primarily for patient with severe neutropenia) was found to be 25% potent, whereas, filgratism dimer had 67% potency compared to the intact molecule.[44] In addition to influencing protein conformation, glycosylation can play a critical role in defining biological functionality. In the case of a mAb, the presence of a core fucose unit in the N-linked oligosaccharide was found to be responsible for decreasing the antibody-dependent cellular cytotoxicity (ADCC), highlighting the importance of glycan identification in comparability studies for the pre- and post-change mAb products.[45] As another example, TNK-Tissue Plasminogen Activator (TNK-tPA)

is a glycosylated protein which contains four glycosylation sites, three are N-linked and one site is O-linked. In one comparability study,[46] with a biosimilar molecule under development, the biosimilar protein had a similar glycosylation pattern as the innovator drug product, except for one N-glycosylation site which was found be only partially glycosylated. The close proximity of the partially glycosylated glycan to the active site raised concerns about its influence on the clot lysis biological activity, resulting in the need for more detailed studies to investigate such effects. Another marketed protein product called Myozyme (Alglucosidase alpha), used to treat patients with Pompe disease, that was produced in two different sites in the U.S. from the same company was found to be not similar in terms of biological activity.[47] These differences observed in the biological activity were attributed to glycosylation differences between proteins from the two manufacturing sites.

1.3.3 Accelerated and Forced Degradation stability studies

Forced degradation studies comprise the group of analytical tests applied on the drug product to elucidate the physicochemical mechanism(s) of protein degradation, whereas, accelerated stability studies measure the rate of given degradation mechanism(s) over time at various temperatures in specific formulations. Evaluating the effect of storage period, excipients and environmental stress on the accelerated (and long term) stability of protein drug

products is an essential part of formulation development and comparability evaluations. Protein drugs encounter different environmental stresses during production, storage, shipment and patient administration. Thus, accelerated stability studies and forced degradation studies are needed to determine the stability profile of a protein drug by subjecting the protein to various stresses including elevated or changing temperatures, freezing, thawing, agitation and oxidative stresses, light, exposure to different interfaces and pH changes.[48-51] The design of successful forced degradation and accelerated stability studies depends on having the appropriate analytical tools to detect, quantify and characterize any degradants, impurities and side products generated during these studies.

For the stability component of a comparability exercise, regulatory guidelines such as ICH Q3C [52], ICH Q5C [53] and ICH Q5E [19] can be used for initial guidance regarding the type of forced degradation and stability studies to be applied. For example, ICH Q3C guideline mentions the importance of developing analytical assays to quantify residual impurities of xylene leaching from rubber stoppers during freeze-drying process. Similarly, ICH Q5E guideline talks about divalent cations leaching from vial stoppers which in turn activate trace amounts of proteases leading to the degradation of the protein drug. These two real-life examples highlight the importance of assessing the effect of process changes made in the final dosage form. Stressing the drug product samples obtained from different manufacturing processes can potentially magnify any small changes in

protein stability helping scientists to reach a conclusion concerning the protein drug's structural integrity, safety and efficacy. It should be pointed out that the regulatory guidance documents discussing forced degradation and accelerated stability studies lack detailed descriptions regarding the analytical procedures and storage conditions, thus leaving it up to protein drug manufacturers to identify specific methods and conditions to test degradation behavior of their specific protein product.

Designing a successful comparability stability study also depends on the type of process or product change being evaluated. For instance, a change in the final dosage form from a liquid to a lyophilized drug product will result in a more stable product and would thus not necessarily be expected to have a similar stability profile. In this case, showing similarity of degradants type would be of primary interest. In an opposite scenario, changing from a lyophilized dosage form to a liquid one, would not only require evaluating the types of degradants but also the protein drug product under additional stress conditions (e.g., mechanical stress) to get an insight about the aggregation behavior of the liquid formulated protein drug. Exposure to new surfaces from changing the primary containers or formulation additives has been reported to induce protein aggregation and oxidation in some protein drug products. In one study,[25] an assessment of the impact of changing the primary packaging from a vial to a pre-filled syringe in terms of conformational integrity and stability of two mAbs was

evaluated. Similar molecular structure, biological activity and degradation profiles were seen for both mAbs in a liquid formulation filled in the vials and syringes with the one exception: a small but statistically significant difference in subvisible particles levels was noted. This relative increase in subvisible particles in the two containers was attributed to the presence of trace amounts of silicon oil in the syringes, which has been reported to have an undesirable effect on proteins stability and aggregation.[54, 55]

In another protein comparability exercise, the biophysical stability of three lots of an IgG1 mAb that were manufactured and filled at different locations was assessed.[56] These three lots were incubated for multiple time points (0, 8 and 16 weeks) under either refrigeration (4 ^{0}C) or heat stressed conditions (40 ^{0}C). No differences between the different lots of the protein in terms of conformational stability as well as in aggregation behavior were detected for the refrigerated lots. However, variations between the different lots stored at 40 ^{0}C at different time points were seen using extrinsic fluorescence spectroscopy (using ANS as a dye), and differences between two of the lots were also detected using intrinsic (Trp) fluorescence spectroscopy. Different aggregation levels were seen for the heat stressed samples as well using static light scattering (SLS) and size exclusion high performance liquid chromatography (SE-HPLC). This example illustrates, as mentioned before, the importance of applying stress on the protein sample to

extract additional information about the protein's critical quality attributes such as HOS that may otherwise not be observed.

1.3.4 Pharmacokinetics Studies

In addition to analytical comparability testing described above, pharmacokinetic studies may need to be evaluated in the form of either non-clinical or clinical studies in which the pharmacokinetic profile of the protein drug is evaluated using animal models (rodents or primates) and/or in humans. These studies are applied as part of comparability assessments to demonstrate product comparison for the pre- and post- change products after drug administration in a relevant animal model or patient population. The need for performing pharmacokinetic studies depends on a variety of factors including the type of structural, functional or stability differences observed analytically in the product after applying the process change. In cases involving an observed non-similarity between the products under comparison, it may be necessary to perform pharmacokinetic study in human subjects to demonstrate comparability.[57] These pharmacokinetic studies are performed using the same route of administration and dose regimens providing comparative results (e.g., absorption, bioavailability as well as elimination parameters like clearance and elimination half-life) that should be highly similar for the two samples being compared.[57]

Structural differences introduced in the post-manufacturing process change drug product can vary in the extent to which they affect pharmacokinetic parameters. Glycosylation plays a central role in defining the circulation and half-life in the human body for glycoproteins. In one example, using a rat animal model, 50% loss in the amount of circulating protein (ceruloplasmin, a copper carrying protein in the blood) was observed after a 20% reduction in sialic acid content of the glycan attached to the protein. [58] In some glycoproteins lacking sialic acid, it has been shown that they have a higher affinity to mannose receptors in the liver cells, leading to a faster clearance and catabolism compared to the fully sialylated ones.[59] The same fate was observed for antibodies containing mannose terminated N-glycans.[60, 61] Multiple comparability studies have examined glycoproteins with different distributions of glycosylation patterns due to a process change (especially those including changes in cell line or cell culture). In one study, the amount of sialic acid in addition to the relative distribution of neutral oligosaccharides were different between the pre and post-change for mAb proteins after changing the producing cells form a murine myeloma cell line (NS0) to Chinese hamster ovary cell line (CHO).[62] Another study demonstrated that using a different clone of the same cell, or changing the cell culture components, resulted in a significant increase in acidic glycoforms of a mAb compared to the original cell line.[25]

Pharmacokinetic parameters, in addition to being sensitive to changes in the glycosylation patterns, have also been reported to be sensitive to changes in the overall charge state of the protein as well. Proteins with specific charge heterogeneity profiles have been shown, after modifying the manufacturing method, to have a different charge distribution profile.[63] Changes in the overall charge state of a protein could alter the electrostatic and hydrophobic interactions between the protein and the negatively charged cell membrane leading to a different pharmacokinetic profile.[64] Using animal studies, minor shifts in the p*I* of a protein (in the range of 0.1-0.2 p*I* units) have been demonstrated to have no effect on the pharmacokinetic profile.[65] Meanwhile, shifts of above 1.0 p*I* units could have a measurable effect. In one study, protein cationization resulted in a longer tissue retention times and a faster clearance, [66] whereas protein anionization tended to cause a decrease in tissue retention time but still increased the whole body clearance [67] (demonstrated in rats and mice, respectively). At the molecular level, changes in the charge heterogeneity profile of a protein molecule could rise from alterations in the primary sequence of the protein as a result of amino acid mutations or chemical degradation (e.g., Asn deamidation).[68] Post-translational modifications (e.g., sialic acid on the glycan residues and C-terminal lysine) on proteins could contribute to the charge heterogeneity profile of a protein.[68] Protein aggregation may also affect the pharmacokinetics profile directly or indirectly through neutralizing antibodies produced from the immune

cells in the body. For example, insulin oligomers have been reported to have a slower absorption and bioavailability upon subcutaneous administration compared to non-aggregated form of the protein.[69]

Taken together, changes to a protein's glycosylation pattern, charge distribution and aggregation profiles upon manufacturing changes could have a measurable effect on its pharmacokinetic profile, which may or may not have an effect on the drug pharmacodynamics, efficacy and safety profiles. The evaluation of such pK affects are almost always carried out first using animal models (either rodents or primates), and if results are inconclusive, human clinical pharmacokinetic comparability studies may be necessary.

1.3.5 Clinical Immunogenicity Studies

Since proteins are complex macromolecules of high molecular weight and naturally occurring structural heterogeneity, any changes to the native structure could potentially reveal antigenic sites that could stimulate an immune response. An immune response could be stimulated by many factors that are generally divided into two categories: extrinsic and intrinsic. Patient immunogenic susceptibility and patient health status (administering co-medications) in addition to the dose and route of administration are all considered extrinsic factors related to the immunogenicity of a protein based drug.[70] Intrinsic factors are those related to the protein or the drug product itself including aggregation propensity,

impurities (e.g., residual host cell protein not removed by the purification steps) and leachables (from container-closure system, which may not be immunogenic by itself but could induce protein aggregation).[71-73] The consequences of an immune reaction against a protein drug could vary significantly, ranging from clinically minor to severe, life-threatening effects. In one unfortunate story, a specific erythropoietin-α drug product (Eprex®) has been associated (in 1998 and peaked in occurrence in 2002) with pure red cell aplasia (PRCA).[74] An increase in neutralizing antibodies titers in patients with chronic renal failure against the protein drug was found, which was correlated after investigation with changes made in the product formulation.[75] Human serum albumin (HSA), used as a stabilizer, was removed from the original formulation and substituted by polysorbate 80 surfactant. This substitution facilitated instability either by the leaching of compounds (tungsten in one theory) [76] from the rubber plunger of the pre-filled syringe causing the protein to unfold and aggregate. Another theory suggested that polysorbate 80 formed micelles with the protein resulting in an adjuvant-like nanoparticle that stimulated the immune system.[77] The route of administration plays a critical role as well in product immunogenicity. It was found that patients who received Eprex® through an intravenous injection (i.v) did not get PRCA unlike those received the drug subcutaneously (s.c).[78] As part of the corrective actions to prevent PRCA in the future, European regulatory authorities

recommended changing the route of administration for Eprex® from s.c to i.v in addition to going back to using HSA as the stabilizer of choice.[74]

Other intrinsic factors that could influence immunogenicity include protein degradation, during manufacturing or storage, resulting in exposure of previously unseen epitopes that could activate the immune system. Glycoproteins bearing different kinds of monosaccharides or different linkages than the naturally occurring ones in the human body could potentially stimulate the immune response as well. These glycan differences are introduced from various mammalian cell lines used to produce a recombinant protein. For example, the presence of galactose-α-1, 3 glycans have been associated with causing anaphylactic shock and an immune response in patients using cetuximab and bovine thrombin, respectively.[79, 80] N-glycolylneuraminic acid (Neu5Gc or NGNA) is a sialic acid glycan that contains an additional oxygen atom compared to the naturally occurring N-acetylneuraminic acid (Neu5AC or NANA) glycan in humans. The presence of this sialic acid form (NGNA) has been associated with immunogenicity risks.[81] A comparison between cetuximab and panitumumab (both antibodies specific for binding epidermal growth factor receptor), concerning the addition of Neu5Gc to the glycan structure during expression in cell culture, showed that cetuximab only was incorporating NGNA to the glycan structure.[82] The addition of NANA to the culture media helped reduce the incorporation of NGNA to the glycoprotein drug. Finally, complete

deglycosylation of a glycoprotein has been associated with increasing immunogenicity incidences. Mechanisms underlying such as effect are not fully understood, however, aggregation resulting from the exposure of normally hidden hydrophobic patches, decreasing solubility and the exposure of antigenic sites or a combination of factors have been proposed, for example, immunogenicity incidences due to deglycosylation were reported for interferon-β [83, 84] and Granulocyte Macrophage Colony-Stimulating factor (GM-CSF).[85]

Protein aggregation events are thought to have a significant impact on the immunogenicity potential of protein drugs. Protein aggregation can be exacerbated by multiple factors including changes in solution conditions (pH, salts, excipients, etc.) [35, 36, 50] and exposure of the protein solution to different environmental stresses (temperature, agitation, freeze-thaw, etc.).[86-88] An immunogenic response in patients receiving an interferon alpha was attributed to the presence of aggregated species in the drug product, seen after alterations applied into the formulation components.[89] A positive correlation between protein aggregation and immunogenicity has been shown as well for other therapeutic proteins, such as insulin,[90] human growth hormone [91] and bovine serum albumin[92] manifesting the important role of protein aggregate detection and characterization in protein drug products.[93, 94]

Immunogenicity prediction in humans using either *in vitro* models or animal studies is difficult, and the development of new approaches to obtain more

reliable immunogenicity tests remains highly desirable.[95] The need to evaluate post-manufacturing change protein drug products for immunogenicity becomes even more important for products with a past history of immunogenicity (the pre-change product), as well for those protein products with manufacturing changes that are considered extensive (cell line) or result in observations for increased levels of aggregates or particles.

1.4 Analytical challenges for future comparability studies

Overall, the type and extent of any comparability exercise depends primarily on the nature of the protein (size, complexity, microheterogeneity), the magnitude and type of manufacturing changes, and the analytical tools available to monitor the structural integrity of a protein. An in depth understanding of the protein including its inherent susceptibility to the different chemical and physical degradation mechanisms, combine with accumulated clinical and manufacturing experience with product, is essential for a successful comparability exercise. Accurate structural determination for protein-based drugs is a difficult task for pharmaceutical and biotechnological industry, in contrast to small molecule drugs, because of their complex three-dimensional structures and microheteogeneity. Major advances have been made in developing analytical tools for primary structure analysis, ranging from chromatographic (size

exclusion, reversed phase and ion-exchange HPLC) and electrophoretic (capillary isoelectric focusing and capillary sodium dodecyl sulfate) separation methods that are typically linked with mass spectrometry detection (intact molecular weight, peptide maps, and oligosaccharides maps) to well characterize a protein's primary structure including post-translational modifications. Although major advances have been made in developing analytical tools for primary structure analysis, major challenges regarding the development of improved analytical techniques for determination of higher order structural integrity of proteins still exist. In fact, the current requirement for performing functional biological potency assays to ensure biological activity is considered an overall check on the higher order structural integrity of a protein. Although multiple high resolution analytical techniques, with the ability to better characterize the high order structures of proteins are available (x-ray crystallography, H/DX-MS and NMR), development of these methodologies for use with protein drug candidates within a pharmaceutical dosage form (containing excipients) still remains as a major challenge.

More well established, commonly available, lower resolution biophysical techniques such as circular dichroism, intrinsic and extrinsic fluorescence spectroscopy, differential scanning calorimetry, static light scattering and turbidity assays are used for the evaluation of secondary/tertiary structures and colloidal stability of a protein as part of a pharmaceutical drug product containing

formulation components. These biophysical methods can be setup as high throughput assays in which analysis can be performed automatically across various environmental conditions such as changes in solution pH and temperature. Environmental stresses, such as elevated temperatures and extreme pH conditions, are frequently used stress factors to evaluate the overall conformational stability of proteins during formulation development, but the use of these types of data sets for comparability analysis has not been explored. By using data sets acquired from multiple low-resolution biophysical techniques that monitor different aspects of a protein's higher-order structural stability as a function of environmental stress, differences in structural integrity may potentially be detected when these differences are not readily apparent when monitored using lower resolution methods under non-stressed conditions (i.e., at low temperatures at neutral pH conditions). Additionally, the evaluation of conformational stability differences may not only be an effective surrogate to monitor differences in higher-order structure between protein samples, but also a useful complement to traditional accelerated stability and forced degradation studies often used in analytical comparability studies as described above.

1.5 Possible applicability of high throughput biophysical analysis of protein stability to comparability studies

Physiochemical characterization for the higher order structural integrity of a protein in two different drug products under comparison is one of the essential elements of a comparability study (as discussed above). Although various lower resolution analytical techniques have been used and developed to test higher order structural comparability between two protein drug samples (i.e., CD, fluorescence and DSC), as discussed above, the use of higher resolution techniques such as NMR, X-ray crystallography and H/D exchange mass spectrometry (that provide structural details about the protein's folded structure and dynamics) remains limited in their wide spread use (e.g., due to high molecular weight, presence of formulation components, and/or analytical complexity) as part of analytical comparability studies. With that being said, the need for a new approaches to better monitor the higher order structural integrity of proteins during comparability studies is of a great interest.

Although lower resolution biophysical techniques such as circular dichroism, intrinsic/extrinsic fluorescence spectroscopy, differential scanning calorimetry, static light scattering and turbidity assays are commonly used techniques to monitor the structural integrity and conformational stability of protein-based drugs, no single technique provides sufficient information to

establish the higher order structural integrity of complex macromolecules such as proteins. Therefore, the use of more than one technique is generally needed for better characterization. The multi-dimensional nature of such analysis makes collection, analysis and visualization of larger data sets problematic. Historically, data analysis of protein conformational stability data was performed by either visual inspection or data fitting of thermal unfolding curves to sigmoidal functions of results from individual instruments. These types of approaches can result in data interpretation that is not only subjective, but limited in terms of the scope and utility.

In 2003, a new data visualization methodology was introduced as a tool for analysis of protein physical stability data obtained from high throughput biophysical instruments, and its application toward formulation screening purposes for protein based drugs was extensively evaluated.[96] This methodology, called Empirical Phase Diagram (EPD), is a data visualization tool that is based on using data sets from multiple low-resolution biophysical techniques to construct a color coded diagram reflecting the different structural phases that the protein would experience during an applied stress conditions (e.g., pH, temperature, ionic strength or protein concentration). The idea of developing such a methodology stemmed from the fact that most comparative experiments using protein thermal melting curves conventionally use visual assessment and T_m/T_{onset} values to determine differences between the different formulations under

comparison, which makes data interpretation across multiple samples difficult and potentially highly subjective. Using bovine granulocyte colony stimulating factor (bGSCF) as a model protein combined with second derivative absorbance spectroscopy as a model biophysical method to characterize the physical stability of the protein across multiple pH and temperature conditions, the first EPD was constructed. This EPD, interestingly, was able to detect six different structural phases that the protein experienced under a combination of two stress conditions used (temperature and pH) that by visual observation of the individual data sets were not easily detected.

An EPD analysis involves the collection of protein physical stability data under different experimental conditions using multiple low-resolution biophysical techniques. The stability data from the experimental conditions and techniques are then entered into *m* x *n* input matrix in which *m* represents the experimental techniques (i.e., circular dichroism, fluorescence spectroscopy, turbidity, etc.) and *n* represents the experimental conditions (i.e., number of pH values x number of temperature measurements). After data normalization, singular value decomposition of the *m* x *n* experimental data matrix is calculated to extract three orthogonal basis vectors associated with the three largest singular values. These results are then mapped to red-green-blue (RGB) color scheme that can be visualized as a function of the stress conditions (e.g., temperature and pH). After an EPD is generated, what remains is the interpretation of the change of colors of

the different areas of the EPD. The colors of the different areas within an EPDs have no physical meaning, instead the change in color signifies a structural change in the protein as detected by the data from experimental techniques. A scientist must refer to the original experimental biophysical data and consider the physical process that generated regions with different colors. Changes in the biophysical signal which corresponds to change in protein's physical stability would be seen in the EPDs as changes from one color to another, a change that would be interpreted as a transition of the protein from one conformational state to another. [96, 97]

Realizing the potential applications of this EPD methodology, a subsequent optimization was carried over the following years with a wide variety of proteins in terms of the number and type of biophysical techniques included in the EPD, clustering analysis and color interpretation.[97] In 2012, radar charts were introduced as an additional data visualization tool for displaying protein physical stability data obtained from multiple biophysical instruments.[98] The major idea of this data visualization approach is to arrange multiple axes, representing the different biophysical techniques, at evenly spaced angles to form a polygonal figure. Polar axes are adjusted to display values from each analytical instrument between zero (representing the starting point or in this case the native state of a protein) and 1 (representing the end point or in this case the structurally altered state). Data acquired from the different biophysical methods are therefore

normalized and mapped to points in the polar coordinates in the radar chart. Radar diagrams are composed of multiple charts arranged in two dimensional coordinates of environmental stress conditions (e.g., temperature and pH). Structural changes of the protein as monitored by the different methods are then visualized in the form of differences in the area of the polygons, where the native-like state of a protein would have a polygon with smaller area compared to structurally disrupted states of the same protein. Unlike EPDs, radar diagrams have the advantage of displaying protein physical stability results from a larger number of experimental techniques, allowing the evaluation of protein structural integrity and conformational stability as a function of the specific biophysical techniques across the experimental conditions.[98]

In this work, the possible use of high throughput biophysical analysis of protein physical stability data along with the data visualization techniques is being evaluated as a way to compare the structural integrity and physical stability of different versions of the same protein to each other (as would be done in comparability studies). Our approach (as will be discussed in detail below) is based on using a variety of different proteins with different sizes, post-translational modifications and inherent stability. Structural differences in the form of known "major" (i.e., point mutations) or "minor" (i.e., post translational modifications) alterations in protein structure were specifically introduced into three different proteins: FGF-1, IgG1 mAb, and IgG1-Fc protein. These different

proteins were subsequently extensively characterized in terms of physical stability properties using multiple low-resolution biophysical techniques described above to monitor different aspects of the higher-order structural of these proteins across a wide range of pH and temperature conditions. These large data sets of biophysical data where then used to construct EPDs and radar charts for data visualization and structural comparison between the different proteins. Using this approach, differences in structural integrity and conformational stability were detected at stress conditions that could not be detected by using the same techniques under ambient conditions (i.e., no stress). Thus, an evaluation of conformational stability differences may serve as an effective surrogate to monitor differences in higher-order structure between protein samples.

1.6 Chapter reviews

1.6.1 An Empirical Phase Diagram Approach to Investigate Conformational Stability of "Second-generation" Functional Mutants of Acidic Fibroblast Growth Factor (FGF-1). (Chapter 2)

FGF-1 is a 16 kDa protein that belongs to β-trefoil family of proteins. It is composed of a six stranded β-barrels closed off at one end by three β-hairpin structures. FGF-1 is an intrinsically unstable protein molecule that is involved in the angiogenesis process. It is being investigated from a pharmaceutical perspective as a candidate for treatment of ischemic disease, including wound

healing in diabetic ulcers, peripheral artery disease, and non-treatable (i.e., ‘‘no option’’) coronary occlusions. Since FGF-1 has intrinsically low thermodynamic stability in conjunction with three reactive cysteine residues, it is vulnerable to irreversible unfolding and aggregation during production and storage, with associated negative consequences for shelf-life, potency, and immunogenicity. FGF-1 is a heparin binding protein and has significant natural affinity for many polyanions, and based on this observation, FGF-1 for human therapeutic use has been formulated with the addition of heparin. The use of heparin as an excipient, however, adds considerable complexity including increased expense, its own pharmacological properties (e.g., as an anticoagulant), animal derived material from pig tissues (with potential for infectious contamination), and the possible induction of adverse inflammatory or allergic reactions in a segment of the targeted patient population. Thus, although heparin or related polyanions used as formulation additives help to address the FGF-1 stability issue, they introduce other undesirable properties. To solve this problem, a site directed mutagenesis approach is used with the goal of altering the temperature and pH stability profile of the FGF-1 mutants to more closely resemble that of wildtype FGF-1 in complexation with heparin. In this chapter, the structural integrity and conformational stability of ten FGF-1 mutants were characterized and compared to the FGF-1 wild-type alone and with heparin. Twelve EPDs were constructed and used to broadly assess the physical stability of these mutants in response to

variations in pH and temperature. In addition, the EPD ability to distinguish stability differences between the FGF-1 variants was evaluated.

1.6.2 High-Throughput Biophysical Analysis and Data Visualization of Conformational Stability of an IgG1 Monoclonal Antibody (mAb) After Deglycosylation. (Chapter 3)

Monoclonal antibodies are glycosylated, multidomain proteins (~MW of 150 kDa) and the extent and type of glycosylation has been shown to influence the conformational stability of mAbs. In this chapter, the structural integrity and conformational stability of an IgG1 mAb, after partial and complete enzymatic removal of the N-linked Fc glycan, was compared to the untreated mAb over a wide range of temperature (10° to 90°C) and solution pH (3 to 8). Subtle to larger stability differences between the different glycoforms were observed. Improved detection of physical stability differences was then demonstrated over a narrower pH range (4.0-6.0) and smaller temperature increments. An additional data visualization method (radar plots) was incorporated to the data assessment as well. Differential scanning calorimetry and differential scanning fluorimetry were then utilized and also showed an improved ability to detect differences in mAb glycoform physical stability. Based on these results, a two-step methodology was used in which mAb glycoform conformational stability is first screened with a wide variety of instruments and environmental stresses, followed by a second

evaluation with optimally sensitive experimental conditions, analytical techniques and data visualization methods. In this chapter, high-through-put biophysical analysis to assess relatively subtle conformational stability differences in protein glycoforms is demonstrated.

1.6.3 Global stability assessment of an IgG1-Fc; mutation, glycosylation and charge variation effects. (Chapter 4)

In this chapter, a model IgG1-Fc protein (~50 kDa protein containing two C_H2 domains and two C_H3 domains) was produced from yeast *Pichia pastoris* and different glycosylation forms were generated to provide insight about the effect of glycosylation differences, and charge heterogeneity differences (due to point mutations and enzymatic treatments of the Fc glycoforms) on the structural integrity and conformational stability of the C_H2 domain from different Fc glycoforms.

Using this yeast expression system, two glycosylation forms of IgG1-Fc were produced and purified. These forms are comprised of different site occupancy: a high mannose di-glycosylated form, where the Fc protein is glycosylated in the two C_H2 domains (glycan-glycan), and high mannose mono-glycosylated form, where the Fc protein is glycosylated at a single C_H2 domain (glycan-Asn). These two glycoforms of the IgG1-Fc molecule were separated using cation exchange and hydrophobic interaction chromatography to obtain the

individual glycoforms of high purity. An aglycosylated IgG1-Fc mutant containing Gln in both C_H2 domains (instead of Asn) was also produced using the same expression system and purified using hydrophobic interaction chromatography. The three Fc glycoforms (di-, mono-, and a-glycoylated species) were then used to study the effect of glycosylation level on the global stability of the C_H2 domain.

In addition to site occupancy, the global physical stability of differentially charged forms of the aglycosylated Fc molecule, specifically in the C_H2 domain, is an additional aspect of antibody stability that was then evaluated in this chapter. Differentially charged forms of the aglycosylated Fc protein were created upon treating the di-glycosylated and mono-glycosylated IgG1-Fc molecules with PNGase F enzyme creating a di-charged (Asp-Asp) and a mono-charged (Asp-Asn) IgG1-Fcs in the C_H2 domsain as an outcome of the enzymatic deglycosylation mechanism. These two molecules were compared to the non-glycosylated (Gln-Gln) IgG1-Fc mutant. An assessment of these charge differences within the C_H2 domain in terms of their impact on structural integrity and physical stability of the Fc protein was also evaluated.

1.6.4 Conclusions and future work. (Chapter 5)

This final chapter summarizes what we learned about the structural integrity and conformational stability of the various proteins examined in

Chapters 2-4 (point mutants of FGF-1, deglycosylated forms of an IgG1 mAb, and different glycoforms of an IgG-1 Fc) and as well as the potential utility of using new data visualization methods for displaying high throughput biophysical stability data (as discussed in the previous chapters) in analytical comparability studies. Suggestions for future work are also discussed.

1.7 References

1- Aggarwal, S. R., What's fueling the biotech engine—2011 to 2012. *Nature Biotechnology* **2012,** *30,* 1191–1197.

2- Manning, M.; Chou, D.; Murphy, B.; Payne, R.; Katayama, D., Stability of Protein Pharmaceuticals: An Update. *Pharmaceutical Research* **2010,** *27* (4), 544-575.

3- Tsai, R. M. M. a. A. M., Misbehaving Proteins, Protein (Mis) Folding, Aggregation, and Stability. **2006**.

4- Møller, M. v. d. W. a. E. H., Immunogenicity of Biopharmaceuticals. **2008**.

5- Rosenberg, A., Effects of protein aggregates: An immunologic perspective. *The AAPS Journal* **2006,** *8* (3), E501-E507.

6- Shirley, B. A., Protein Stability and Folding, Theory and Practice. **1995.**

7- Bee, J. S.; Randolph, T. W.; Carpenter, J. F.; Bishop, S. M.; Dimitrova, M. N., Effects of surfaces and leachables on the stability of biopharmaceuticals. *Journal of Pharmaceutical Sciences* **2011,** *100* (10), 4158-4170.

8- Narhi, L. O.; Schmit, J.; Bechtold-Peters, K.; Sharma, D., Classification of protein aggregates. *Journal of Pharmaceutical Sciences* **2012,** *101* (2), 493-498.

9- Wang, W., Protein aggregation and its inhibition in biopharmaceutics. *International Journal of Pharmaceutics* **2005,** *289* (1–2), 1-30.

10- Brych, S. R.; Gokarn, Y. R.; Hultgen, H.; Stevenson, R. J.; Rajan, R.; Matsumura, M., Characterization of antibody aggregation: Role of buried, unpaired cysteines in particle formation. *Journal of Pharmaceutical Sciences* **2010,** *99* (2), 764-781.

11- Davies, M. J., Singlet oxygen-mediated damage to proteins and its consequences. *Biochemical and Biophysical Research Communications* **2003,** *305* (3), 761-770.

12- Banks, D. D.; Latypov, R. F.; Ketchem, R. R.; Woodard, J.; Scavezze, J. L.; Siska, C. C.; Razinkov, V. I., Native-state solubility and transfer free energy as predictive tools for selecting excipients to include in protein formulation development studies. *Journal of Pharmaceutical Sciences* **2012,** *101* (8), 2720-2732.

13- Hari, S. B.; Lau, H.; Razinkov, V. I.; Chen, S.; Latypov, R. F., Acid-Induced Aggregation of Human Monoclonal IgG1 and IgG2: Molecular Mechanism and the Effect of Solution Composition. *Biochemistry* **2010,** *49* (43), 9328-9338.

14- Majhi, P. R.; Ganta, R. R.; Vanam, R. P.; Seyrek, E.; Giger, K.; Dubin, P. L., Electrostatically Driven Protein Aggregation: β-Lactoglobulin at Low Ionic Strength. *Langmuir* **2006,** *22* (22), 9150-9159.

15- Hamada, H.; Arakawa, T.; Shiraki, K., Effect of Additives on Protein Aggregation. *Current Pharmaceutical Biotechnology* **2009,** *10* (4), 400-407.

16- Reichert, J. M., Which are the antibodies to watch in 2013, *mAbs* **2013,** *5* (1), 1-4.

17- GUIDANCE CONCERNING DEMONSTRATION OF COMPARABILITY OF HUMAN BIOLOGICAL PRODUCTS; AVAILABILITY. *Federal Register* **April 26, 1996,** *61* (82).

18- Committee for Proprietary Medicinal Products. Guideline on comparability of medicinal products containing biotechnology-derived proteins as active substance. Non-clinical and clinical issues. EMEA/CPMP/3097/02/Final2003.

19- ICH Q5E: Comparability Biotechnological/Biological Products Subject to Changes in Their Manufacturing Process. Fed. Reg. 70(125) 2003: 37861–37862; www. ich.org/LOB/media/MEDIA1196.pdf

20- EXPERT COMMITTEE ON BIOLOGICAL STANDARDIZATION. GUIDELINES ON EVALUATION OF SIMILAR BIOTHERAPEUTIC PRODUCTS (SBPs). World Health Organization 2009.

21- Chirino, A. J.; Mire-Sluis, A., Characterizing biological products and assessing comparability following manufacturing changes. *Nat Biotech* **2004,** *22* (11), 1383-1391.

22- Federici, M.; Lubiniecki, A.; Manikwar, P.; Volkin, D. B., Analytical lessons learned from selected therapeutic protein drug comparability studies. *Biologicals* **2013,** *41* (3), 131-147.

23- Berkowitz, S. A.; Engen, J. R.; Mazzeo, J. R.; Jones, G. B., Analytical tools for characterizing biopharmaceuticals and the implications for biosimilars. *Nat Rev Drug Discov* **2012,** *11* (7), 527-540.

24- Li, C.; Rossomando, A.; Wu, S.-L.; Karger, B. L., Comparability analysis of anti-CD20 commercial (rituximab) and RNAi-mediated fucosylated antibodies by two LC-MS approaches. *mAbs* **2013,** *5* (4), 565-575.

25- Lubiniecki, A.; Volkin, D. B.; Federici, M.; Bond, M. D.; Nedved, M. L.; Hendricks, L.; Mehndiratta, P.; Bruner, M.; Burman, S.; DalMonte, P.; Kline, J.; Ni, A.; Panek, M. E.; Pikounis, B.; Powers, G.; Vafa, O.; Siegel, R., Comparability assessments of process and product changes made during development of two different monoclonal antibodies. *Biologicals* **2011,** *39* (1), 9-22.

26- Skrlin, A.; Radic, I.; Vuletic, M.; Schwinke, D.; Runac, D.; Kusalic, T.; Paskvan, I.; Krsic, M.; Bratos, M.; Marinc, S., Comparison of the physicochemical properties of a biosimilar filgrastim with those of reference filgrastim. *Biologicals* **2010,** *38* (5), 557-566.

27- Walsh, G.; Jefferis, R., Post-translational modifications in the context of therapeutic proteins. *Nat Biotech* **2006,** *24* (10), 1241-1252.

28- Beck, A.; Sanglier-Cianférani, S.; Van Dorsselaer, A., Biosimilar, Biobetter, and Next Generation Antibody Characterization by Mass Spectrometry. *Analytical Chemistry* **2012,** *84* (11), 4637-4646.

29- Zaia, J., Mass Spectrometry and the Emerging Field of Glycomics. *Chemistry & Biology* **2008,** *15* (9), 881-892.

30- Brooks, S., Strategies for Analysis of the Glycosylation of Proteins: Current Status and Future Perspectives. *Molecular Biotechnology* **2009,** *43* (1), 76-88.

31- Pompach, P.; Chandler, K. B.; Lan, R.; Edwards, N.; Goldman, R., Semi-Automated Identification of N-Glycopeptides by Hydrophilic Interaction Chromatography, nano-Reverse-Phase LC–MS/MS, and Glycan Database Search. *Journal of Proteome Research* **2012,** *11* (3), 1728-1740.

32- Desaire, H., Glycopeptide Analysis, Recent Developments and Applications. *Molecular & Cellular Proteomics* **2013,** *12* (4), 893-901.

33- Leymarie, N.; Zaia, J., Effective Use of Mass Spectrometry for Glycan and Glycopeptide Structural Analysis. *Analytical Chemistry* **2012,** *84* (7), 3040-3048.

34- Baković, M. P.; Selman, M. H. J.; Hoffmann, M.; Rudan, I.; Campbell, H.; Deelder, A. M.; Lauc, G.; Wuhrer, M., High-Throughput IgG Fc N-Glycosylation Profiling by Mass Spectrometry of Glycopeptides. *Journal of Proteome Research* **2013,** *12* (2), 821-831.

35- Manikwar, P.; Majumdar, R.; Hickey, J. M.; Thakkar, S. V.; Samra, H. S.; Sathish, H. A.; Bishop, S. M.; Middaugh, C. R.; Weis, D. D.; Volkin, D. B., Correlating excipient effects on conformational and storage stability of an IgG1 monoclonal antibody with local dynamics as measured by hydrogen/deuterium-exchange mass spectrometry. *Journal of Pharmaceutical Sciences* **2013,** *102* (7), 2136-2151.

36- Majumdar, R.; Manikwar, P.; Hickey, J. M.; Samra, H. S.; Sathish, H. A.; Bishop, S. M.; Middaugh, C. R.; Volkin, D. B.; Weis, D. D., Effects of Salts from the Hofmeister Series on the Conformational Stability, Aggregation Propensity, and Local Flexibility of an IgG1 Monoclonal Antibody. *Biochemistry* **2013,** *52* (19), 3376-3389.

37- Cauchy, M.; Hefford, M. A., Excipient exchange in the comparison of preparations of the same biologic made by different manufacturing processes: An exploratory study with recombinant human growth hormone (rhGH). *Biologicals* **2010,** *38* (6), 637-643.

38- DeFelippis, M. R.; Larimore, F. S., The role of formulation in insulin comparability assessments. *Biologicals* **2006,** *34* (1), 49-54.

39- Narhi, L. O.; Arakawa, T.; Aoki, K. H.; Elmore, R.; Rohde, M. F.; Boone, T.; Strickland, T. W., The effect of carbohydrate on the structure and stability of erythropoietin. *Journal of Biological Chemistry* **1991,** *266* (34), 23022-6.

40- Kai Zheng, C. B. a. R. B., The impact of glycosylation on monoclonal antibody conformation and stability. *mAbs* **2011,** *3* (6), 568-576.

41- Mimura, Y.; Church, S.; Ghirlando, R.; Ashton, P. R.; Dong, S.; Goodall, M.; Lund, J.; Jefferis, R., The influence of glycosylation on the thermal stability and effector function expression of human IgG1-Fc: properties of a series of truncated glycoforms. *Molecular Immunology* **2000,** *37* (12-13), 697-706.

42- Raju, T. S.; Scallon, B. J., Glycosylation in the Fc domain of IgG increases resistance to proteolytic cleavage by papain. *Biochemical and Biophysical Research Communications* **2006,** *341* (3), 797-803.

43- Raju, T. S.; Scallon, B., Fc Glycans Terminated with N-Acetylglucosamine Residues Increase Antibody Resistance to Papain. *Biotechnology Progress* **2007,** *23* (4), 964-971.

44- Skrlin, A.; Krnic, E. K.; Gosak, D.; Prester, B.; Mrsa, V.; Vuletic, M.; Runac, D., Correlation of liquid chromatographic and biological assay for potency assessment of filgrastim and related impurities. *Journal of Pharmaceutical and Biomedical Analysis* **2010,** *53* (3), 262-268.

45- Shields, R. L.; Lai, J.; Keck, R.; O'Connell, L. Y.; Hong, K.; Meng, Y. G.; Weikert, S. H. A.; Presta, L. G., Lack of Fucose on Human IgG1 N-Linked Oligosaccharide Improves Binding to Human FcγRIII and Antibody-dependent Cellular Toxicity. *Journal of Biological Chemistry* **2002,** *277* (30), 26733-26740.

46- Jiang, H.; Wu, S.-L.; Karger, B. L.; Hancock, W. S., Characterization of the Glycosylation Occupancy and the Active Site in the Follow-on Protein Therapeutic: TNK-Tissue Plasminogen Activator. *Analytical Chemistry* **2010,** *82* (14), 6154-6162.

47- Kozlowski, S.; Woodcock, J.; Midthun, K.; Behrman Sherman, R., Developing the Nation's Biosimilars Program. *New England Journal of Medicine* **2011,** *365* (5), 385-388.

48- Cordes, A. A.; Carpenter, J. F.; Randolph, T. W., Accelerated stability studies of abatacept formulations: Comparison of freeze–thawing- and agitation-induced stresses. *Journal of Pharmaceutical Sciences* **2012,** *101* (7), 2307-2315.

49- Miller, M. A.; Rodrigues, M. A.; Glass, M. A.; Singh, S. K.; Johnston, K. P.; Maynard, J. A., Frozen-state storage stability of a monoclonal antibody: Aggregation is impacted by freezing rate and solute distribution. *Journal of Pharmaceutical Sciences* **2013,** *102* (4), 1194-1208.

50- Wang, T.; Kumru, O. S.; Yi, L.; Wang, Y. J.; Zhang, J.; Kim, J. H.; Joshi, S. B.; Middaugh, C. R.; Volkin, D. B., Effect of ionic strength and pH on the physical and chemical stability of a monoclonal antibody antigen-binding fragment. *Journal of Pharmaceutical Sciences* **2013,** *102* (8), 2520-2537.

51- Britt, K. A.; Schwartz, D. K.; Wurth, C.; Mahler, H.-C.; Carpenter, J. F.; Randolph, T. W., Excipient effects on humanized monoclonal antibody

interactions with silicone oil emulsions. *Journal of Pharmaceutical Sciences* **2012,** *101* (12), 4419-4432.

52- ICH Q3C: Impurities — Guideline for Residual Solvents. Fed. Reg. 68(219) 2003: 64352–64353; www.ich.org/LOB/media/ MEDIA423.pdf.

53- ICHQ3C: Stability testing of Biotechnological / Biological products. Fed Regis 52(125)1996: 44928 -44935; www.ich.org/LOB/media/ MEDIA263.pdf.

54- Jones, L. S.; Kaufmann, A.; Middaugh, C. R., Silicone oil induced aggregation of proteins. *Journal of Pharmaceutical Sciences* **2005,** *94* (4), 918-927.

55- Thirumangalathu, R.; Krishnan, S.; Ricci, M. S.; Brems, D. N.; Randolph, T. W.; Carpenter, J. F., Silicone oil- and agitation-induced aggregation of a monoclonal antibody in aqueous solution. *Journal of Pharmaceutical Sciences* **2009,** *98* (9), 3167-3181.

56- Maity, H.; Lai, Y.; Srivastava, A.; Goldstein, J., Principles and Applications of Selective Biophysical Methods for Characterization and Comparability Assessment of a Monoclonal Antibody. *Current Pharmaceutical Biotechnology* **2012,** *13* (10), 2078-2101.

57- Putnam, W. S.; Prabhu, S.; Zheng, Y.; Subramanyam, M.; Wang, Y.-M. C., Pharmacokinetic, pharmacodynamic and immunogenicity comparability assessment strategies for monoclonal antibodies. *Trends in Biotechnology* **2010,** *28* (10), 509-516.

58- van den Hamer, C. J. A.; Morell, A. G.; Scheinberg, I. H.; Hickman, J.; Ashwell, G., Physical and Chemical Studies on Ceruloplasmin. *Journal of Biological Chemistry* **1970,** *245* (17), 4397-4402.

59- Stockert, R. J., The asialoglycoprotein receptor: relationships between structure, function, and expression. *Physiological Reviews* **1995,** *75* (3), 591-609.

60- Kanda, Y.; Yamada, T.; Mori, K.; Okazaki, A.; Inoue, M.; Kitajima-Miyama, K.; Kuni-Kamochi, R.; Nakano, R.; Yano, K.; Kakita, S.; Shitara, K.; Satoh, M., Comparison of biological activity among nonfucosylated therapeutic IgG1 antibodies with three different N-linked Fc oligosaccharides: the high-mannose, hybrid, and complex types. *Glycobiology* **2007,** *17* (1), 104-118.

61- Goetze, A. M.; Liu, Y. D.; Zhang, Z.; Shah, B.; Lee, E.; Bondarenko, P. V.; Flynn, G. C., High-mannose glycans on the Fc region of therapeutic IgG antibodies increase serum clearance in humans. *Glycobiology* **2011,** *21* (7), 949-959.

62- Kilgore, B. R.; Lucka, A. W.; Patel, R.; Andrien, B. A.; Dhume, S. T., Comparability and Monitoring Immunogenic N-linked Oligosaccharides from Recombinant Monoclonal Antibodies from Two Different Cell Lines using HPLC with Fluorescence Detection and Mass Spectrometry. In *Post-translational Modifications of Proteins*, 2008; Vol. 446, pp 333-346.

63- He, X. Z.; Que, A. H.; Mo, J. J., Analysis of charge heterogeneities in mAbs using imaged CE. *ELECTROPHORESIS* **2009,** *30* (5), 714-722.

64- Khawli LA, M. M., Sharifi J, Hu P, Epstein AL., Pharmacokinetic characteristics and biodistribution of radioiodinated chimeric TNT-1, -2, and -3 monoclonal antibodies after chemical modification with biotin. *Cancer Biother Radiopharm* **2002,** *17* (4), 359-70.

65- Harris, R. Heterogeneity of recombinant antibodies: linking structure to function. *Developments in biologicals* **2005,** *122*, 117-27.

66- Hong, G.; Bazin-Redureau, M. I.; Scherrmann, J. M. G., Pharmacokinetics and organ distribution of cationized colchicine-specific IgG and fab fragments in rat. *Journal of Pharmaceutical Sciences* **1999,** *88* (1), 147-153.

67- M Dellian, F. Y., V S Trubetskoy, V P Torchilin and R K Jain, Vascular permeability in a human tumour xenograft: molecular charge dependence. *British Journal of Cancer* **2000,** *82*, 1513–1518.

68- Sosic, Z.; Houde, D.; Blum, A.; Carlage, T.; Lyubarskaya, Y., Application of imaging capillary IEF for characterization and quantitative analysis of recombinant protein charge heterogeneity. *ELECTROPHORESIS* **2008,** *29* (21), 4368-4376.

69- Pezron, I.; Mitra, R.; Pal, D.; Mitra, A. K., Insulin aggregation and asymmetric transport across human bronchial epithelial cell monolayers (Calu-3). *Journal of Pharmaceutical Sciences* **2002,** *91* (4), 1135-1146.

70- Bal, S. M.; Slütter, B.; Verheul, R.; Bouwstra, J. A.; Jiskoot, W., Adjuvanted, antigen loaded N-trimethyl chitosan nanoparticles for nasal and intradermal vaccination: Adjuvant- and site-dependent immunogenicity in mice. *European Journal of Pharmaceutical Sciences* **2012,** *45* (4), 475-481.

71- Ohkuri, T.; Nagatomo, S.; Oda, K.; So, T.; Imoto, T.; Ueda, T., A Protein's Conformational Stability Is an Immunologically Dominant Factor: Evidence That Free-Energy Barriers for Protein Unfolding Limit the Immunogenicity of Foreign Proteins. *The Journal of Immunology* **2010,** *185* (7), 4199-4205.

72- Johnson, R.; Jiskoot, W., Models for evaluation of relative immunogenic potential of protein particles in biopharmaceutical protein formulations. *Journal of Pharmaceutical Sciences* **2012,** *101* (10), 3586-3592.

73- Rosenberg, A. S.; Verthelyi, D.; Cherney, B. W., Managing uncertainty: A perspective on risk pertaining to product quality attributes as they bear on immunogenicity of therapeutic proteins. *Journal of Pharmaceutical Sciences* **2012,** *101* (10), 3560-3567.

74- Pure Red-Cell Aplasia and Recombinant Erythropoietin. *New England Journal of Medicine* **2002,** *346* (20), 1584-1586.

75- Boven, K.; Knight, J.; Bader, F.; Rossert, J.; Eckardt, K.-U.; Casadevall, N., Epoetin-associated pure red cell aplasia in patients with chronic kidney disease: solving the mystery. *Nephrology Dialysis Transplantation* **2005,** *20* (suppl 3), iii33-iii40.

76- Seidl, A.; Hainzl, O.; Richter, M.; Fischer, R.; Böhm, S.; Deutel, B.; Hartinger, M.; Windisch, J.; Casadevall, N.; London, G.; Macdougall, I., Tungsten-Induced Denaturation and Aggregation of Epoetin Alfa During Primary Packaging as a Cause of Immunogenicity. *Pharmaceutical Research* **2012,** *29* (6), 1454-1467.

77- Relationship between biopharmaceutical immunogenicity of epoetin alfa and pure red cell aplasia. *Current Medical Research and Opinion* **2003,** *19* (5), 433-434.

78- Schellekens, H., How to predict and prevent the immunogenicity of therapeutic proteins. In *Biotechnology Annual Review*, El-Gewely, M. R., Ed. Elsevier: 2008; Vol. Volume 14, pp 191-202.

79- Chung, C. H.; Mirakhur, B.; Chan, E.; Le, Q.-T.; Berlin, J.; Morse, M.; Murphy, B. A.; Satinover, S. M.; Hosen, J.; Mauro, D.; Slebos, R. J.; Zhou, Q.; Gold, D.; Hatley, T.; Hicklin, D. J.; Platts-Mills, T. A. E., Cetuximab-Induced Anaphylaxis and IgE Specific for Galactose-α-1,3-Galactose. *New England Journal of Medicine* **2008,** *358* (11), 1109-1117.

80- Schoenecker, J.; Hauck, R.; Mercer, M.; Parker, W.; Lawson, J., Exposure to Topical Bovine Thrombin During Surgery Elicits a Response Against the Xenogeneic Carbohydrate Galactose α1-3Galactose. *Journal of Clinical Immunology* **2000,** *20* (6), 434-444.

81- Hokke, C. H.; Bergwerff, A. A.; van Dedem, G. W. K.; van Oostrum, J.; Kamerling, J. P.; Vliegenthart, J. F. G., Sialylated carbohydrate chains of recombinant human glycoproteins expressed in Chinese hamster ovary

cells contain traces of N-glycolylneuraminic acid. *FEBS Letters* **1990,** *275* (1–2), 9-14.

82- Darius Ghaderi, R. E. T., Vered Padler-Karavani,Sandra Diaz & Ajit Varki, Implications of the presence of N-glycolylneuraminic acid in recombinant therapeutic glycoproteins. *Nature Biotechnology* **2010,** *28,* 863–867.

83- Runkel, L.; Meier, W.; Pepinsky, R. B.; Karpusas, M.; Whitty, A.; Kimball, K.; Brickelmaier, M.; Muldowney, C.; Jones, W.; Goelz, S., Structural and Functional Differences Between Glycosylated and Non-glycosylated Forms of Human Interferon-β (IFN-β). *Pharmaceutical Research* **1998,** *15* (4), 641-649.

84- Rudick, R. A.; Simonian, N. A.; Alam, J. A.; Campion, M.; Scaramucci, J. O.; Jones, W.; Coats, M. E.; Goodkin, D. E.; Weinstock-Guttman, B.; Herndon, R. M.; Mass, M. K.; Richert, J. R.; Salazar, A. M.; Munschauer, F. E.; Cookfair, D. L.; Simon, J. H.; Jacobs, L. D.; *, T. M. S. C. R. G., Incidence and significance of neutralizing antibodies to interferon beta-1a in multiple sclerosis. *Neurology* **1998,** *50* (5), 1266-1272.

85- Gribben, J. G.; Devereux, S.; Thomas, N. S. B.; Keim, M.; Jones, H. M.; Goldstone, A. H.; Linch, D. C., Development of antibodies to unprotected glycosylation sites on recombinant human GM-CSF. *The Lancet* **1990,** *335* (8687), 434-437.

86- Sahin, E.; Weiss, W. F.; Kroetsch, A. M.; King, K. R.; Kessler, R. K.; Das, T. K.; Roberts, C. J., Aggregation and pH–temperature phase behavior for aggregates of an IgG2 antibody. *Journal of Pharmaceutical Sciences* **2012,** *101* (5), 1678-1687.

87- Thirumangalathu, R.; Krishnan, S.; Ricci, M. S.; Brems, D. N.; Randolph, T. W.; Carpenter, J. F., Silicone oil- and agitation-induced aggregation of a monoclonal antibody in aqueous solution. *Journal of Pharmaceutical Sciences* **2009,** *98* (9), 3167-3181.

88- Cordes, A. A.; Carpenter, J. F.; Randolph, T. W., Accelerated stability studies of abatacept formulations: Comparison of freeze–thawing- and agitation-induced stresses. *Journal of Pharmaceutical Sciences* **2012,** *101* (7), 2307-2315.

89- Braun, A.; Kwee, L.; Labow, M.; Alsenz, J., Protein Aggregates Seem to Play a Key Role Among the Parameters Influencing the Antigenicity of Interferon Alpha (IFN-α) in Normal and Transgenic Mice. *Pharmaceutical Research* **1997,** *14* (10), 1472-1478.

90- Robbins, D. C.; Cooper, S. M.; Fineberg, S. E.; Mead, P. M., Antibodies to Covalent Aggregates of Insulin in Blood of Insulin-Using Diabetic Patients. *Diabetes* **1987,** *36* (7), 838-841.

91- MOORE, W. V.; LEPPERT, P., Role of Aggregated Human Growth Hormone (hGH) in Development of Antibodies to hGH. *Journal of Clinical Endocrinology & Metabolism* **1980,** *51* (4), 691-697.

92- Cleland, J. L.; Powell, M. F.; Shire, S. J., The development of stable protein formulations: a close look at protein aggregation, deamidation, and oxidation. *Critical reviews in therapeutic drug carrier systems* **1993,** *10* (4), 307-377.

93- Wuchner, K.; Büchler, J.; Spycher, R.; Dalmonte, P.; Volkin, D. B., Development of a microflow digital imaging assay to characterize protein particulates during storage of a high concentration IgG1 monoclonal antibody formulation. *Journal of Pharmaceutical Sciences* **2010,** *99* (8), 3343-3361.

94- Jiskoot, W.; Randolph, T. W.; Volkin, D. B.; Middaugh, C. R.; Schöneich, C.; Winter, G.; Friess, W.; Crommelin, D. J. A.; Carpenter, J. F., Protein instability and immunogenicity: Roadblocks to clinical application of injectable protein delivery systems for sustained release. *Journal of Pharmaceutical Sciences* **2012,** *101* (3), 946-954.

95- Geertje J. D. van Mierlo, N. H. P. C., Diana Wouters, Gerrit Jan Wolbink, Margreet H. L. Hart, Theo Rispens, Niels-Christian Ganderup, C. Frieke Kuper, Lucien Aarden, and André H. Penninks, The minipig as an alternative non-rodent model for immunogenicity testing using the TNFα blockers adalimumab and infliximab. *Journal of Immunotoxicology* **2013,** *0* (0), 1-10.

96- Kueltzo, L. A.; Ersoy, B.; Ralston, J. P.; Middaugh, C. R., Derivative absorbance spectroscopy and protein phase diagrams as tools for comprehensive protein characterization: A bGCSF case study. *Journal of Pharmaceutical Sciences* **2003,** *92* (9), 1805-1820.

97- Maddux, N. R.; Joshi, S. B.; Volkin, D. B.; Ralston, J. P.; Middaugh, C. R., Multidimensional methods for the formulation of biopharmaceuticals and vaccines. *Journal of Pharmaceutical Sciences* **2011,** *100* (10), 4171-4197.

98- Kim, J. H.; Iyer, V.; Joshi, S. B.; Volkin, D. B.; Middaugh, C. R., Improved data visualization techniques for analyzing macromolecule structural changes. *Protein Science* **2012,** *21* (10), 1540-1553.

99- Li, C. H.; Nguyen, X.; Narhi, L.; Chemmalil, L.; Towers, E.; Muzammil, S.; Gabrielson, J.; Jiang, Y., Applications of circular dichroism (CD) for structural analysis of proteins: qualification of near- and far-UV CD for protein higher order structural analysis. *Journal of Pharmaceutical Sciences* **2011,** *100* (11), 4642-4654.

100- Amezcua, C. A.; Szabo, C. M., Assessment of higher order structure comparability in therapeutic proteins using nuclear magnetic resonance spectroscopy. *Journal of Pharmaceutical Sciences* **2013,** *102* (6), 1724-1733.

101- Dimitrov, D., Therapeutic Proteins. In *Therapeutic Proteins*, Voynov, V.; Caravella, J. A., Eds. Humana Press: 2012; Vol. 899, pp 1-26.

Chapter 2

An Empirical Phase Diagram Approach to Investigate Conformational Stability of "Second-generation" Functional Mutants of Acidic Fibroblast Growth Factor (FGF-1)

2.1 Introduction

Acidic fibroblast growth factor-1 (FGF-1) is a potent angiogenic factor being investigated as a pro-angiogenic biopharmaceutical drug candidate for treatment of ischemic disease, including wound healing in diabetic ulcers, peripheral artery disease, and non treatable (i.e. ‘‘no option’’) coronary occlusions.[1–4] Significant hurdles, however, remain in the successful realization of FGF-1 as a biopharmaceutical drug, principally related to its intrinsically low thermodynamic stability[5] in conjunction with three reactive cysteine residues (free thiols) buried within the protein interior.[6] These features contribute to irreversible unfolding and aggregation of this 16 kDa protein during production and storage, with associated negative consequences for shelf-life, potency, and immunogenicity.

A substantial number of formulation studies have been performed on FGF-1 with the goal of identifying pharmaceutical excipients that can stabilize the protein during long term storage and administration.[7–9] FGF-1 has significant affinity for polyanions such as heparin/heparan sulfate, which as formulation additives can dramatically stabilize FGF-1 against unfolding by both heat and extremes of pH[10] as well as against metal catalyzed oxidation of free cysteine residues.[7,9] Based on these observations, FGF-1 for human therapeutic use has been formulated with the addition of both heparin and antioxidants. The use of heparin as an excipient, however, adds considerable complexity including

increased expense, its own pharmacological properties (e.g., as an anticoagulant), animal derived material from pig tissues (with potential for infectious contamination), and the possible induction of adverse inflammatory or allergic reactions in a segment of the targeted patient population. Thus, although heparin or related polyanions used as formulation additives solve the FGF-1 stability issue, they introduce other undesirable properties.

An alternative approach to the use of co-solutes to increase protein stability is to directly alter the protein's physical properties by chemical modification or mutagenesis. One approach that has been used to increase the circulating half-life of proteins is ''PEGylation'' [covalent attachment of polyethylene glycol (PEG), a biocompatible polymer]. This increases the molecular mass of a protein and thereby reduces renal clearance (i.e., glomerular filtration of biomolecules is size dependent) and substantially increases the circulating half-life.[11] Furthermore, the attached PEG molecule can mask regions of the protein surface that would otherwise be susceptible to proteolytic attack or immune recognition, increasing the circulating half-life and reducing immunogenicity.[12] PEGylation has either little effect or destabilizes the thermodynamic stability of proteins[13]; thus, the beneficial properties of PEGylation are primarily associated with modulation of renal clearance and reduction of the irreversible pathways associated with degradation and insolubility. One problem with PEGylation is that it can interfere with functional

regions on the protein's surface, reducing receptor/ligand affinity by two or more orders of magnitude.[12,14]

Mutating proteins to improve properties for human therapeutic application is a practical approach since over 30 mutant proteins have been approved for use as human biopharmaceuticals.[15] These include mutations that contribute to increased yields during purification, increased in vivo functional half-life, or improved activity. Examples include mutations of buried free-cysteine residues in beta-interferon (BetaseronVR) and interleukin-2 (ProleukinVR) as well as other mutations hypothesized to increase thermostability. Thus, a mutational approach to improve the physical properties of proteins is a viable route to develop ''second-generation'' protein biopharmaceuticals.

In the present report, mutations are introduced into human FGF-1 with the goal of altering the temperature and pH stability profile to more closely resemble that of FGF-1 in complexation with heparin. These mutations target increases in thermostability as well as a reduction in the number of buried free cysteine residues. Furthermore, these mutations select positions with limited surface accessibility. Using empirical phase diagrams (EPDs) to broadly assess the structural integrity of proteins in response to variations in pH and temperature, mutants of FGF-1 are identified to achieve the design goal of matching, or exceeding, the protective effects of heparin as an additive.[16,17] These mutants

represent potential ‘‘second-generation’’ forms of FGF-1 that may be successfully formulated for use as a human therapeutic in the absence of heparin.

We also take advantage of the revised EPD approach used in this study to compare the relative conformational stability of FGF-1 mutants to assess the value and utility of this multidimensional vector based approach as a novel analytical comparability tool.[18,19] Comparability assessments in biopharmaceutical development are conducted to determine the similarities (and differences) of various preparations of a biopharmaceutical drug used in clinical development in terms of a protein drug's physicochemical properties as they relate to its safety and efficacy.[20,21] Currently, one of the major analytical challenges in this area is to identify new biophysical approaches that complement in vitro/in vivo potency assays to better assess higher order structure and conformational stability of biopharmaceutical drug candidates. Although the series of FGF-1 mutants evaluated in this study are different molecular entities, the updated EPD data analytical approach used in this study could potentially be applied to biopharmaceutical comparability assessments of different preparations of the same protein drug.

2.2 Experimental section

2.2.1 Materials

Recombinant FGF-1 proteins (WT and mutants, except for Symfoil-4P) utilized a synthetic gene for the 140 amino acid form of human FGF-1[40–43] containing an additional amino-terminal six His tag as previously described.[44] The design strategy of the Symfoil-4P mutant used complete gene synthesis and was reported previously.[26] The FGF-1 protein mutants used in this study are listed in Table I. The QuikChange ™ site directed mutagenesis protocol (Agilent Technologies, Santa Clara, CA) was used to introduce all point mutations and was confirmed by nucleic acid sequence analysis (Biomolecular Analysis Synthesis and Sequencing Laboratory, Florida State University). All expression and purification protocols followed previously published procedures involving sequential chromatographic steps using Ni-NTA resin and heparin Sepharose CL-6B affinity resin.[44] Three of the mutant proteins, SYM6ΔΔ/K12V/P134V, SYM10ΔΔ (=SYM7ΔΔ/K12V/P134V/H93G) and Symfoil-4P, which have no affinity for heparin, were purified by Ni-NTA chelation and Superdex 75 size exclusion chromatography as reported previously.[6,26] The purified protein in each case was exchanged into 50 mM sodium phosphate, 0.1 M NaCl, 10 mM ammonium sulfate, 2 mM dithiothreitol (DTT), and pH 7.5 (‘‘crystallization buffer’’). The purified A66C mutant protein contains a mixture of reduced and oxidized forms. To isolate the fully oxidized form of A66C, the purified protein

was exchanged into crystallization buffer without DTT and subsequently air oxidized at room temperature for 3 weeks. An extinction coefficient of E280 nm (0.1%, 1 cm) =1.26 [7,45] was used to determine protein concentration for FGF-1 with the exception of C83T/C117V/L44F/ F132W, SYM6ΔΔ/K12V/P134V, SYM10ΔΔ, and Symfoil- 4P. Due to the variation in number of Trp and Tyr residues in these mutants, the extinction coefficient was determined by the method of Gill and von Hippel or densitometry analysis as reported previously.[6,10,11] The resulting E280 nm (0.1%, 1 cm) values utilized were: C83T/C117V/L44F/F132W, 1.58; SYM6ΔΔ/K12V/P134V and SYM10ΔΔ, 1.31; Symfoil-4P, 0.32.

Heparin sodium salt, grade 1-A from porcine intestinal mucosa, was purchased from Sigma–Aldrich (St. Louis, MO). All other chemicals were purchased from Sigma–Aldrich (St. Louis, MO) or Fisher Scientific (Pittsburg, PA).

2.2.2 Methods

2.2.2.1 Sample preparation

The purified FGF-1 proteins (WT and mutants) were dialyzed against 20 mM citrate-phosphate buffers at pH 3–8 and adjusted to an ionic strength of 0.15 M with NaCl, using a 3.5 kDa molecular-weight cutoff (Pierce, Rockford, IL) membrane. The dialysis step was carried out overnight at 4 ^{0}C. A mixture of WT

FGF-1 and heparin was prepared by adding heparin to the protein solution to achieve a 3:1 (w/w) ratio of heparin to protein.

2.2.2.2 Circular dichroism spectroscopy

Far-UV CD spectra were recorded using either a Jasco J-810 (Tokyo, Japan) or Chirascan (Applied Photophysics) instruments, both equipped with a peltier type temperature controller. The protein concentration used was 0.2 mg/mL using a 0.1 cm path length quartz cuvette in a total volume of 0.2 mL. Full CD spectra were collected before and after temperature ramping at 10 ^{0}C for wavelengths ranging from 260 to 200 nm with a resolution of 0.2 nm and a bandwidth of 1 nm over the pH range 3–8 at one unit intervals. The CD signal intensity changes at 228 nm were followed as the temperature was raised from 10 to 90 ^{0}C at 2.5 ^{0}C intervals with a scanning speed of 15 ^{0}C/h and 5 min equilibration time at each temperature.

2.2.2.3 Intrinsic fluorescence spectroscopy and static light scattering (SLS)

Intrinsic fluorescence measurements were recorded using a two-channel, four positions PTI Quantum Master fluorometer (Brunswick, New Jersey) equipped with a peltier temperature controlled cell holder. Spectra were obtained using excitation at 280 nm with emission spectra recorded between 290 and 390 nm at a resolution of 1 nm. Spectra were also obtained from 10 to 90 ^{0}C at 2.5 ^{0}C

intervals in a 0.2 cm path length rectangular reduced volume cuvette containing 0.2 mL protein solution. Buffer spectra were collected and subtracted from protein samples. Fluorescence emission peak positions and intensities were determined by a ‘‘dpoly’’ method using Origin 7.0 software. SLS intensity for the same sample was followed by using a right angle detector located 180^0 relative to the other detector, and the peak intensity change at 280 nm was followed as the temperature was raised.

2.2.2.4 Extrinsic fluorescence spectroscopy

Measurements were performed using ANS to detect exposure of apolar regions of the protein as the temperature was increased. A protein concentration of 0.08 mg/ mL was used, and ANS was added to the protein solution to achieve an optimal ANS: protein molar ratio of 10:1. The resulting mixture was excited at 374 nm, and the emission spectra were recorded from 400 to 600 nm with a resolution of 1 nm.

2.2.2.5 Empirical phase diagrams

EPDs are designed to summarize and visualize physical characterization data as a colored diagram with two-dimensional axes of environmental stress conditions such as temperature and pH. The theory and calculation procedures to create EPDs are described in detail elsewhere.[16,17] The EPDs of FGF-1 and its

mutants were constructed based on the following biophysical measurements: intrinsic fluorescence intensity ratio at two wavelengths (I305/I330 nm), intrinsic fluorescence peak intensity, CD at 228nm, SLS and ANS fluorescence intensity at 480nm. Complete data sets are presented in Supporting Information section. Data from the individual biophysical measurements (except for the I305/I330 nm fluorescence intensity ratio) were normalized as described previously.[16,17] All calculations were performed using MATLAB software (The Mathworks Inc., Natick, MA).

Two revisions of the data analysis methodologies are used in this work to improve the ability of EPDs to compare the conformational stability profiles of the FGF-1 mutants. First, the EPD data analysis technique was extended to better pursue direct color comparison of EPDs from multiple samples. Previously, regions of color transition, but not the color itself, have been compared between EPDs. Similar colors in different EPDs could not be interpreted, even if proteins had similar conformational states, because each EPD was generated separately using an arbitrary RGB color mapping scheme. In contrast, the colors of EPDs made with the revised methodology can be directly compared with each other, assuming the meaning of the results from the different biophysical measurements is consistent between different samples. In brief, experimental data sets are represented as n-dimensional vectors where n refers to the number of experiment techniques (five in this case). The condition space of the original EPD method

consists of two environmental conditions (typically temperature and solution pH) whereas in this revised version the space is extended to incorporate multiple samples. Therefore, a sample condition space is defined with three components: sample, temperature, and solution pH. For a total of m conditions (=number of samples x number of temperature measurements x number of pH measurements), singular value decomposition of the m x n experimental data matrix is calculated to extract three orthogonal basis vectors associated with the three largest singular values, which are then mapped to RGB colors and visualized as EPDs.

The EPDs generated in this way are considered to display similar conformational behaviors across the different proteins based on an assumption that the collected experimental data represents similar physical behavior. If, however, the same data values represent different conformational states, these proteins are not processed together to generate EPDs for comparison purposes. For this reason, we divided WT FGF1 with and without heparin, as well as the 10 mutants into two groups (I and II) to generate EPDs (Table I), due to the significant differences in their intrinsic fluorescence behavior (see Supporting Information). This evaluation was done manually by visual assessment of the fluorescence data from each protein. Group I proteins include WT FGF-1 (A), WT FGF-1 with heparin (B), and the mutants L26D/ H93G (C), C83T/C117V/K12V (D), P134V/C117V (E), K12V/C117V (F), A66C (G), and K12V/C117V/P134V (H). Group II proteins include C83T/C117V/L44F/ F132W

(I), SYM6ΔΔ/K12V/P134V (J), Symfoil-4P (K), and SYM10ΔΔ (L). Mutants in Group I contain a single Trp residue which is quenched in the protein's native state. Mutants in Group II contain either an unquenched Trp residue in the native state or do not contain a Trp residue. These differences lead to different fluorescence peak positions and intensities and the data sets cannot be directly compared. In summary for this work, the EPDs for FGF-1 proteins in each group (I and II) were created together as can be seen in Figures 5 and 6, respectively; therefore, the colors of EPDs should be compared directly within these two groups but not between the two groups.

The second revision implemented with the EPD methodology is the application of mathematical clustering analysis to computationally identify regions of structural transitions (e.g., color changes). Previously, structural transitions in the EPDs were estimated by visual inspection of the EPD with comparisons to the individual biophysical data sets. The subtle or gradual change in colors often presented in the EPD, however, makes the location of the transitions difficult to be determined visually. Therefore, clustering analysis that utilizes the same m x n experimental data matrix as the EPD can provide complementary information for structural transitions.

In this research, k-means clustering algorithm was chosen for the clustering analysis and implemented using a MATLAB toolbox downloaded from

http://www.dcorney.com/ClusteringMatlab.html. The performance of various clustering algorithms will be the subject of future work.

k-Means clustering is a mathematical procedure in which a number (m) of experimental observations are partitioned into k groups or clusters. Clusters are based on the proximity of observations to proximate means. Observations are defined as n-dimensional vectors (a1, a2, . . ., an). The method then partitions m observations into k-sets (k < n) P ¼ [P1, P2, . . .Pk] to minimize the ‘‘within-cluster sum of squares’’. More formally:

$$\arg\min \sum_{i=1}^{k} \sum_{aj \in Pi} \|aj - \mu i\|^2$$

in which μi is the mean of point in Pi.

The number of clusters (k) is determined after several diagnostic runs with various integral numbers. Generally, k = 2–5 works well for protein characterization data because k should, to a first approximation, correspond to the number of conformational states portrayed in the EPD. When constructing an EPD, the clustering results are used to draw the boundary between different clusters. The clustering results identify regions of conformational changes in FGF-1 mutants (due to environmental stresses such as temperature and pH), and

help to identify and compare regions displaying native state behaviors, and can be used to compare mutant FGF-1 proteins across the two groups, even though the two groups of EPDs display two different color sets.

2.3 Results

2.3.1 Selection of FGF-1 mutants

A combination of wild-type (WT) and 10 different FGF-1 mutants were chosen for analysis in this study. The mutant proteins were developed via a series of protein stability and folding studies with FGF-1 and were identified experimentally as having enhanced stability, functional half-life, or mitogenic activity.[6,22–28] The previously described thermodynamic stability properties and available in vitro mitogenic activity as well as in vivo half-life values are summarized in Table I. The rationale used for the selection of mutants examined in this study is based on the results in Table I (WT FGF-1 and mutants are labeled A–L). For example, the L26D/H93G (C) mutant (developed as part of a study evaluating the effect of the consensus β-turn motif Asx-Pro-Asx-Gly on FGF-1 stability and folding [28]) combines a destabilizing mutation (L26D), and an essentially off-setting stabilizing mutation (H93G), resulting in the overall thermostability essentially unchanged in comparison to WT FGF-1 (A) ($\Delta\Delta G$ = 0.9 kJ/mol, calculated based on differential scanning calorimetry). This mutant is therefore a thermostability control for the EPD analysis. Two of the FGF-1

mutants [SYM6ΔΔ/ K12V/P134V (J) and SYM10ΔΔ (L)] were selected to evaluate the effect of significantly elevated thermostability. These mutants (developed to test the effect of symmetry on FGF-1 protein folding and design [22,29]) exhibit diminished mitogenic activity towards 3T3 fibroblasts, which is postulated to be due to an effect of enhanced stability which prevents structure (dynamic) changes essential to the formation of receptor complexes.[29] Alternatively, the P134V/C117V (E) mutant has enhanced stability (ΔΔG = - 9.3 kJ/mol) yet exhibits similar mitogenic activity in comparison to WT FGF-1 (A). Other examples include K12V/C117V (F) and K12V/C117V/ P134V (H) which are stabilizing mutations that, in the absence of heparin, achieve similar mitogenic potency to that of WT formulated in the presence of heparin (mutants E, F, and H were designed to stabilize N- and C-termini β-strand interactions, a region of known structural weakness within FGF- 1 [24]) The mutants C83T/C117V/K12V (D), C83T/ C117V/L44F/F132W (I), and oxidized A66C (G) have eliminated one or more free thiols, in comparison to WT FGF-1 (A). These mutations substantially increase their in vitro functional half-life with varying effects on thermostability (by mutating exclusively at solvent-inaccessible positions, thereby limiting immunogenic potential [6,27]). Finally, Symfoil-4P (K), a synthetic ultra stable β-trefoil protein (designed as a hyperthermophile, purely symmetric polypeptide [26,29]), was selected to evaluate its EPD profile in the context of its use as a nonfunctional protein engineering ‘‘scaffold.’’[26] For the biophysical

characterization work performed in this study, the FGF-1 mutants in Table I were subdivided into two groups (I and II) due to the significant differences in their intrinsic fluorescence behavior (see ‘‘Methods section’’).

Due to the large amount of biophysical stability data generated in this work for WT FGF-1, both with and without heparin, as well as the 10 mutants of FGF-1, one mutant [K12V/C117V/P134V or (H) in Table I] was selected as an example to be compared with WT FGF-1 with heparin (B in Table I) and without heparin (A in Table I) in the main text. The data generated in this study for the other nine FGF- 1 mutants are provided in Supporting Information. The biophysical characterization of WT FGF-1 in the presence and absence of heparin by the original EPD methodology has been determined previously,[10] but was repeated in this work to provide a direct comparison to the FGF-1 mutants, especially in terms of evaluating of stability profiles using the revised EPD methodology.

2.3.2 Biophysical measurements of FGF-1 and mutants

2.3.2.1 Circular dichroism

Far-ultraviolet (UV) circular dichroism (CD) analysis was used to characterize the secondary (and tertiary) structure of WT FGF-1 (A in Table I), WT FGF-1 with heparin (B in Table I), and 10 mutants of FGF-1 (C-L in Table I). The mutant K12V/C117V/P134V was selected as an example to represent CD

spectra at different solution pH values (pH 3–8) at 10 ^{0}C (Fig. 1A). The CD spectra of K12V/C117V/P134V from pH 4 to 8 are similar in nature, with a broad positive peak at around 228 nm and a strong negative peak near 205 nm. The negative peak near 205 nm is consistent with the expected class II β-protein structure.[5,30] The positive band at 228 nm is presumably a combination of contributions from β-turns, loops and aromatic side chains [31–33] and is potentially tertiary structure sensitive. At pH 3, the positive peak at 228 nm is greatly diminished, which suggests an alteration of protein tertiary structure under acidic conditions. Because significant secondary structure still appears preserved, this suggests the possible preserve of a molten globule state.[34,35] WT FGF-1 (with and without heparin) display similar CD spectra from pH 5 to 8 with a positive peak at 228 nm and a negative peak at 205 nm (Supporting Information Figs. 1A and 2A). For WT FGF-1 without heparin at pH 3 as well as WT FGF-1 with heparin at pH 3–4, the CD spectra show a negative peak broadened toward 215 nm, which could be explained by the formation of intermolecular β-sheet structure.[5–7,9] At pH 4, WT FGF-1 without heparin shows a CD spectrum similar to K12V/ C117V/P134V at pH 3, with only a negative peak at 205 nm (Supporting Information Fig. 1A).

To monitor structural changes of the proteins, CD signals at 228 nm were collected as a function of temperature from 10 to 90 ^{0}C. At elevated temperature, the positive peak diminished under all pH conditions examined, whereas the

negative peak shifted toward 215 nm (data not shown). As a result, at pH 5–8, the CD signals at 228 nm decreased from positive to negative as the temperature increased, as shown in Figure 1C for mutant K12V/C117V/P134V, Figure 1B for WT FGF-1, and Figure 1D for WT FGF-1 with heparin. This structural transition occurs between 40 and 50 ^{0}C for WT FGF-1, 50–60 ^{0}C for K12V/C117V/P134V and 60–70 ^{0}C for WT FGF-1in the presence of heparin. Thus, K12V/C117V/ P134V shows a significantly higher thermal stability than WT FGF-1, although it is still less stable than WT FGF-1 with heparin.

The CD thermal transitions monitored at 228 nm at pH 3–4 are different when comparing K12V/ C117V/P134V, WT FGF-1, and WT FGF-1 with heparin, for example, for K12V/C117V/P134V at pH 4, the CD signal at 228 nm shows a similar positive to negative transition as pH 5–8, albeit at lower temperature (30 ^{0}C). In contrast, the CD signal at 228 nm for K12V/C117V/P134V at pH 3 does not show a major structural transition. Similarly, WT FGF-1 at pH 3–4 does not show any significant structural transitions. In contrast, WT FGF-1 with heparin at pH 3–4 shows a transition from negative to less negative ellipticity, probably due to the precipitation of protein out of solution.

2.3.2.2 Intrinsic fluorescence spectroscopy

Intrinsic fluorescence spectra were used to monitor the tertiary structure of WT FGF-1 (with and without heparin) as well as the 10 FGF-1 mutants. Because the WT FGF-1 contains eight Tyr and a single Trp residue quenched in the native state, the proteins were excited at 280 nm to simultaneously collect fluorescence from both Tyrosine and Trp residues. The intrinsic fluorescence spectra of K12V/C117V/P134V at 10 ^{0}C are displayed in Figure 2A. The spectra from the mutant at pH 5–8 have a single peak at 305 nm, which corresponds to the emission of Tyr residues. In contrast, the spectra at pH 3 show a major peak at 305 nm, but a significant broad shoulder at 340 nm, which corresponds to the emission of the previously quenched Trp residues. Trp fluorescence is not observed at pH 5–8 because when the protein is properly folded at near neutral pH conditions, the fluorescence of the single Trp residue is quenched by positive charges from neighboring His and Lys residues.[5,36] At pH 3, the structure of WT FGF-1 is altered, and the nearby His and Lys side chains are moved away from the indole ring of Trp, resulting in dequenching of Trp fluorescence. The intrinsic fluorescence spectrum of the K12V/ C117V/P134V mutant at pH 4 show intermediate behavior compared with pH 3 and 5–8. The intrinsic fluorescence spectra of WT FGF-1 and WT FGF-1 with heparin at 10 ^{0}C are shown in Supporting Information Figures 1C and 2C, respectively. The fluorescence spectra for WT FGF-1 both with and without heparin at pH 3–4 is composed of

contributions from Trp and Tyr, whereas Tyr contributions dominate as described above for pH 5–8.

The ratio of the fluorescence intensity at 305 nm and 330 nm (I305/I330) has been shown to sensitively monitor the change in FGF-1 tertiary structure as a function of pH or temperature.[10] A higher value (~ 3) of I305/I330 for proteins in Group I (see Table I) indicates a more native-like, properly folded structure, whereas a lower value (~1) indicates altered structure. Thus, intrinsic fluorescence spectra were obtained from 10 to 90 ^{0}C at 2.5 ^{0}C intervals and I305/I330 values were calculated and plotted as a function of temperature to monitor changes in tertiary structure for the K12V/C117V/P134V mutant and WT FGF-1 with and without heparin (Fig. 2B–D).

As shown in Figure 2B for the K12V/C117V/ P134V mutant at pH 3, the fluorescence intensity ratio started at ~1 and increased gradually as the temperature was increased, without any obvious structural transition, indicating that the higher order structure is already altered at pH 3 at 10 ^{0}C. In contrast, the fluorescence intensity ratio for pH 5–8 started at about 3 and then decreased to ~0.7. The fluorescence intensity ratio for the mutant at pH 4 is between the values observed at pH 3 and pH 5–8 (starting at ~2 and decreasing to ~1.1 between 25 and 40 ^{0}C). The thermal transitions for the mutant occurred between 20 and 55 ^{0}C for pH 4–7, with an apparent bi-phasic transition observed between pH 5 and 8. The first transition is more gradual than the second phase. For WT FGF-1 with

and without heparin, the fluorescence intensity ratio at both pH 3 and 4 shows no obvious structural transitions, indicating the expected structural alterations in WT FGF-1 at both pH values. In contrast, for pH 5–8, the ratio quickly decreased from 3 to ~0.7. By comparing the temperature at the completion of this structural transition for pH 5–8, the transition ended at ~45 ^{0}C for WT FGF-1, ~55 ^{0}C for the K12V/ C117V/P134V, and about 60 ^{0}C for WT FGF-1 with heparin.

For FGF-1 mutant proteins in Group II (see Table I), however, the ratio of the fluorescence intensity at 305 nm and 330 nm (I305/I330) has a different biophysical meaning because these mutants contain either an unquenched or missing Trp residue. Both a His and Lys residue, which quench the Trp residue in WT FGF, were deleted from SYM6ΔΔ/K12V/ P134V (J in Table I) and SYM10ΔΔ (L in Table I). Thus, the I305/I330 value is close to 1 even in the native state of protein (Supporting Information Figs. 4F and 5F). In contrast, C83T/C117V/L44F/F132W (I in Table I) has one extra Trp residue, which is not quenched in the native state. As a result, the I305/ I330 value is below 1 across the temperature range from pH 3 to 8 (Supporting Information Fig. 8F). In the case of Symfoil-4P (K in Table I), the protein contains no Trp residues but does have three Tyr residues, so the I305/I330 value is above 3 up to 70– 80 ^{0}C (Supporting Information Fig. 6F). Due to the difference of I305/I330 values in the native state, Symfoil-4P (K in Table I) has a different color scheme in the EPDs

(discussed below in Fig. 6) even in the low temperature region compared with the other mutants in Group II.

2.3.2.3 1-Anilino-8-naphthalnesulfonate fluorescence

1-Anilino-8-naphthalnesulfonate (ANS) has been extensively used to detect the exposure of apolar binding sites on the surface of proteins and to detect the presence of molten globule-like states.[30, 37, 38] At pH 3 and 4, substantial ANS fluorescence was observed for K12V/C117V/P134V (Fig. 3A), WT FGF-1 (Supporting Information Fig. 1H), and WT FGF-1 with heparin (Supporting Information Fig. 2H) at 10 ^{0}C. Above pH 5, however, much less fluorescence is observed in the presence of these samples at 10 ^{0}C. Thus, ANS fluorescence spectra indicate that the tertiary structure of FGF-1 is altered in acidic condition even at low temperature, consistent with CD and intrinsic fluorescence results.

The ANS fluorescence intensity at 480 nm was monitored from 10 to 90 ^{0}C at 2.5 ^{0}C intervals. K12V/ C117V/P134V manifested an increase in ANS fluorescence intensity at ~40 ^{0}C for pH 5 and ~50 ^{0}C at higher pH values (Fig. 3B). As shown in Figure 3C, at pH 5–8, WT FGF-1 shows an increase in ANS fluorescence intensity starting at 20 ^{0}C. By including heparin with WT FGF-1, the onset temperature of ANS binding was delayed to 55 ^{0}C for pH 5–8 (Fig. 3D). At pH 3–4, the major trend is a decrease in ANS fluorescence intensity as temperature increases for all three proteins. At pH 4, the K12V/C117V/ P134V

mutant shows slightly more neutral pH-like structural transitions (compared with WT FGF-1 with and without heparin), probably because the K12V/C117V/P134V mutant has more native-like structure at pH 4.

2.3.2.4 Static light scattering

Both acidic pH conditions and elevated temperatures cause aggregation/precipitation of WT FGF-1.[2, 3] Due to the low protein concentration used during dialysis, however, no gross precipitation was observed after dialysis at pH 3–4. The temperature induced aggregation of FGF-1 was followed by the static light scattering (SLS) signal at 280 nm. As shown in Figure 4A, very little scattering was observed at low temperatures for the K12V/C117V/P134V mutant under all pH conditions. An increase in light scattering intensity started at ~45 ^{0}C for pH 5–8 and ~55 ^{0}C for pH 4. No significant aggregation could be detected by light scattering for pH 3 up to 90 ^{0}C. A decrease in light scattering signal was observed for pH 5–8 above ~60 ^{0}C due to the precipitation of protein. For WT FGF-1 at pH 3, light scattering initiated at a higher level than other pH conditions, probably due to acidic buffer induced aggregation, although no obvious visible precipitation was observed. The onset of WT FGF-1 aggregation at pH 4–8 started at ~40 ^{0}C. For WT FGF-1 with heparin, the light scattering signal for both pH 3 and 4 started at higher values than all other pH conditions, immediately followed by a gradual increase and then decrease. This aggregation started at ~45 ^{0}C for pH 5 and ~60 ^{0}C for all other pH values. At a solution pH between 6 and 8,

protein aggregation started at 40 ^{0}C, 45 ^{0}C, and 60 ^{0}C for WT FGF-1, K12V/C117V/P134V, and WT FGF-1 with heparin, respectively. Again, the K12V/C117V/P134V mutant displayed improved stability under acidic conditions.

2.3.2.5 Empirical phase diagrams

The EPD approach has been developed to combine large amounts of data from multiple measurements to evaluate the overall conformational stability of proteins and other macromolecular systems under different environmental stresses.[16, 17, 39] As shown in Figures 5 and 6, EPDs were generated for WT FGF-1 (with and without heparin) and for the 10 different FGF-1 mutants. All of the measurements as a function of temperature and solution pH (as described above and in Supporting Information section) were summarized into RGB color plots in a two-dimensional space of pH and temperature using the revised EPD approach described in ‘‘Method section.’’ As explained in more detail in ‘‘Method section,’’ the EPDs for the FGF-1 mutants were generated in two groups (I and II). Group I (Fig. 5) includes proteins A–H in Table I and Group II (Fig. 6) includes proteins I–L in Table I. Colors can be compared directly within each group. A clustering method was then used to generate three distinct regions for each group of EPDs (not each EPD). The location of boundary of the individual

regions can be used to compare the conformational stability among and between the two groups.

As shown in Figure 5, the EPD for WT FGF-1 (A) has two distinct regions, a blue area (Region 2) and a green area (Region 1). The green region (Region 1) covers the low temperature and neutral pH range, which represents the native, most stable form of the protein. A structural transition occurs at ~44 ^{0}C for pH 6 and 7, which are the most stable pH conditions for WT FGF-1 (A). Although a third light blue region is present around the boundary between Regions 1 and 2, which represents molten globule-like behavior,[34, 35] this subtle color difference was not defined as a separate region by this clustering analysis. On the addition of heparin to WT FGF-1 (B), a third region (pink) appears between Regions 1 and 2 as well as at low temperatures at pH 3 and 4. The formation of this third region is primarily due to the strong negative CD signal at low temperatures for pH 3 and 4 and at high temperatures at pH 5–8 (Fig. 1D). From inspection of the CD spectra of WT FGF-1 with heparin (B) (Supporting Information Fig. 2A), it is apparent that intermolecular β-sheet structure has formed at pH 3 and 4 at 10 ^{0}C and pH 5–8 at higher temperatures. As the temperature increased, protein aggregates started to form as indicated by increased light scattering (Fig. 4C), which is followed by a slight decrease presumably due to precipitation of protein. This third region in the EPD appears to be unique to WT FGF-1 with heparin (B). The structural transition between

Regions 2 and 3 for WT FGF-1 with heparin occurred at 60 ^{0}C, which is about 16 ^{0}C more stable than WT FGF-1 without heparin.

The EPDs for 6 of the FGF-1 mutants are also shown in Figure 5. The EPDs for the mutants show 2 regions (green for Region 1 and blue for Region 2). The K12V/C117V/P134V (H) mutant is most stable at pH 6 and 7, with a transition at 52 ^{0}C, which is ~8 ^{0}C higher than WT FGF-1. At pH 4, structural transitions are present at ~30 ^{0}C, which differs from WT FGF-1 and most of the other mutants where transitions at pH 4 cluster with pH 3. Thus, K12V/ C117V/P134V (H) has enhanced resistance to acidic unfolding. The K12V/C117V (F) mutant is similar to K12V/C117V/P134V (H), except for a lower overall thermal stability (~4 ^{0}C less).

The EPDs for the other four mutants of FGF-1 are shown in Figure 6. The EPDs of C83T/C117V/ L44F/F132W (I), SYM6ΔΔ/K12V/P134V (J), and SYM10ΔΔ (L) have Regions 1 (purple) and 2 (orange). Region 2 is at low temperature and in the neutral pH range. It thus represents the native, stable region. Both SYM6ΔΔ/K12V/P134V (J) and SYM10ΔΔ (L) show a very high degree of enhanced physical stability. In contrast, the EPD of Symfoil-4P (K) manifests a Regions 1 (purple) and 3 (light blue/green) due to the difference in the I305/I330 value, as explained above, where Region 3 represents the native stable region. As expected, SYM10ΔΔ (L) and Symfoil-4P (K), a synthetic ultra stable β-trefoil protein, are the most conformationally stable mutants observed by the

EPD analysis. The EPDs and clustering of the FGF-1 mutants are consistent with the thermodynamic conformational stability data previously obtained for the mutants (see Table I).

2.4 Discussion

The stability of FGF-1 is strongly dependent on complexation with polyanions such as heparin.[7, 8] This stabilization is important endogenously where the biological activity of this (and many other) growth factors requires interaction with polyanionic proteoglycans and protein receptors on the cell surface. In addition, the use of FGF-1 as a therapeutic agent requires the presence of heparin or other polyanions because the protein is unstable during storage and administration in its absence. In this work, we have analyzed a series of FGF-1 mutants with the goal of reducing or eliminating the need for exogenous heparin by enhancing the protein's intrinsic stability. Refer to Table I for the description of each FGF-1 mutant and Figures 5 and 6 for the summary of the biophysical stability results which will be the focus of the rest of this discussion. Rather than the usual reliance on evaluating protein stability from a single, unique biophysical technique (e.g., CD, intrinsic and ANS fluorescence, light scattering, etc.), we have evaluated the protein stability data from multiple experimental methods holistically in the form of a multivariable vector-based approach designated the

EPD to provide a broad picture of the physical behavior of the FGF-1 mutants as a function of temperature and pH.[17]

Increases in stability in this context can be viewed as an expansion of the apparent phase boundaries obtained in the EPD (i.e., the region of abrupt color change). For example, when comparing WT FGF-1 in the absence and presence of heparin, this boundary is moved to significantly higher temperature (Fig. 5) with an accompanying dramatic increase in biological activity (the EC50 is approximately 120 x lower as shown in Table I). Several of the mutants [e.g., Symfoil-4P (K), SYM6ΔΔ/K12V/ P134V (J), and SYM10ΔΔ (L)] display even greater increase in conformational stability, but demonstrate little biological activity. In contrast, a number of the FGF-1 mutants [K12V/C117V (F), C83T/C117V/ L44F/F132W (I), A66C (G), and K12V/C117/P134V (H)] display improved free energies of unfolding relative to WT, major increases in mitogenic activity in the absence of heparin (Table I), with EPDs similar to those of WT in the presence of heparin (Fig. 5). Thus, these FGF-1 mutants seem to be good candidates for future therapeutic applications from a stability and potency point of view.

Because the biophysical data for WT FGF-1(with and without heparin) and the other six mutants (Table I and Fig. 5) were mathematically processed together as the same data set, the colors from these EPDs can be directly compared with each other. Different color regions within the same EPD reflect

different physical states of protein under the indicated pH and temperature condition. Color changes indicate transitions in these states. Note that these are not necessarily thermodynamic states because reversibility between them is frequently not present. To facilitate the visualization of different color regions in EPDs, a clustering method was used to divide each EPD into different regions based on the input data (see below for further discussion).

The FGF-1 mutants in Figure 6 have different fluorescence ratios (I305/I330 nm) in their native states. This effect is due to the deletion of a Lys, and thus the Trp fluorescence in SYM6ΔΔ/K12V/ P134V (J) and SYM10ΔΔ mutants (L) (see Table I) is not quenched in the native state. Thus, the I305/I330 profile for these two mutants is quite different from the others (see Supporting Information Figs. 4F and 5F). C83T/C117V/L44F/F132W (I in Table I) has an additional Trp residue which is not quenched in the native state. Symfoil-4P (L in Table I) does not have any Trp residues. As a result, EPDs for these SYM6ΔΔ/K12V/P134V (J) and SYM10ΔΔ (L) mutants were generated separately (Fig. 6), and their colors are compared with each mutant within this group. Nonetheless, the location of the cluster boundaries for the phase transitions shown in the EPDs for the various mutants can be compared with each other.

FGF-1 is known to form molten globule-like states under conditions of acidic pH as well as at moderately elevated temperatures at higher pH. This molten globule conformation is visually identified as a light blue region between

the dark blue (Region 2) and green (Region 1) areas identified by the clustering boundary for the WT FGF and many of the mutants' EPDs in Figure 5. This observation of the formation of a molten globule state for FGF-1 under environmental stress is consistent with previous work.[10] It should be noted, however, that the clustering methodology used in this work was not able to identify this subtle color change. Thus, the current version of the clustering analysis identifies the transition region between large conformational changes (e.g., between the native and unfolded, aggregated states of the FGF-1 mutants) but is not currently able to consistently identify the more subtle color changes represented by the molten globule state. The clustering methodology used in this work is a prototype version, and by exploring different clustering methods (work in progress), automatic clustering analysis might be able to identify the more subtle color differences (e.g., the molten globule state for FGF-1) that are observed visually by human sight in the future. Nonetheless, this version of the clustering analysis was able to identify several FGF-1 mutants, for example K12V/C117V/ P134V (H), which display an expanded native state (Region 1 in Fig. 5). These FGF-1 mutants are stable, bioactive forms of the growth factor that are not heparin dependent.

A second purpose of this study was to test the ability of EPDs to distinguish the conformational stability of a series of mutant proteins. We have previously successfully utilized the EPD method for the development of stabilized

pharmaceutical formulations of macromolecular systems such as biopharmaceutical drugs and vaccines.[17, 39] Instead of relying on one or only a few biophysical parameters, EPDs use a two-dimensional ‘‘stimulation/response’’ color pattern diagram. As is evident from Figures 5 and 6, both dramatically different and highly similar EPDs are produced with only a few mutational differences between proteins. Thus, this approach offers a unique methodology to compare proteins that is not based on structure alone, but rather uses the way a protein responds to environmental stress (e.g., pH and temperature) as a comparative principle. The EPD approach is not limited to temperature and pH but can also be used to evaluate the effect of protein concentration as well as solute and ionic strength among other solution variables.[17, 39] We have recently shown that use of methods sensitive to the internal motions of proteins (e.g., isotope exchange, ultrasonic spectroscopy, solute spectral quenching, etc.) in the context of EPDs can also provide insight into more dynamic aspects of a protein behavior. Thus, the EPD approach would seem to offer an improved method to analyze the effect of mutation on protein structure.

In addition, it should be possible in the future to evaluate the revised EPD methodology developed in this work to compare stability of different mutants, as a new analytical approach to assess comparability.[18, 19] During the pharmaceutical development of a protein therapeutic drug candidate or vaccine, comparability assessments are performed to determine if a protein’s key physicochemical

properties have changed (or not) across different preparations used during clinical trials. These analytical assessments typically involve a combination of routine quality control tests (e.g., sodium dodecyl sulfate polyacrylamide gel electrophoresis, size exclusion-high performance liquid chromatography, isoelectric focusing, etc.), more sophisticated analysis using mass spectrometry and biophysical methods (e.g., intact MW analysis, peptide and oligosaccharide maps, differential scanning calorimetry, analytical ultracentrifugation, etc.), and stability profiles under accelerated and storage temperature conditions. [20, 21] It has recently been shown that comparison of accelerated temperature stability profiles can be an effective and sensitive way to perform comparability assessments.[20] Because the EPD methodology provides a rapid, high throughput approach to collect and evaluate conformational stability data under accelerated conditions of temperature and pH, this approach could potentially be useful as a comparability assessment tool. The EPD method is currently being evaluated in our laboratories for its utility in examining the conformational stability of different preparations of the same protein with modest changes in post translational modifications (e.g., glycosylation patterns).

In summary, the conformational stability of WT and 10 different FGF-1 mutants was examined as a function of temperature and solution pH by a series of biophysical techniques, and the resulting data sets were analyzed with an EPD methodology. The revised version of the EPD methodology used in this work

resulted in effective and convenient comparisons of the effect of temperature and solution pH on the structural properties of a wide range of FGF-1 mutants. The conformational stability profiles of several of the FGF-1 mutants were comparable to the WT FGF-1 in the presence of heparin. Thus, candidate FGF-1 mutants were identified with enhanced stability profiles in the absence of heparin and can be considered promising second-generation therapeutic FGF-1 candidates. These mutants are currently undergoing preclinical pharmacokinetic studies in animal.

Table 1: Summary of Stability Parameters and Biological Activity Values for WT FGF-1 and 10 FGF-1 Mutants.

FGF-1 protein (reference)	Symbol	ΔΔG (kJ/mol)	EC50 (ng/mL) (-) heparin	EC50 (ng/mL) (+) heparin	Half-life (h)	Heparin Binding
Group I						
WT (without and with heparin)	*A and B*	_	*58.4 ± 25.4*	*0.48 ± 0.08*	*1.0*	*Yes*
L26D/H93G [28]	*C*	*- 0.9*	*N.A.*	*N.A.*	*N.A.*	*Yes*
C83T/C117V/K12V [6]	*D*	*- 1.9*	*0.93 ± 0.25*	*0.36 ± 0.12*	*40.4*	*Yes*
P134V/C117V [24]	*E*	*- 8.8*	*46.8 ± 6.7*	*N.A.*	*N.A.*	*Yes*
K12V/C117V [24]	*F*	*- 9.3*	*4.2 ± 1.7*	*N.A.*	*N.A.*	*Yes*
A66C (oxi) [27, 46]	*G*	*- 10.2*	*5.43 ± 3.96* [46]	*0.36 ± 0.20* [46]	*14.2* [46]	*Yes*
K12V/C117V/P134V [24]	*H*	*- 19.1*	*1.80 ± 0.90*	*N.A.*	*N.A.*	*Yes*
Group II						
C83T/C117V/L44F/F132W [6]	*I*	*- 0.4*	*0.74 ± 0.19*	*0.51 ± 0.15*	*42.6*	*Yes*
SYM6ΔΔ/K12V/P134V [29]	*J*	*- 35.0*	*741 ± 302*	*N.A.*	*N.A.*	*No*
Symfoil-4P [26]	*K*	*- 44.1*	*N.A.*	*N.A.*	*N.A.*	*No*
SYM10ΔΔ [29]	*L*	*-47.0*	*N.D.* [29]	*N.A.*	*N.A.*	*No*

Conformational stability (ΔΔG, calculated based on DSC), mitogenic activity (EC50), and in vivo half values are listed from the references provided. FGF-1 proteins in Group I contain a single Trp residue which is quenched at the native state. FGF-1 proteins in Group II contain either an unquenched Trp residue in the native state or do not contain the Trp residue. N.A., not available; N.D., not detected.

Figure 1

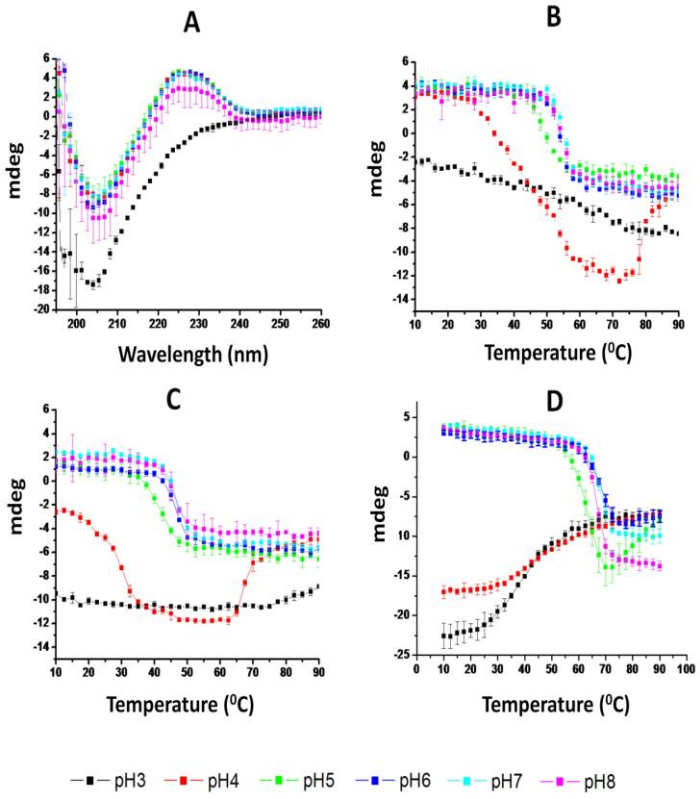

Far UV CD analysis of WT FGF-1 and a representative FGF-1 mutant. (A) CD spectra of the K12V/C117V/P134V mutant measured at 10_C at different pH values. (B–D) CD signal at 228 nm as measured as a function of temperature at indicated pH values for (B) K12V/C117V/P134V, (C) WT FGF-1, and (D) WT FGF-1 with heparin. Data points are an average of two independent analyses. Complete CD data sets for the other nine FGF-1 mutants are provided in Supporting Information section. See Table I for a further description of each mutant including K12V/C117V/P134V (H in Table I).

Figure 2

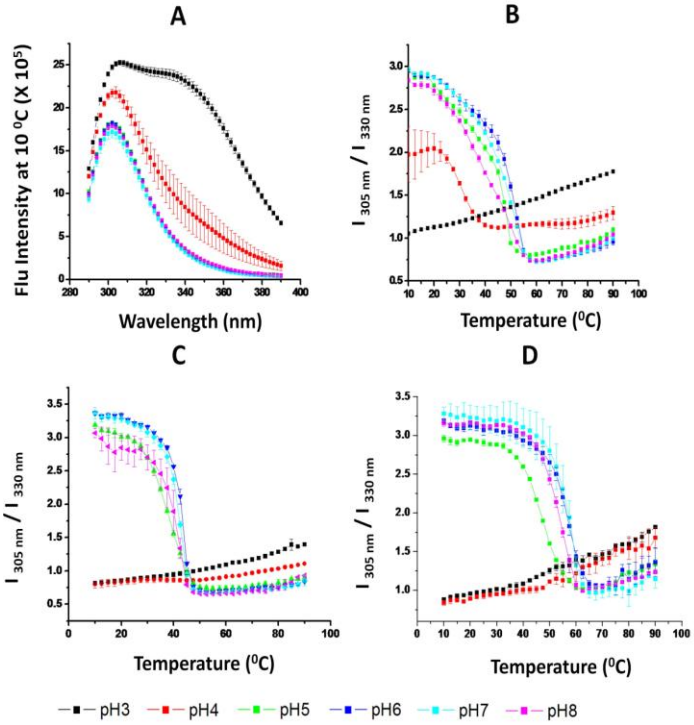

Intrinsic fluorescence analysis of WT FGF-1 and a representative FGF-1 mutant. (A) Fluorescence emission spectra (excited at 280 nm) of the K12V/C117V/P134V mutant measured at 10_C at different pH values. (B–D) Fluorescence intensity ratio (I305/I330) as measured as a function of temperature at indicated pH values for (B) K12V/C117V/P134V, (C) WT FGF-1, and (D) WT FGF-1 with heparin. Data points are an average of two separate experiments. Complete intrinsic fluorescence data sets for other nine FGF-1 mutants are provided in Supporting Information section. See Table I for a further description of each mutant including K12V/C117V/P134V (H in Table I).

Figure 3

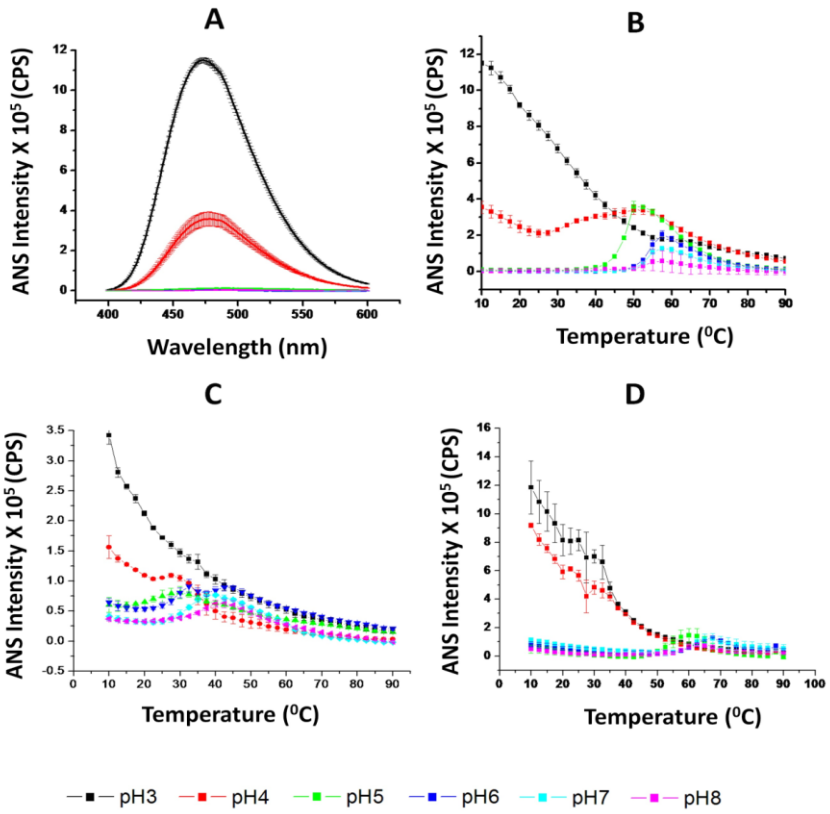

ANS fluorescence analysis of WT FGF-1 and a representative FGF-1 mutant. (A) ANS fluorescence spectra of K12V/C117V/P134V measured at 10_C at different pH values. (B–D) ANS fluorescence intensity ratio as measured as a function of temperature at indicated pH values for (B) K12V/C117V/P134V, (C) WT FGF-1, and (D) WT FGF-1 with heparin. Data points are an average of two independent experiments. The complete ANS fluorescence data sets for the other nine FGF-1 mutants are provided in Supporting Information section. See Table I for a further description of each mutant including K12V/C117V/P134V (H in Table I).

Figure 4

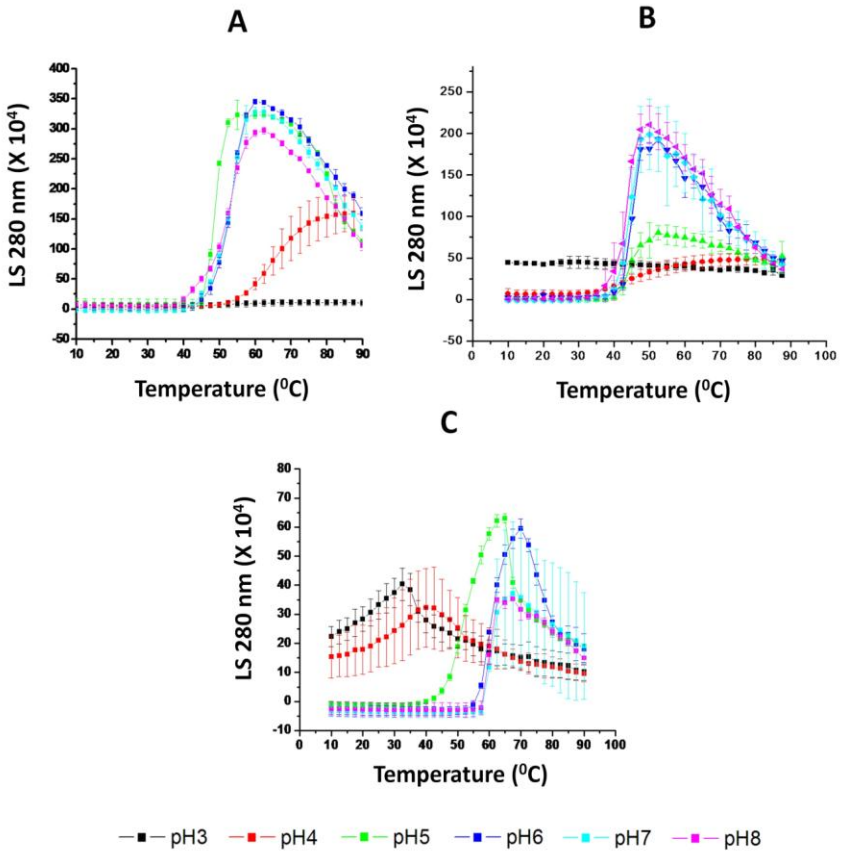

Static light scattering analysis of WT FGF-1 and a representative FGF-1 mutant as a function of temperature at the indicated pH values. (A) K12V/C117V/P134V, (B) WT FGF-1, and (C) WT FGF-1 with heparin. Data points are an average of two independent experiments. The complete static light scattering data set for the other nine FGF-1 mutants is provided in Supporting Information section. See Table I for a further description of each mutant including K12V/C117V/P134V (H in Table I).

Figure 5

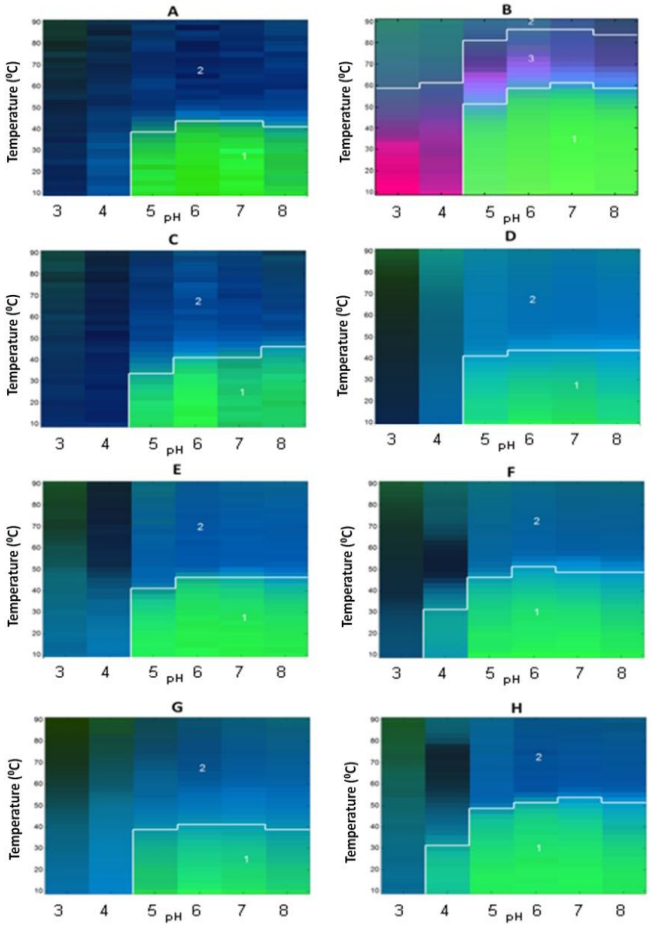

Empirical Phase Diagrams (EPDs) for WT FGF-1 (A), WT FGF-1 with heparin (B), and 6 different FGF-1 mutants without heparin (C–H). The EPDs were constructed based on intrinsic fluorescence intensity ratio at two wavelengths (I305/I330 nm), intrinsic fluorescence intensity, CD at 228 nm, static light scattering (SLS) and ANS fluorescence intensity at 480 nm. All FGF-1 mutants in this Figure contain a single Trp residue which is quenched at the native state.

Figure 6

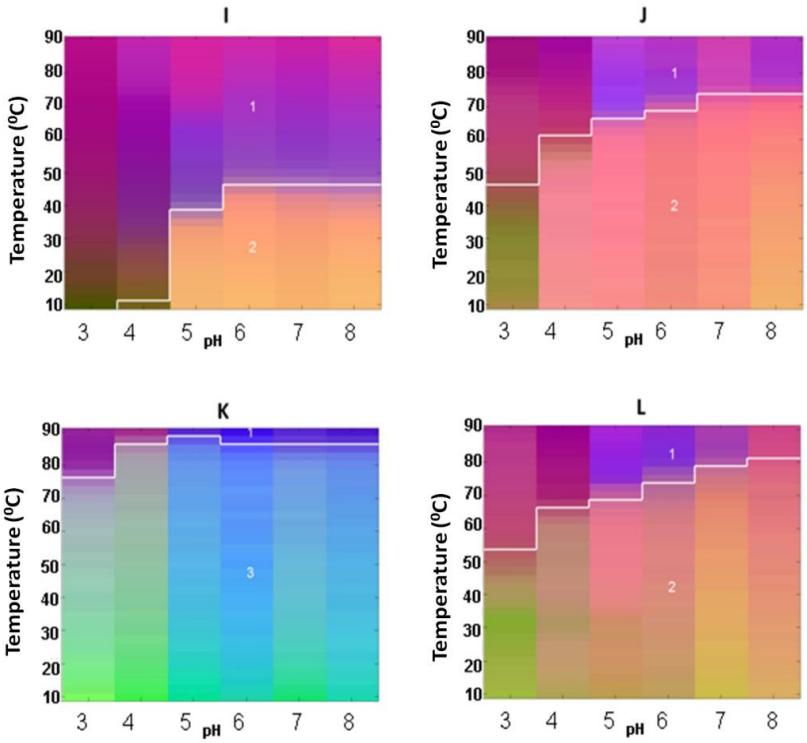

Empirical Phase Diagrams (EPDs) for four different FGF-1 mutants without heparin (I–L). The EPDs were constructed based on intrinsic fluorescence intensity ratio at two wavelengths (I305/I330 nm), intrinsic fluorescence intensity, CD at 228 nm, static light scattering (SLS) and ANS fluorescence intensity at 480 nm. FGF-1 mutants in this Figure contain either an unquenched Trp residue in the native state or do not contain the Trp residue. See Table I for description of each mutant.

Supplemental Figures Legend

Proteins Figures: The following description applies to all FGF1 protein mutants in supplemental figures 1 to 11:

A- Far-UV CD spectra at 10 ^{0}C

B- Far-UV CD signals at 228 nm as a function of temperature.

C- Intrinsic fluorescence spectra at 10 ^{0}C

D- Intrinsic fluorescence intensity change as a function of temperature

E- Intrinsic fluorescence peak position change as a function of temperature

F- Intrinsic fluorescence intensity ratio at 305 and 330 nm (I_{305}/I_{330}) change as a function of temperature

G- Static light scattering intensity change as a function of temperature

H- ANS spectra at 10 ^{0}C

I- ANS fluorescence intensity change as a function of temperature

Within each figure, the following applies, pH 3 (black), pH 4 (red), pH 5 (green), pH 6 (blue), pH 7 (cyan), pH 8 (purple).

Supplementary figure 1: WT FGF-1 data summery.

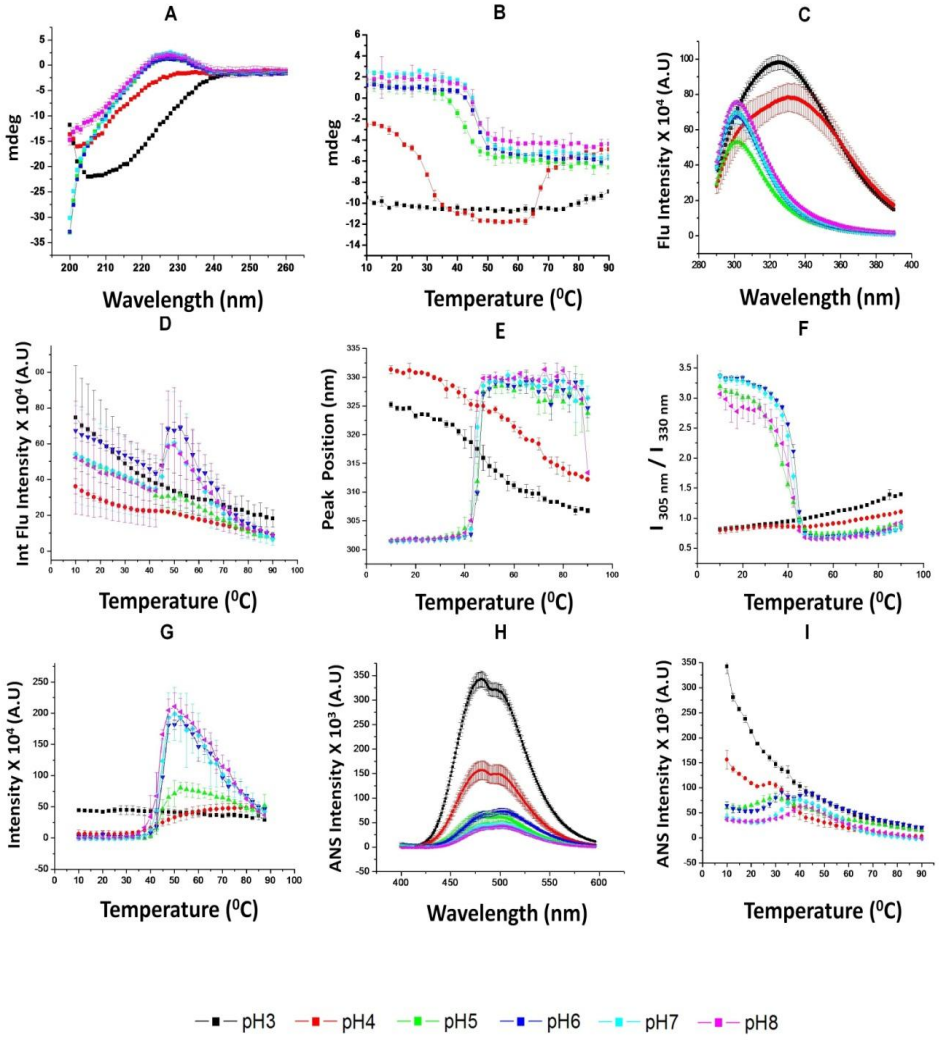

Supplementary figure 2: WT FGF-1 with (3X) Heparin data summery.

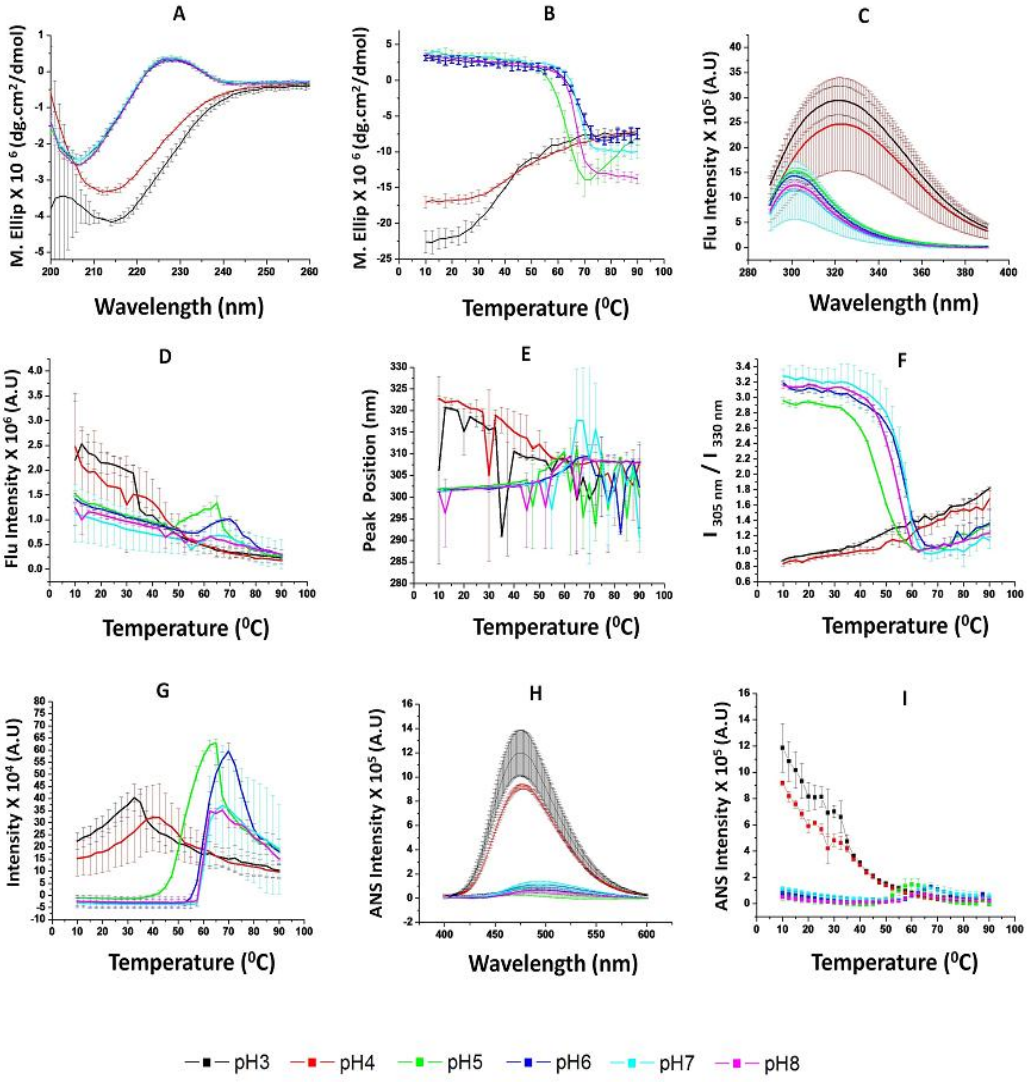

Supplementary figure 3: L26D/H93G FGF-1 data summery.

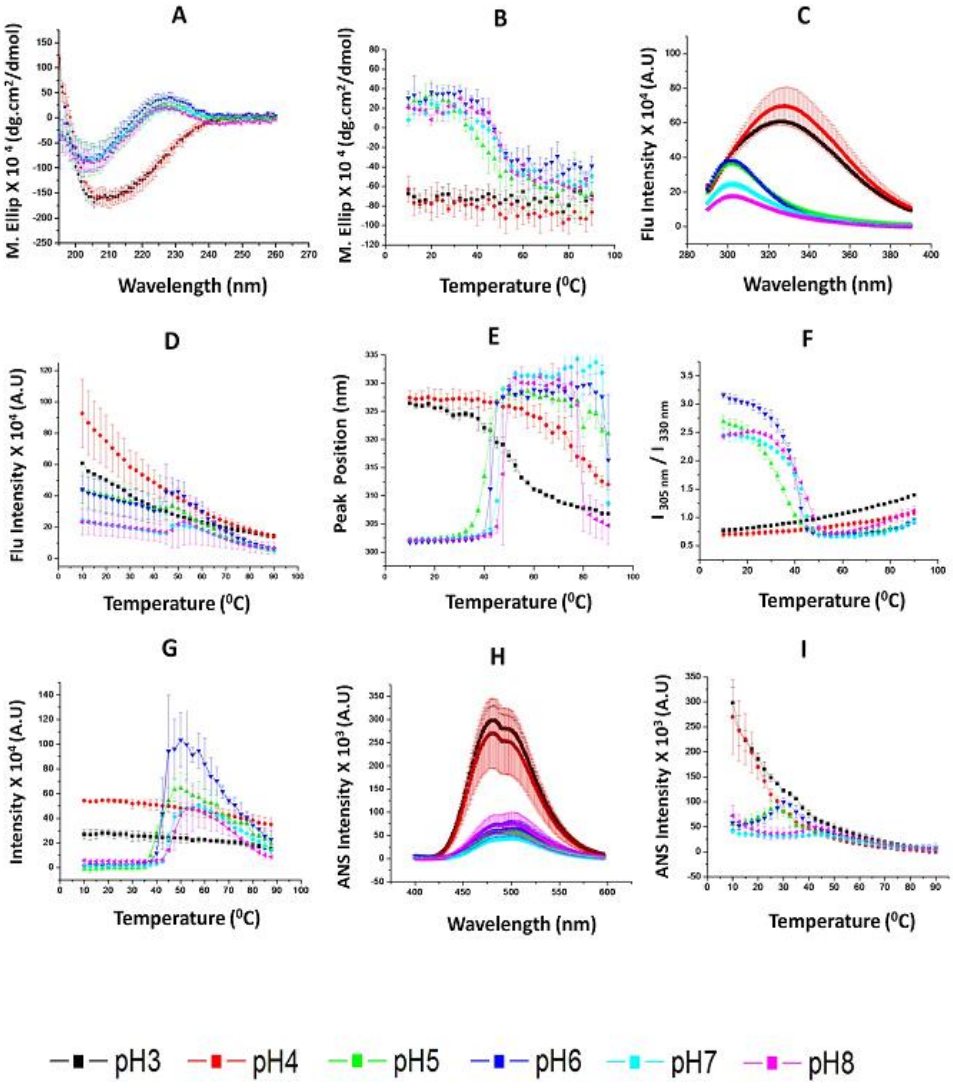

Supplemental figure 4: SYM6ΔΔ/K12V/P134V data summery.

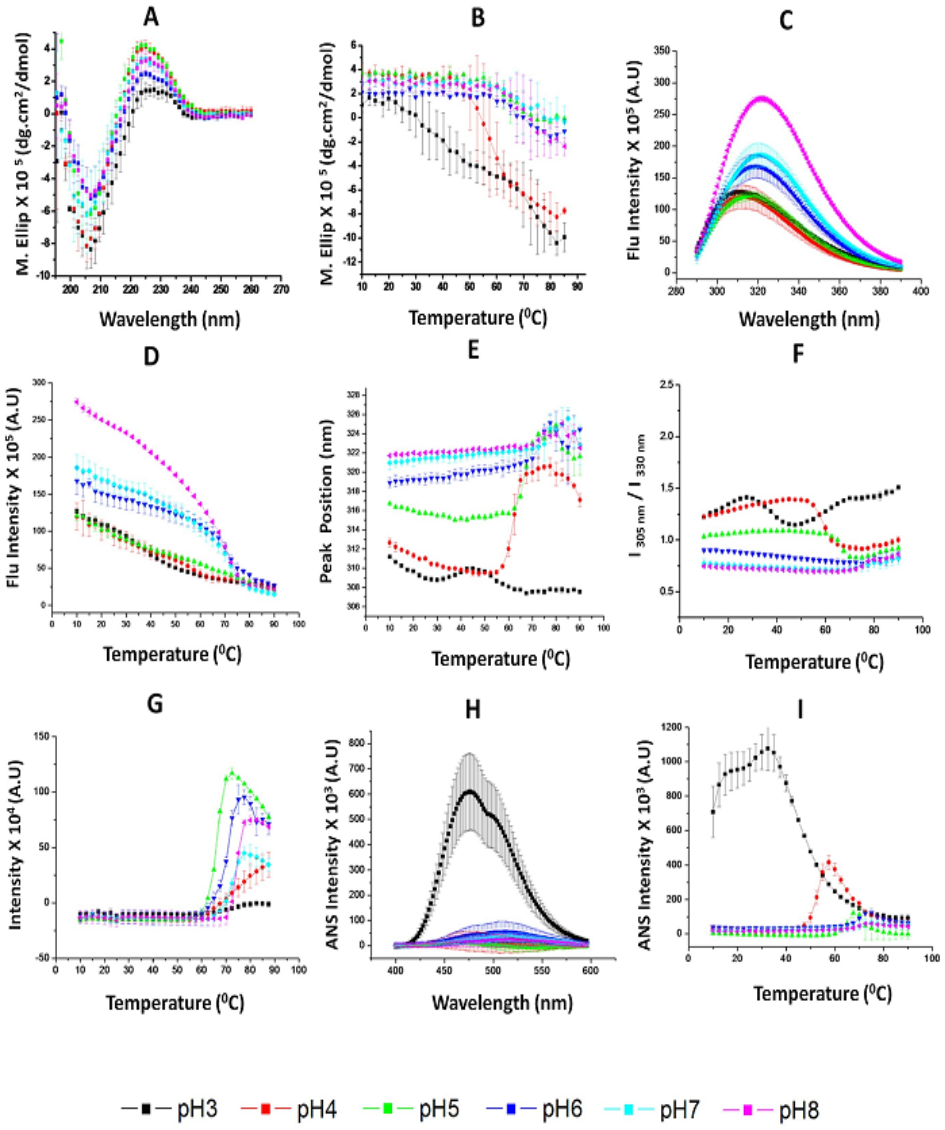

Supplemental figure 5: SYM7ΔΔ/K12V/P134V/H93G data summery

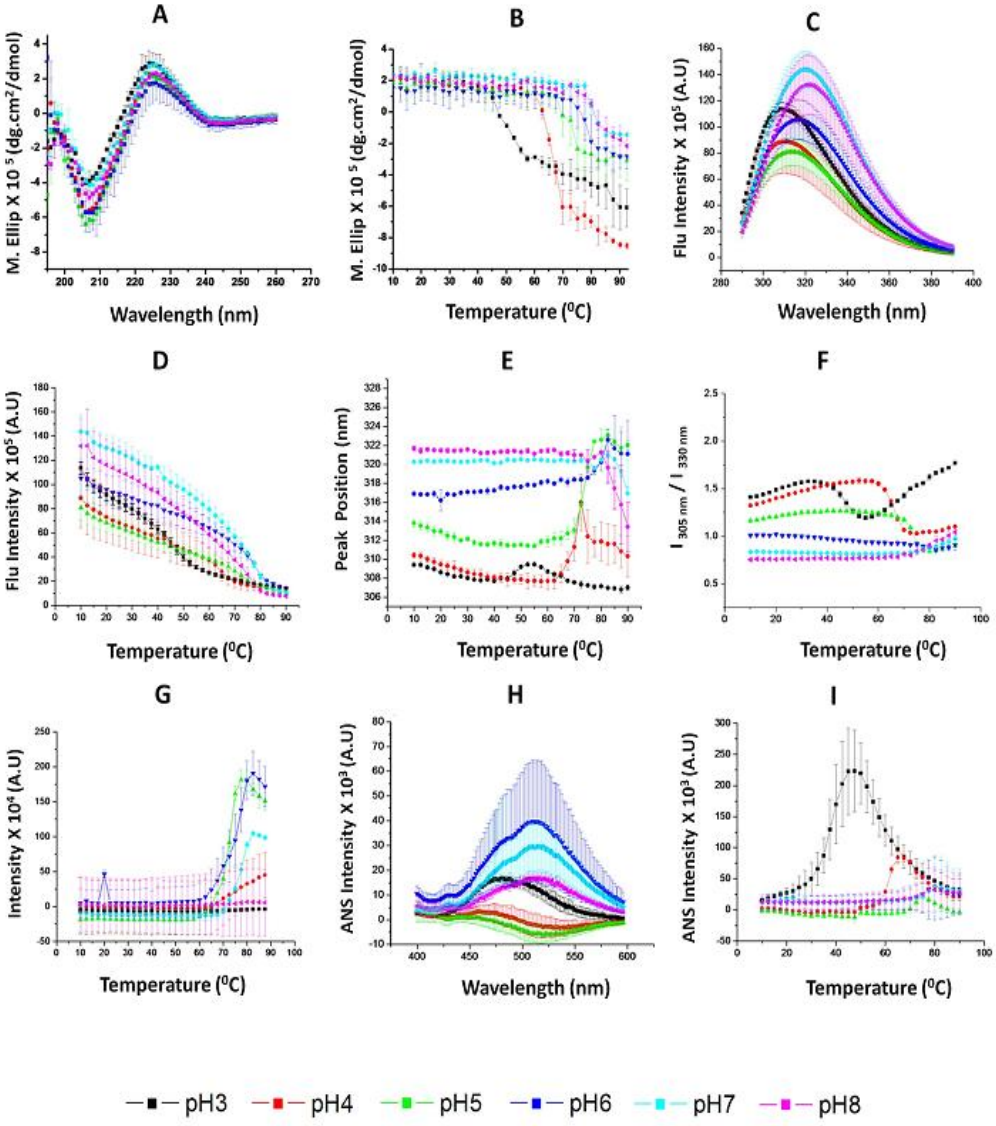

Supplemental figure 6: Symfoil-4P data summery

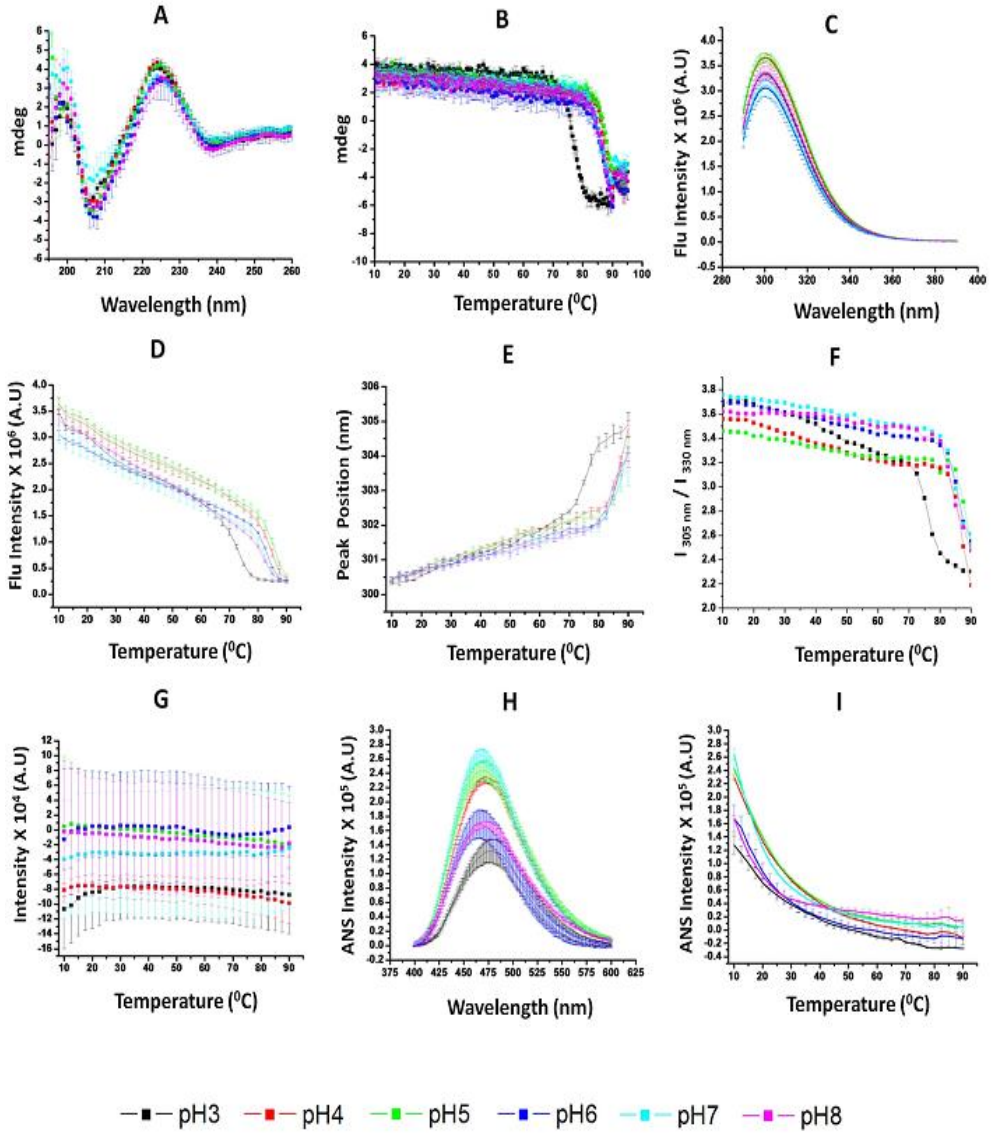

Supplemental figure 7: P134V/C117V data summery

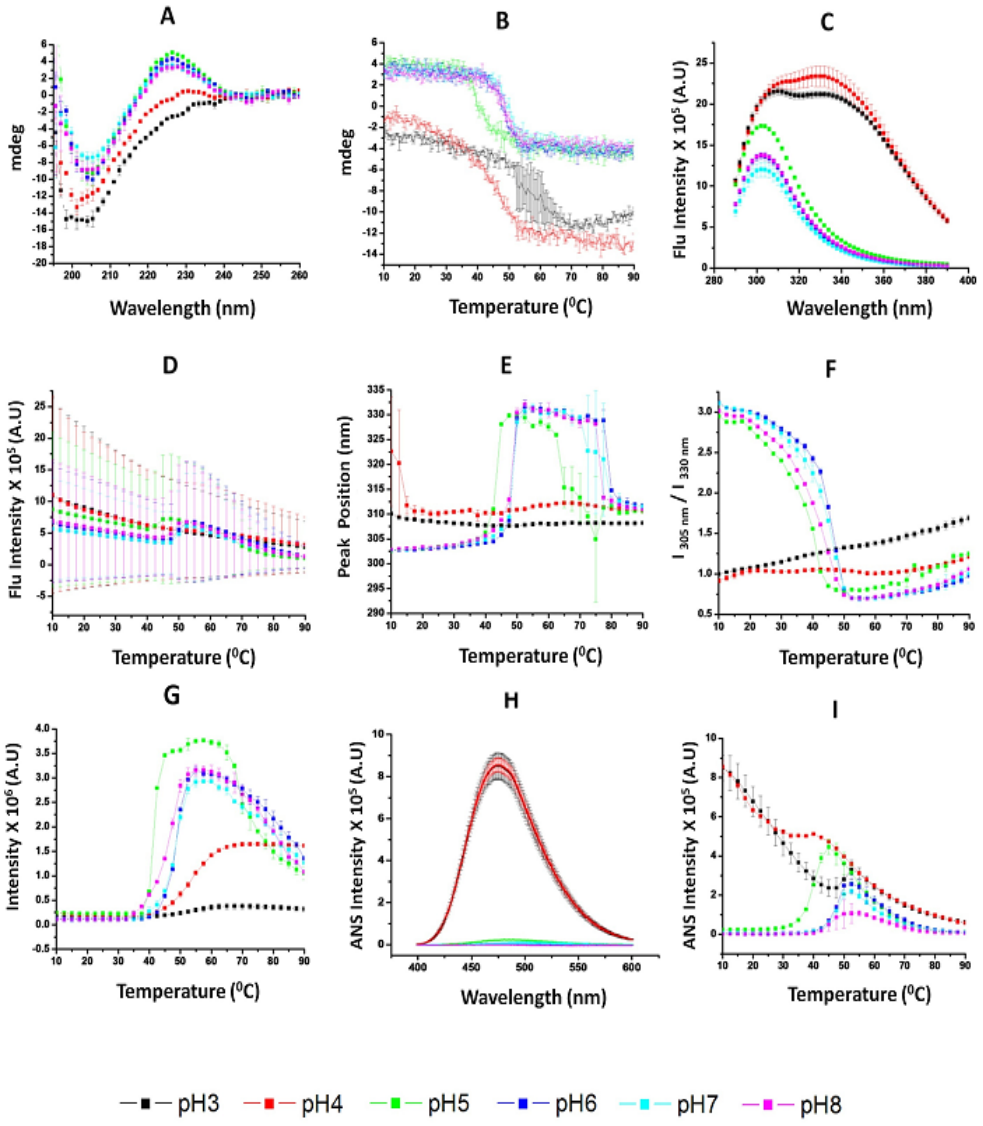

Supplemental figure 8: C83T/C117V/L44F/F132W data summery

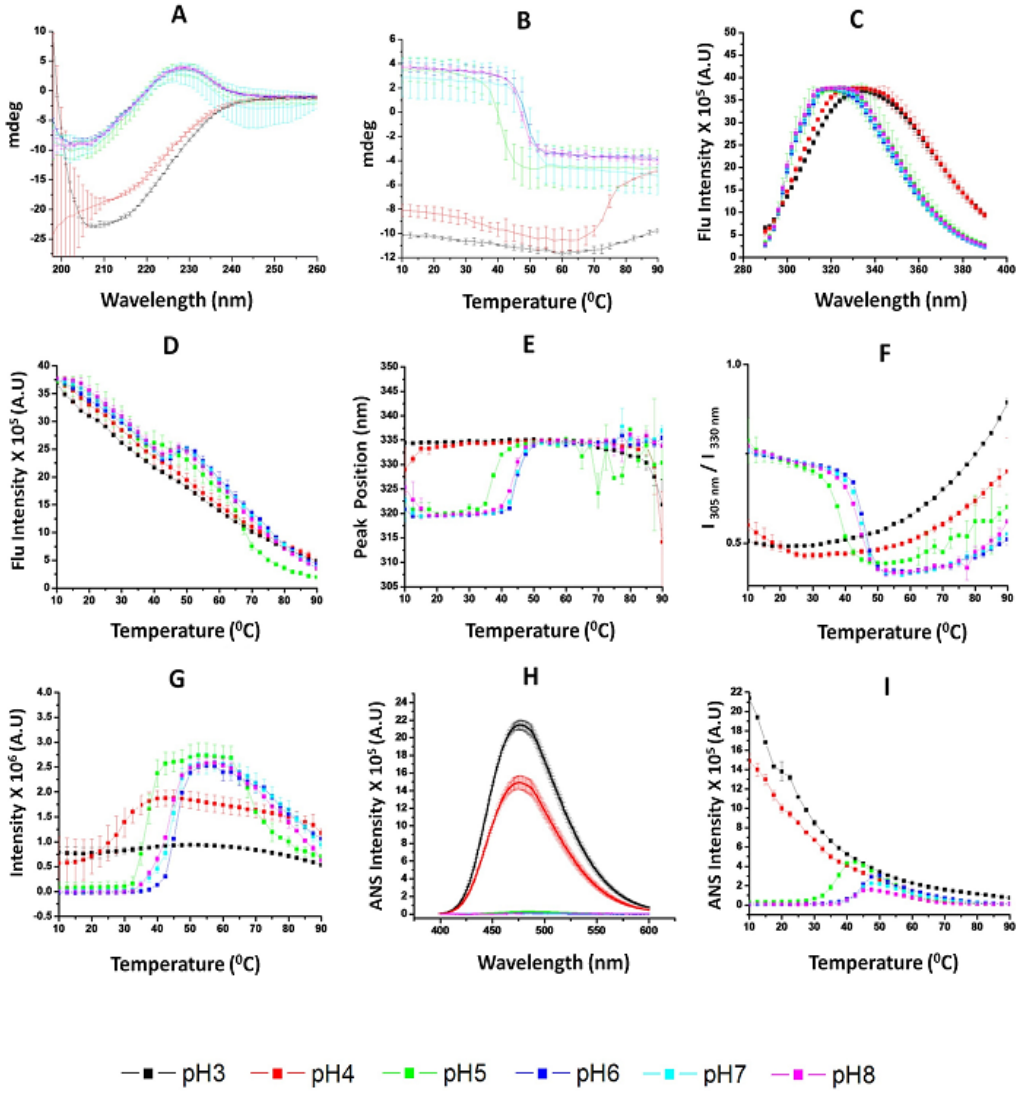

Supplemental figure 9: A66C data summery

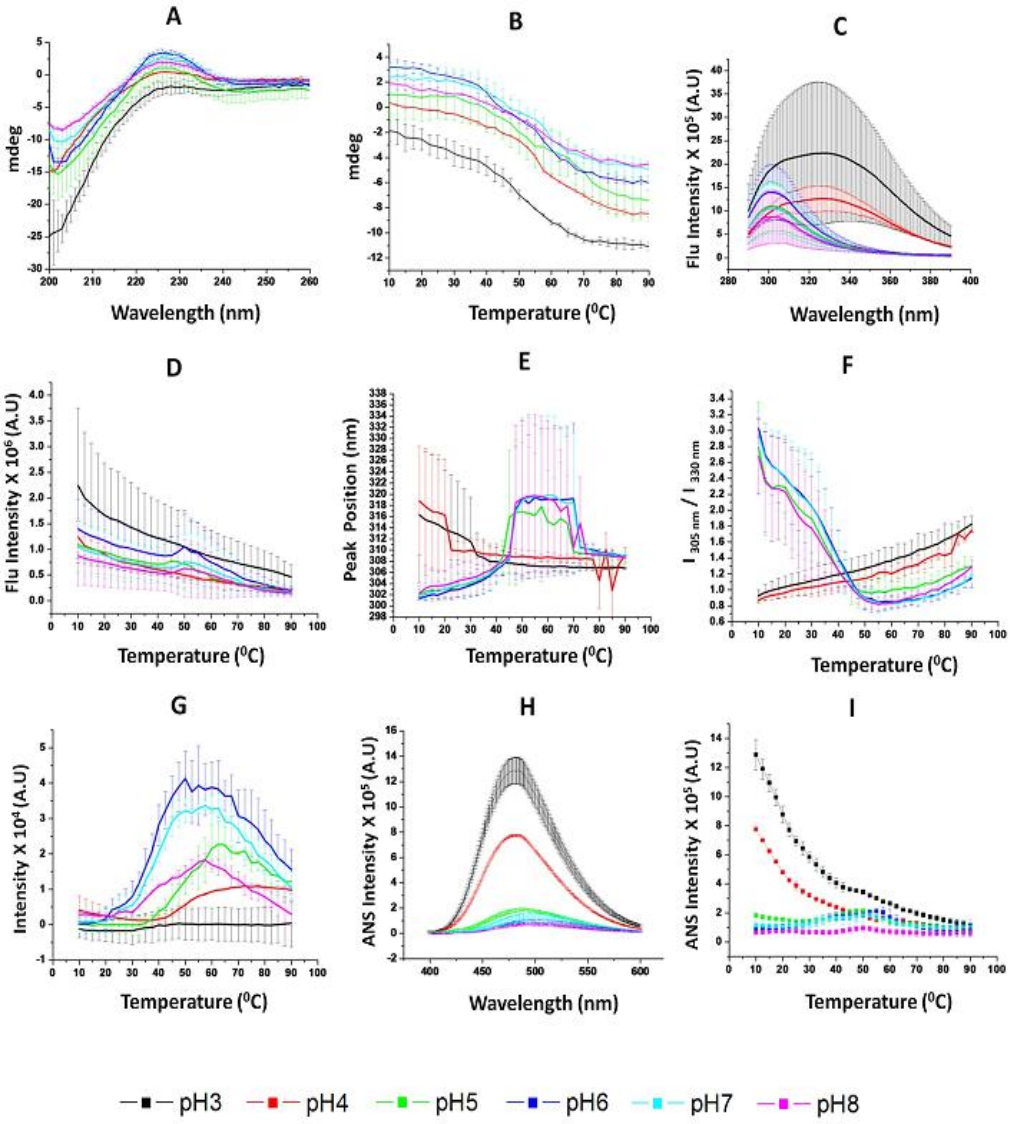

Supplemental figure 10: C83T-C117V-K12V data summery

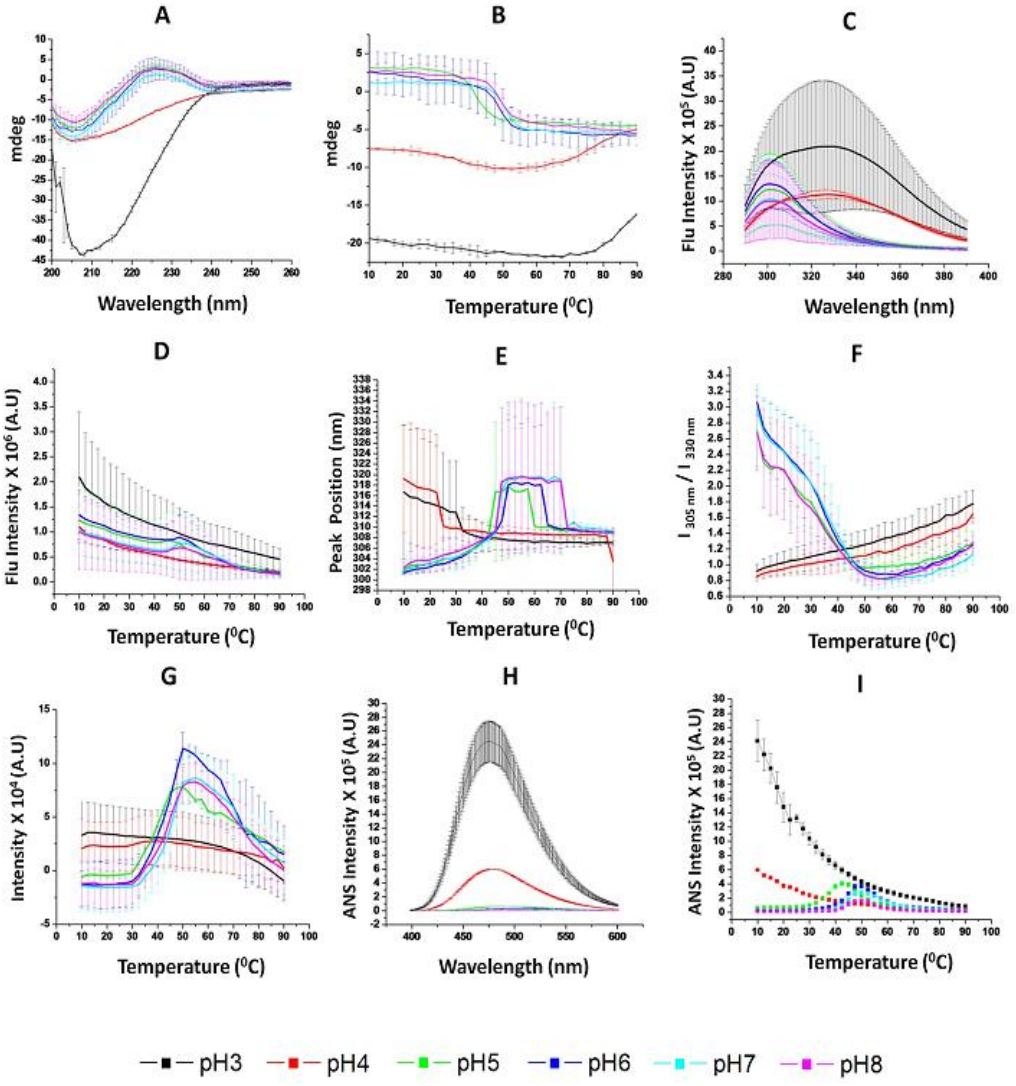

Supplemental figure 11: C117V-K12V data summery

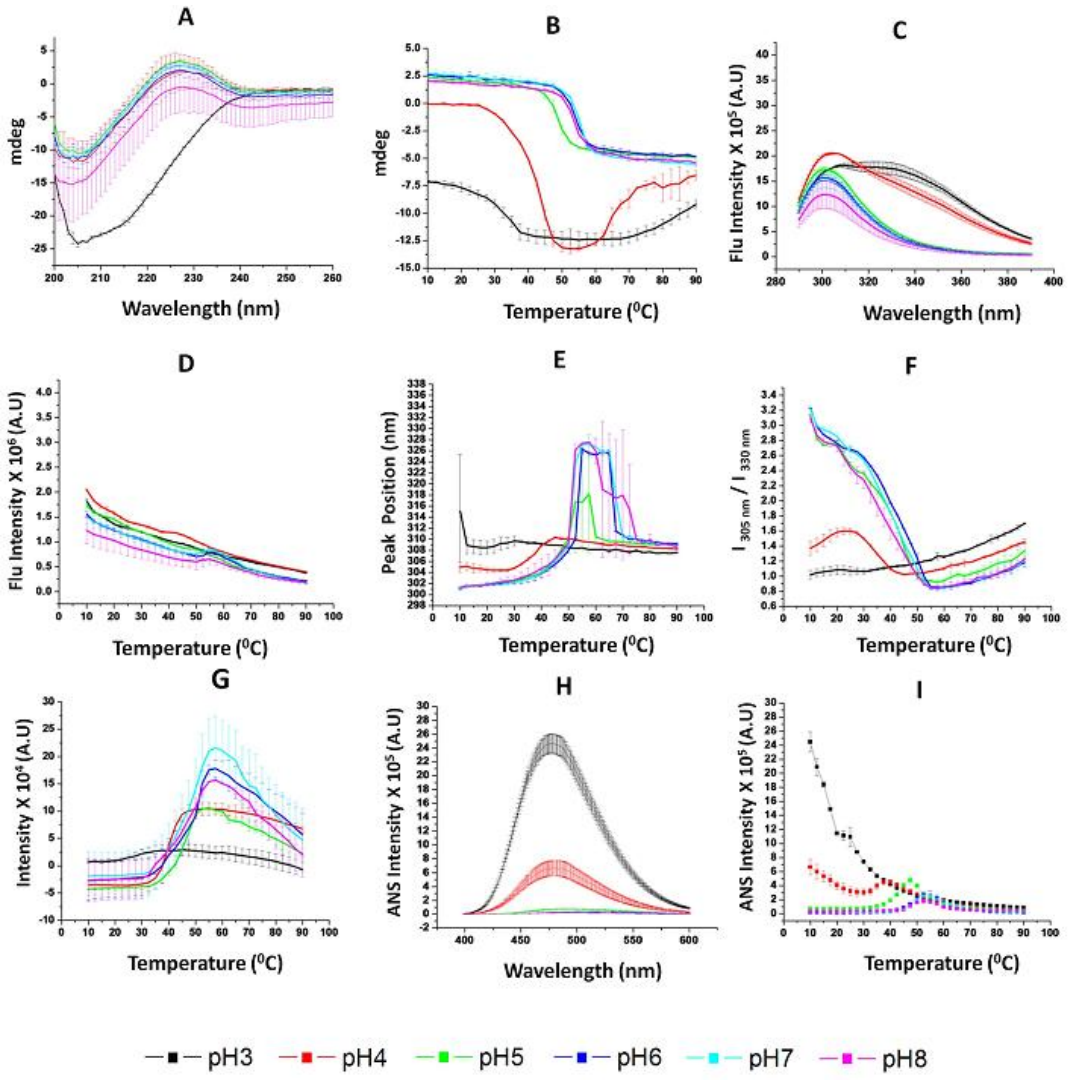

2.5 References

1. Ioli V, Wiens B, Mellin T, Thomas K, Ellis R, Ryan J, White CJ (1992) Effect of topically applied acidic fibroblast growth factor (FGF-1) on healing of chronic venous stasis and diabetic ulcers. Abstracts of the 5th Annual Symposium on Advanced Wound Care. p 150.

2. Schumacher B, Pecher P, von Specht BU, Stegmann T (1998) Induction of neoangiogenesis in ischemic myocardium by human growth factors: first clinical results of a new treatment of coronary heart disease. Circulation 97:645–650.

3. Comerota AJ, Throm RC, Miller KA, Henry T, Chronos N, Laird J, Sequeira R, Kent CK, Bacchetta M, Goldman C, Salenius JP, Schmieder FA, Pilsudski R (2002) Naked plasmid DNA encoding fibroblast growth factor type 1 for the treatment of end-stage unreconstructible lower extremity ischemia: preliminary results of a phase I trial. J Vasc Surg 35:930–936.

4. Wagoner L, Merrill W, Jacobs J, Conway G, Boehmer J, Thomas K, Stegmann T (2007) Angiogenesis protein therapy with human fibroblast growth factor (FGF-1): results of a phase I open label, dose escalation study in subjects with CAD not eligible for PCI or CABG. Circulation 116:443.

5. Copeland RA, Ji H, Halfpenny AJ, Williams RW, Thompson KC, Herber WK, Thomas KA, Bruner MW, Ryan JA, Marquis-Omer D, Sanyal G, Sitrin RD, Yamazaki S, Middaugh CR (1991) The structure of human acidic fibroblast growth factor and its interaction with heparin. Arch Biochem Biophys 289:53–61.

6. Lee J, Blaber M (2009) The interaction between thermostability and buried free cysteines in regulating the functional half-life of fibroblast growth factor-1. J Mol Biol 393:113–127.

7. Tsai PK, Volkin DB, Dabora JM, Thompson KC, Bruner MW, Gress JO, Matuszewska B, Keogan M, Bondi JV, Middaugh CR (1993) Formulation design of acidic fibroblast growth factor. Pharm Res 10:649–659.

8. Mach H, Volkin DB, Burke CJ, Middaugh CR, Linhardt RJ, Fromm JR, Loganathan D, Mattsson L (1993) Nature of the interaction of heparin with acidic fibroblast growth factor. Biochemistry 32:5480–5489.

9. Volkin DB, Tsai PK, Dabora JM, Gress JO, Burke CJ, Linhardt RJ, Middaugh CR (1993) Physical stabilization of acidic fibroblast growth factor by polyanions. Arch Biochem Biophys 300:30–41.

10. Fan H, Li H, Zhang M, Middaugh CR (2007) Effects of solutes on empirical phase diagrams of human fibroblast growth factor 1. J Pharm Sci 96:1490–1503.
11. Harris JM, Chess RB (2003) Effect of PEGylation on pharmaceuticals. Nature Rev Drug Discov 2:214–221.

12. Chapman AP (2002) PEGylated antibodies and antibody fragments for improved therapy: a review. Adv Drug Deliv Rev 54:531–545.

13. Monfardini C, Schiavon O, Caliceti P, Morpurgo M, Harris JM, Veronese FM (1995) A branched monomethoxypoly(ethylene glycol) for protein modification. Bioconjug Chem 6:62–69.

14. Basu A, Yang K,WangM, Liu S, Chintala R, Palm T, Zhao H, Peng P,Wu D, Zhang Z,Hua J, HsiehMC, Zhou J, Petti G, Li X, Janjua A, Mendez M, Liu J, Longley C, Zhang Z, Mehlig M, Borowski V, Viswanathan M, Filpula D (2006) Structure-function engineering of interferon-beta-1b for improving stability, solubility, potency, immunogenicity, and pharmacokinetic properties by site-selective mono- PEGylation. Bioconjug Chem17:618–630.

15. Kurtzman AL, Govindarajan S, Vahle K, Jones JT, Heinrichs V, Patten PA (2001) Advances in directed protein evolution by recursive genetic recombination: applications to therapeutic proteins. Curr Opin Biotechnol 12:4171–4197.

16. Kueltzo LA, Ersoy B, Ralston JP, Middaugh CR (2003) Derivative absorbance spectroscopy and protein phase diagrams as tools for comprehensive protein characterization: a bGCSF case study. J Pharm Sci 92:1805–1820.

17. Maddux NR, Joshi SB, Volkin DB, Ralston JP, Middaugh CR (2011) Multidimensional methods for the formulation of biopharmaceuticals and vaccines. J Pharm Sci 100:4171–4197.

18. Chirino AJ, Mire-Sluis A (2004) Characterizing biological products and assessing comparability following manufacturing changes. Nat Biotechnol 22:1383–1391.

19. Lubiniecki AS, Marcia Federici M (2006) Comparability is not just analytical equivalence. Biologicals 34:45–47.

20. Lubiniecki A, Volkin DB, Federici M, Bond MD, Nedved ML, Hendricks L, Mehndiratta P, Bruner M, Burman S, Dalmonte P, Kline J, Ni A, Panek ME, Pikounis B, Powers G, Vafa O, Siegel R (2011) Comparability assessments of process and product changes made during development of two different monoclonal antibodies. Biologicals 39:9–22.

21. Schenerman MA, Hope JN, Kletke C, Singh JK, Kimura R, Tsao EI, Folena-Wasserman G (1999) Comparability testing of a humanized monoclonal antibody (Synagis) to support cell line stability, process validation, and scaleup for manufacturing. Biologicals 27:203–215.

22. Brych SR, Dubey VK, Bienkiewicz E, Lee J, Logan TM, Blaber M (2004) Symmetric primary and tertiary structure mutations within a symmetric superfold: a solution, not a constraint, to achieve a foldable polypeptide. J Mol Biol 344:769–780.

23. Culajay JF, Blaber SI, Khurana A, Blaber M (2000) Thermodynamic characterization of mutants of human fibroblast growth factor 1 with an increased physiological half-life. Biochemistry 39:7153–7158.

24. Dubey VK, Lee J, Somasundaram T, Blaber S, Blaber M (2007) Spackling the crack: stabilizing human fibroblast growth factor-1 by targeting the N and C terminus beta-strand interactions. J Mol Biol 371:256–268.

25. Kim J, Brych SR, Lee J, Logan TM, Blaber M (2003) Identification of a key structural element for protein folding within beta-hairpin turns. J Mol Biol 328:951–961.

26. Lee J, BlaberM(2011) Experimental support for the evolution of symmetric protein architecture from a simple peptide motif. Proc Natl Acad Sci U S A 108:126–130.

27. Lee J, Blaber M (2009) Structural basis of conserved cysteine in the fibroblast growth factor family: evidence for a vestigial half-cystine. J Mol Biol 393:128–139.

28. Lee J, Dubey VK, Longo LM, Blaber M (2008) A logical OR redundancy within the Asx-Pro-Asx-Gly type I beta-turn motif. J Mol Biol 377:1251–1264.

29. Lee J, Blaber SI, Dubey VK, Blaber M (2011) A polypeptide ‘‘building block’’ for the beta-trefoil fold identified by ‘‘top-down symmetric deconstruction". J Mol Biol 407:744–763.

30. Srimathi T, Kumar TK, Kathir KM, Chi YH, Srisailam S, Lin WY, Chiu IM, Yu C (2003) Structurally homologous all beta-barrel proteins adopt different mechanisms of folding. Biophys J 85:459–472.

31. Manning MC, Illangasekare M, Woody RW (1988) Circular dichroism studies of distorted alpha-helices, twisted beta-sheets, and beta turns. Biophys Chem 31: 77–86.

32. Khan MY, Villanueva G, Newman SA (1989) On the origin of the positive band in the far-ultraviolet circular dichroic spectrum of fibronectin. J Biol Chem 264: 2139–2142.

33. Berova N, Nakanishi K, Woody RW (2000) Circular dichroism: principles and applications, 2nd ed. Wiley.

34. Mach H, Middaugh CR (1995) Interaction of partially structured states of acidic fibroblast growth factor with phospholipid membranes. Biochemistry 34:9913–9920.

35. Mach H, Ryan JA, Burke CJ, Volkin DB, Middaugh CR (1993) Partially structured self-associating states of acidic fibroblast growth factor. Biochemistry 32: 7703–7711.

36. Pineda-Lucena A, Nunez De Castro I, Lozano RM, Munoz-Willery I, Zazo M, Gimenez-Gallego G (1994) Effect of low pH and heparin on the structure of acidic fibroblast growth factor. Eur J Biochem 222:425–431.

37. Semisotnov GV, Rodionova NA, Razgulyaev OI, Uversky VN, Gripas AF, Gilmanshin RI (1991) Study of the ‘‘molten globule’’ intermediate state in protein folding by a hydrophobic fluorescent probe. Biopolymers 31: 119–128.

38. Matulis D, Lovrien R (1998) 1-Anilino-8-naphthalene sulfonate anion-protein binding depends primarily on ion pair formation. Biophys J 74:422–429.

39. Joshi S, Bhambhani A, Zeng Y, Middaugh CR (2010) Formulation and process development strategies for manufacturing biopharmaceuticals. Wiley & Sons Publication.

40. Linemeyer DL, Menke JG, Kelly LJ, DiSalvo J, Soderman D, Schaeffer MT, Ortega S, Gimenez-Gallego G, Thomas KA (1990) Disulfide bonds are neither

required, present, nor compatible with full activity of human recombinant acidic fibroblast growth factor. Growth Factors 3:287–298.

41. Blaber M, DiSalvo J, Thomas KA (1996) X-ray crystal structure of human acidic fibroblast growth factor. Biochemistry 35:2086–2094.

42. Gimenez-Gallego G, Conn G, Hatcher VB, Thomas KA (1986) The complete amino acid sequence of human brain-derived acidic fibroblast growth factor. Biochem Biophys Res Commun 138:611–617.

43. Cuevas P, Carceller F, Ortega S, Zazo M, Nieto I, Gimenez- Gallego G (1991) Hypotensive activity of fibroblast growth factor. Science 254:1208–1210.

44. Brych SR, Blaber SI, Logan TM, Blaber M (2001) Structure and stability effects of mutations designed to increase the primary sequence symmetry within the core region of a beta-trefoil. Protein Sci 10:2587–2599.

45. Zazo M, Lozano RM, Ortega S, Varela J, Diaz-Orejas R, Ramirez JM, Gimenez-Gallego G (1992) High-level synthesis in Escherichia coli of shortened and full length human acidic fibroblast growth factor and purification in a form stable in aqueous solutions. Gene 113:231–238.

46. Lee J, Blaber M (2010) Increased functional half-life of fibroblast growth factor-1by recovering a vestigial disulfide bond. J Proteins Proteomics 1:37–42.

Chapter 3

High-Throughput Biophysical Analysis and Data Visualization of Conformational Stability of an IgG1 Monoclonal Antibody (mAb) After Deglycosylation

3.1 Introduction

Monoclonal antibodies (mAbs) have emerged as a key category of therapeutic protein drugs with over 30 mAbs currently approved in the USA and Europe and many hundreds under clinical development.[1, 2] The commonly used IgG mAb includes two light chains and two heavy chains forming a homo-dimeric, multidomain structure containing an N-linked glycosylation site in each of the two C_H2 domains found in the Fc portion of the heavy chain.[3, 4] The glycosylation pattern of the Fc region of IgG molecules plays a key role in IgG functionality and clearance, where the type and amount of glycan moieties control the ability and affinity of the Fc region to bind to the various Fc receptors *in vivo*.[5-11] These Fc receptors are responsible for Fc effector function activities and regulating clearance of IgGs from circulation *in vivo*.[12-18]

The extent and type of glycosylation has been shown to influence the conformational stability of proteins in general and mAbs in particular.[19] There are several studies examining the effect of deglycosylation on the structure and stability of the Fc region of IgGs.[20, 21] These studies typically use a single measurement type (e.g., differential scanning calorimetry) over limited solution conditions (e.g., one or two pH values) to examine the effect of varying mAb glycosylation patterns.[22-26, 30] In addition, the protease sensitivity of an IgG (e.g., papain digestion), has been used to examine mAb stability, in which more cleavage has been noted when the Fc was deglycosylated.[34, 35] Recent studies have

also examined the conformational stability of purified Fc domains as function of varying glycosylation.[20, 21, 27-30, 32] Interactions between the glycan moieties and specific residues within the C_H2 domains are responsible for stabilizing the structure of the C_H2 domain, and disruption of these non-covalent interactions by partial or full deglycosylation leads to destabilization of the entire domain.[20, 21, 30-33] The effect of deglycosylation on the structural integrity of the C_H2 domain has been examined by a variety of structural analysis including X-ray crystallography, [56] SAXS [40] and HDX-MS [54, 55] as well as examined by molecular modeling.[6, 57]

The pharmaceutical properties (e.g., storage stability and solubility) of mAbs are also affected by glycosylation, although not necessarily in predictable ways. For example, the solubility of an IgG1 was increased dramatically after the introduction of an additional glycosylation site on the Fab domain.[36] In contrast, an isolated cryoimmunoglobulin species from human serum, known to have dramatically reduced cold solubility, was shown to contain an additional glycosylation moiety in the variable region of the antibody.[37] The aggregation propensity of IgGs may increase upon deglycosylation, which has been attributed to the destabilization of the C_H2 domain as well as exposure of an aggregation-prone regions within the C_H2 domain that are masked in the native IgG by the glycan moiety.[28, 38, 39, 59, 60]

Due to the potential for changes in critical quality attributes for biotech drugs as a result of manufacturing and/or formulation modifications,

comparability studies are performed in which the pre and post-change drug candidates are evaluated to ensure that these process and product changes do not affect the drug's structure, safety and function.[41-44] Structural equivalence between pre and post-change protein drug candidates is evaluated in a step-wise fashion which may include analytical, biological and clinical evaluations.[41] The effect of varying glycosylation profiles on the design of comparability assessments of protein therapeutics, including effects on Fc effector function activity of mAbs, has recently been reviewed.[42, 45]

Analytical characterization for comparability evaluations includes determination of primary and higher-order structural integrity using a combination of methods.[43, 46] A combination of chromatographic (SE, RP and IE-HPLC) and electrophoretic (cIEF, cSDS) methods are typically utilized along with mass spectrometry (intact molecular weight, peptide and oligosaccharides maps) to characterize protein's primary structure and post-translational modifications (e.g., glycosylation patterns). In contrast, analytical methods available to examine higher-order structure are typically lower resolution in nature (e.g., CD, fluorescence), ultimately resulting in the requirement for functional potency assays to be performed to ensure biological activity. Since accelerated or long term stability studies are typically monitored as part of comparability assessments, [43, 46] there is a need for new analytical methods for

determining the higher-order structure of protein drug candidates that would provide a more comprehensive picture of their structural integrity and stability.

In the past decade, multiple papers have appeared from our laboratories describing the ability of empirical phase diagrams (EPDs) to summarize physical stability data and use this information for formulation development of therapeutic proteins and vaccines.[47-52] These EPDs are created through the utilization of large data sets from high throughput analysis of a protein's conformational stability as a function of environmental stresses (e.g., temperature and pH) by multiple lower-resolution biophysical techniques (e.g., CD, fluorescence, light scattering, etc.), followed by the application of multidimensional mathematical analysis techniques, to produce a colored diagram representing structural changes as a function of environmental stress. Furthermore, the ability of EPDs to detect major conformational stability changes in a series of site-directed mutants of acidic fibroblast growth factor (FGF-1) was recently demonstrated.[50] Recent work has also established additional data visualization methods such as radar charts, Chernoff faces and comparative signature diagrams to better compare protein samples.[51, 53]

The purpose of this study is to test the feasibility of using high through-put biophysical analysis and data visualization methods to rapidly evaluate, over a wide range of solution conditions, differences in the structural integrity and conformational stability of an IgG1 mAb of varying glycosylation patterns. This

work required, for the first time, incorporation of differential scanning calorimetry and differential scanning fluorimetry data into the EPD analysis. We also included radar chart methods to better visualize conformational stability data differences across the IgG1 glycoforms.

3.2 Materials and Methods

3.2.1 Materials

An IgG1 mAb solution was received from Janssen R&D/J&J at 40 mg/ml and frozen in aliquots at -80^0 C. Reagent chemicals were purchased from Sigma–Aldrich (St. Louis, MO) or Fisher Scientific (Pittsburg, PA).

3.2.2 Methods

3.2.2.1 Deglycosylation of IgG mAb

Fully deglycosylated mAb was prepared using PNGase F from Prozyme™ (San Leandro, CA). Samples of mAb were diluted to 10 mg/ml with reaction buffer (100 mM Tris, 100 mM NaCl, pH 7.5), and then 20 µl (200 µg) of the diluted protein sample was added to 172 µl of the reaction buffer and 8 µl of PNGase F to achieve a 1:100 (w/w) enzyme: protein ratio. The mixture was incubated at 37 ^{0}C for 15 h. Partially deglycosylated IgG was produced using Endoglycosydase F2 (Endo F2) from Prozyme™ (San Leandro, CA). Samples of mAb were diluted to 10 mg/ml using deionized water. Twenty µl (200 µg) of the

diluted protein sample was then added to 38 µl of deionized water, followed by addition of 10 µl of 5X reaction buffer (250 mM sodium acetate, pH 4.5), and 2 µl of Endo F2 to the mixture. The mixture was incubated for 1h at 37 ^{0}C.

3.2.2.2 Electrospray Ionization Mass Spectrometry (ESI-MS)

To confirm deglycosylation, antibody samples with and without reduction, using 10 mM dithiotreitol (DTT), were diluted to 0.25 mg/ml with 0.1% formic acid. Ten µL of this solution (approximately 16 pmoles of intact mAb or 50 pmoles of Fc monomer) was injected into the sample loop of the LC (Agilent Technologies 1200 Series) with a two pump system. An isocratic loading pump carried the sample from the loop to a Protein Concentration and Desalting Micro Trap (Bruker-Michrom, Auburn, CA, USA) for 5 min desalting with 0.1% formic acid at 200 µL/min. A gradient pump eluted the protein from the trap at 50 µL/min flow rate using a 5-60 % linear acetonitrile gradient in 3 min followed by a 60-95% gradient in 1 min for cleaning the trap onto the electrospray ionization (4 kV capillary) source of a time of flight mass spectrometer (model 6220, Agilent Technologies).The mobile phases used for gradient elution were 0.1% formic acid and 90% acetonitrile /10% water /0.1% formic acid. The mass spectrometer was operated in 2 GHz extended dynamic range mode with fragmentor voltage of 150V, desolvation gas flow rate of 10 L/min at 325 °C and nebulizer pressure of 20 psig. Mass spectra were acquired over an m/z range of

300-3200 with an acquisition rate of 1 spectrum per second with reference mass correction. The raw mass spectral data was processed using Agilent Mass Hunter Qualitative Analysis (version B.04). The mass spectra were deconvoluted at specific mass ranges to search for intact or reduced mAb species.

3.2.2.3 Sample Preparation for Stability Assessments

Samples were dialyzed overnight at 4^0 C using a 10 kDa molecular-weight cutoff membrane (Pierce, Rockford, IL) against 20 mM citrate-phosphate buffer to achieve the targeted pH range (3-8 with one pH unit increment or 3.5-6.0 with 0.5 pH increments). The ionic strength in all buffers was adjusted to 0.15 using NaCl. Protein concentration was determined at each pH using Agilent 8453 spectrophotometer (Palo Alto, California) and adjusted to 1 mg/ml. For physical measurements, two different sets of experimental parameters were evaluated: (1) for the pH range of 3-8, the temperature was raised from 10 ^{0}C to 90 ^{0}C at 2.5 ^{0}C intervals using a 180 sec equilibration time, or (2) for the pH range of 3.5-6.0, 1.25 ^{0}C intervals were used as a temperature ramp with a 30 sec equilibration time.

3.2.3 Biophysical Measurements

3.2.3.1 Far-UV Circular Dichroism Spectroscopy

Far-UV Spectra ranging from 260 to 200 nm with a resolution of 1 nm and a bandwidth of 1 nm was collected first at 10 ^{0}C using Chirascan (Applied photophysics) equipped with four cells peltier type temperature controller. A protein concentration of 0.2 mg/ml using 0.1 cm path length quartz cells with a total volume of 200 µl was used. The CD signal intensity change at 217 nm as a function of temperature was collected, and buffer subtracted from all protein samples.

3.2.3.2 Intrinsic (Trp) Fluorescence Spectroscopy and Static Light Scattering (SLS)

Intrinsic fluorescence and SLS were measured using a dual-channeled, four positioned Photon Technology International (PTI) Quantum master fluorometer (Brunswick, Ney Jersey) equipped with a turreted peltier temperature controller. A protein sample of 0.2 mg/ml in 0.2 cm path length quartz cell containing a total volume of 200 µl was used. Samples were excited at 295 nm with emission spectra collected from 300 to 400 nm at a resolution of 1 nm, collection rate of 1 nm/sec, and an integration time of 1 sec. The slit width used for both excitation and emission was 4 nm, while 0.25 nm was the slit width used for light scattering. As the intrinsic fluorescence signal was collected, SLS signal

was collected simultaneously using 180^0 angle detector relative to the other, and the SLS peak intensity at the wavelength of excitation (295 nm). Spectra and SLS were was followed with temperature increase as describe in detail elsewhere.[32] Fluorescence peak position and intensity changes were determined by center of spectral mass "MSM" method using Origin™ 7.0 software. This method shifts in the actual peak position of approximately 10 nm, but produces more reproducible values of the wavelength maximum. Buffer spectra were determined and subtracted from all protein samples.

3.2.3.3 Extrinsic Fluorescence Spectroscopy with ANS

Extrinsic fluorescence was measured using a four positioned Photon Technology International (PTI) Quantum master fluorometer (Brunswick, Ney Jersey) equipped with a turreted peltier temperature controller. The dye 1-analino-8-naphthalene sulfonate (ANS) was used to detect the exposure of the apolar regions of the protein. A protein concentration of 0.2 mg/ml was used; ANS was added to the protein to achieve a protein:ANS molar ratio of 1:15 and a total volume of 200 µl using 0.2 cm path length quartz cells. Samples were excited at 374 nm and emission spectra were collected in the range of 400 to 600 nm with a 1 nm resolution, 1 nm/sec collection rate, and 1 sec integration time. A slit width of 3 nm was used for both excitation and emission. Buffer spectra were determined and subtracted from all protein samples.

3.2.3.4 Differential Scanning Calorimetry (DSC)

DSC measurements were carried out using MicroCal™ capillary Auto DSC instrument (MicroCal,LLC, Northampton, Massachusetts). A protein concentration of 0.2 mg/ml in a total volume of 600 µl was used with a temperature ramp from 10 ^{0}C to 90 ^{0}C and a scanning rate of 60 ^{0}C/hr. A pH range of 4-6 with 0.5 pH unit increment was evaluated. Buffer thermograms were subtracted from the corresponding sample thermograms. DSC thermograms were integrated, before being utilized in the construction of the EPD, to get a sigmoidal curve, in a step to get a better representation of the data in the EPD.

3.2.3.5 Differential Scanning Fluorimetry (DSF)

DSF measurements were performed using MX3005P QPCR system (Agilent Technologies), with a protein concentration of 0.2 mg/ml and total sample volume of 100 µl. SYPRO™ orange purchased from Invitrogen, Inc. (Carlsbad, CA) supplied in a concentrated form (5000x) dissolved in DMSO. The dye was diluted to 40x and then added to the protein samples to achieve 1x dye concentration for measurements. Using FAM filter sets, the mixture was excited at 492 nm and the emission intensity change with temperature at 516 nm was followed. Temperature was raised from 25 ^{0}C to 90 ^{0}C using 60 ^{0}C/hr as a heating rate and 1 ^{0}C as a step size. Data were transferred to Excel software (Microsoft, Redmond, WA) for data analysis. A pH range of 4-6 with 0.5 pH unit increment

was used, and buffers were run and subtracted from all samples. DSF curves were integrated, before being utilized in the construction of the EPD, to get a sigmoidal curve, in a step to get a better representation of the data in the EPD.

3.2.3.6 Construction of Empirical Phase Diagrams (EPDs) and Radar Charts

EPDs are constructed to summarize and visualize the conformational stability of IgG1 mAbs using data sets from selected experimental techniques as a function of pH and temperature. The experimental measurements are organized in the form of a multi-dimensional vector matrix and analyzed by Singular value decomposition (SVD) as described in detail elsewhere.[51, 52] Results are mapped to a RGB color scheme and visualized as changes in color which indicate changes in the physical states of the protein. Additional data visualization scheme with radar charts was also used to analyze the data as described in detail elsewhere.[51] A radar chart can have any number of polar axes each of which is mapped to an experimental technique. A polygon drawn by connecting all points in the polar axes represents changes in the physical states of the protein. Similar to an EPD, difference in the shapes of polygons indicate changes in the conformational state of a protein. Apparent boundaries between states can be assessed visually or by use of computational aid such as k-Means clustering. A detailed explanation of radar charts and clustering methods can be found elsewhere.[50]

3.3 Results

3.3.1 Deglycosylation of the IgG1 mAb

The IgG1 mAb used in this study had a glycosylation pattern typically observed for recombinant mAbs produced from SP2/0 cells with ~75% consisting of G1F, G2F and G0F structures, and the remaining ~25% being spread over various charged species (e.g., mono and disialylated glycoforms) as described in detail elsewhere.[43] The ability of the different enzymes to remove the two major glycans (G0F, G1F) was monitored by mass spectrometry analysis of the heavy chain Fc from reduced mAb samples (Table 1). Mass spectrometric analysis of the reduced mAb samples showed no significant changes to the light chain (data not shown) while the heavy chain manifested a molecular weight consistent with the specific enzymatic treatments (Table 1). For example, partial deglycosylation was achieved by the treatment with endoglycosydase F2 (Endo F2) which cleaves between two GlcNAc residues and leaves Asn 297 in the protein backbone attached to GlcNAc-Fuc. Full deglycosylation was achieved using N-Glycanase (PNGase F) which fully removes the glycan (see Table 1) and deamidates the Asn to Asp, adding a negative charge to both C_H2 domains. Additional confirmation was obtained by SDS-PAGE and capillary isoelectric focusing analysis which qualitatively showed the expected shifts in migration of fully deglycosylated mAb in terms of molecular weight and charge heterogeneity due to glycan removal (data not shown).

3.3.2 Initial biophysical characterization of a native and fully deglycosylated IgG1

The secondary structure of the native and fully deglycosylated IgG1 mAb was evaluated by far-UV CD analysis from 260 nm to 200 nm at 10 ^{0}C (Figure 1A, 2A). Both samples share the same structural features across all pH values in the form of a broad negative peak at 217 nm, indicating the expected β-sheet rich structure. By following the CD intensity change at 217 nm with increasing temperature (Figures 1B, 2B), the two IgG1 glycoforms show similarity in their secondary structure stability behavior at higher pH values (pH 6-8) with an onset temperature of ~60 ^{0}C. A lower pH, however, (pH range 3-5), the native IgG1 shows a trend toward enhanced stability compared to its deglysosylated form, with ~1 ^{0}C difference in the onset temperature.

At 10 ^{0}C, the native IgG1 produced a higher ANS intensity at pH 3 than other pH values, suggesting increased exposure of apolar regions at low pH (Figure 1C). For the fully deglycosyalted IgG1, higher ANS intensity was observed at all pH values compared to native IgG1 (Figure 2C). Thermal stability was studied by following the ANS intensity change at 486 nm with increasing temperature as shown in Figures 1D and 2D. The native and deglycosylated forms of the mAb show a similar transition at high pH values (pH 6-8) with one, major structural transition observed starting at ~60 ^{0}C. Differences between the two IgG1 forms are observed, however, in more acidic environments (pH 3-5),

including an additional structural transition at lower temperatures. At pH 3, the first transition begins at approximately 10 ^{0}C for the native IgG1, while the protein is already structurally altered at 10 ^{0}C for the fully deglycosylated form, suggesting that the fully deglycosylated IgG1 is experiencing a higher degree structural disruption at pH 3. In contrast, the second transition starts at ~35 ^{0}C for both samples. Two structural transitions are seen at pH 4 for both IgG1s, with a similar onset temperature for the second transition (~57 ^{0}C), but a different onset temperatures in the first transition (~35 ^{0}C for the native IgG vs. ~25 ^{0}C for the fully deglycosylated IgG). The native IgG1 at pH 5 shows only one structural transition starting at ~60 ^{0}C while the deglycosylated form manifest two transitions at ~42 and ~60 ^{0}C.

Intrinsic (Trp) fluorescence spectroscopy was used to probe the overall tertiary structure stability of the native and fully deglycosylated mAb. Comparing the two spectra at 10 ^{0}C, no major differences were observed at all pH values (data not shown). By following the intensity change with increasing temperature for the IgG1 in the native (Figure 1E) and fully deglycosylated states (Figure 2E), similar structural transitions are seen including an initial decrease in fluorescence intensity (due to the intrinsic temperature dependent decrease in quantum yield of the tryptophan's indol ring), a second sudden increase in fluorescence intensity (indicating the start of a tertiary structure unfolding event), and a third transition marked by a sudden decrease in fluorescence intensity consistent with

aggregation/precipitation. The major unfolding event (second transition) for both IgG1 forms starts earlier at pH 3 (~38 ^{0}C) and pH 4 (~55 ^{0}C) compared to other pH values. Approximate 2-3 ^{0}C stability difference for the IgG1 in the native state (~62.5 ^{0}C) was observed for pH (5-8) compared to the fully deglycosylated IgG (~60 ^{0}C). Peak position changes as a function of increasing temperature were also analyzed. The peak position for the native IgG1 (Figure 1F) was 340 nm (shifted from an actual value of 330 nm due to the use of "spectral central of mass" method) for all pH values at 10°C representative of native/folded tertiary structure. The peak position gradually increased with increasing temperature followed by a decrease at around 65 ^{0}C (except at pH 3) suggesting aggregation/precipitation. The fully deglycosylated IgG1 (Figure 2F) at 10 ^{0}C was in a partially unfolded state as indicated by the red shifted peak position (345 nm at pH 3 and 342 nm for the pH range 4-8 using MSM analysis). With increasing temperature, both proteins showed a gradual increase in their peak position as a result of gradual unfolding followed by aggregation/ precipitation and concomitant loss of signal.

Figures 1G and 2G show the temperature induced aggregation behavior of the native and fully deglycosylated IgG1, respectively, as measured by static light scattering. Comparing the two IgG1 forms, pH 3 shows a similar trend with no increase in light scattering intensity even up to 90 ^{0}C, whereas, the native and deglycosylated IgG1 at pH 4 starts aggregating at 64.5 ^{0}C and 62 ^{0}C, respectively,

with a greater intensity upon aggregation for the deglycosylated form. At pH 5 and 6, native IgG1 starts aggregating at ~62.5 ^{0}C and ~65 ^{0}C compared to ~60 ^{0}C and ~62.5 ^{0}C for the deglycosylated IgG1, implying a destabilizing influence of removal of the sugar moiety.

The thermal melting curves from CD, ANS, fluorescence peak intensity, fluorescence peak position, and SLS analysis were used to generate EPDs for the native (Figure 1H) and fully deglycosylated mAbs (Figure 2H). Comparing the two EPDs, three major regions are identified that signify different conformational states. The green region represents the IgG1 in its stable native state and the blue region in a structurally perturbed, partially unfolded state. The purple/red region represents an aggregated state. Both IgG1 forms have similar transition temperatures in the native to the unfolded state events (blue region) in the pH range of 6-8, suggesting no detectable differences in conformational stability between the native and fully deglycosylated IgGs in this pH range. In contrast, notable differences in conformational stability between the two IgG1 forms were seen under more acidic conditions of pH 3-5. Comparing the native (green) region of the EPDs at pH 5 for the two IgG1 forms, a large stability difference is observed, in which the native IgG1 starts transitioning to the unfolded state at ~57.5 ^{0}C and the fully deglycosylated form at ~47.5 ^{0}C. At pH 4, conformational stability differences are even more dramatic, with transitions to the unfolded state appearing at ~47.5 ^{0}C and ~35 ^{0}C for the native and fully deglycosylated IgG1,

respectively. For both IgG1 forms at pH 3, the structurally perturbed state initiates at 10 ^{0}C with this unfolded state undergoing aggregation at ~50 ^{0}C.

3.3.3 Optimization of experimental parameters to better compare conformational stability of Native and Fully Deglycosylated mAb glycoforms

Based on the studies above, EPD data analysis permitted a rapid, visual assessment of conformational thermal stability differences between the native and fully deglycosylated IgG1 in the pH range of 3 to 5. Given the size of the temperature steps (2.5 ^{0}C) and pH steps (one pH unit), however, it was difficult to analyze these stability differences in more detail. Thus, a narrower pH range (3.5 to 6 in 0.5 pH increments) with smaller temperature increments (1.25°C) was used to generate a new set of EPDs for both IgG1 mAb forms. Using the same techniques, a more detailed EPD was generated for native protein (Figure 3A) and deglycosylated protein (Figure 3C). The data from these experiments are provided in Supplementary Figures S1 and S2. These improved EPDs resulted in observation of four structural regions including a blue region, where both IgG1 forms are in their stable-native like states, a dark black region, immediately above the blue region probably representing the IgG's in a molten globule-like state. The third region (green) represents a highly structurally altered, extensively unfolded state, while the purple/red region comprising protein that is aggregating and/or precipitating. Comparing the blue regions of the two IgG1 forms to each

other, we see this region covers most of the native state, but covers a much smaller area in the fully deglycosylated form. This more clearly illustrates conformational stability differences between the two IgG1 forms. For example, in the pH range of 3.5-4.5, a noticeable difference in the structural transition temperatures from the native to the molten globular and unfolded states are observed. Transition temperature differences were less substantial in the pH range of 5-6 in the EPD with an ~2-3 ^{0}C stability difference between the two IgG1 forms.

We used the same data set to generate radar charts, a newly developed data visualization method for protein biophysical data.[51] Radar charts for the native and fully deglycosylated IgG1 mAb forms are shown in Figures 3C and 3D, respectively. The reference radar chart guide to the right of the figure shows the position of the five analytical techniques that are being evaluated. Consequently, five radii are projecting out from the center of the chart creating one larger pentagonal image. According to the clustering analysis (K=3), for both IgG forms, the radar charts are divided into three regions, regions I, II, and III. These three regions are similar to the three regions describe above with EPD analysis (i.e., native-like state, structurally altered state, and more extensively altered form with aggregation). Region I is of small quadrilateral shape and corresponds to minimal change in the signals, thus representing the more stable-native like state. Region I covers 60% (Figure 3C) vs. 42% (Figure 3D) of the

total area of the radar charts for the untreated and fully deglycosylated IgG1 mAbs, respectively.

3.3.4 Conformational Stability of Three Different IgG1 mAb Glycoforms Analyzed with Optimized Analytical and Data Visualization Methods

As a final set of experiments, three forms of the IgG1 mAb of varying glyscoylation were analyzed: the untreated control, the fully deglycoyslated PNGase F treated protein, and a partially deglycosylated form generated by treatment with Endo F2 (see Table 1). In addition, as noted above, since various biophysical techniques (Figures 1-3) differed in their ability to detect the destabilizing effect of deglycosylation, we selected the most sensitive methods described above (extrinsic fluorescence spectroscopy with ANS and static light scattering) for the additional experiments described below. In addition, we also employed differential scanning calorimetry (DSC) and differential scanning fluorimetry (DSF) which have previously been shown to be capable of detecting conformational stability differences in deglycosylated IgG1 mAbs.[21, 24, 27, 28, 30-33] Finally, the pH range of analysis was also narrowed to pH 4.0-6.0 to better focus on the structural transition regions and due to complex, irreproducible behavior of DSC and DSF results when heated at pH 3.5 and below (data not shown). The ANS, DSC and DSF data are discussed below and the SLS data for the three mAb samples are provided in Supplementary Figure S3.

The thermal melting curves for the native (black), partially (green), and fully deglycosylated (red) mAbs in the presence of ANS are shown in Figure 4. At 10 ^{0}C, at all pH values tested, the fully deglycosylated IgG1 has the highest ANS intensity value, followed by the partially deglycosylated IgG1. The ANS intensity differences between the three IgG1 glycoforms at 10 ^{0}C decreases as the pH increases. As the temperature is increased, two transitions are evident for the three IgG glycoforms at lower pH with only a single transition observed at higher pH values. The loss of the first transition occurs at pH 5.0, 5.5, and 6.0 for the native, partially deglycosylated and the fully deglycosylated IgG1 mAbs, respectively. The second thermal transition temperature seems to be less affected by the glycosylation state of the mAbs, since the three samples display similar transition temperatures (~68°C at pH 4.5-6.0 and ~65°C at pH 4.0).

Figure 5 shows DSC thermograms of the three IgG1s at pH 4-6. The second and third endothermic peaks observed by DSC are very similar in terms of melting temperatures (74 ^{0}C and 82.5 ^{0}C, respectively). The first endothermic peak onset temperature, however, shows both a solution pH and glycosylation pattern dependence. In the pH range of 4 to 5, the transition onset temperature initiates earlier in the case of the deglycosylated IgG, followed by the partially deglycosylated and then the native IgG1. The latter two samples show similarity in their onset temperature, except at pH 4.5 where the partially deglycosylated IgG1 seems to be less stable than the native molecule. At pH 5, the first peak

starts merging with the second peak for both the native and partially deglycosylated IgGs, ultimately forming a shoulder. The first peak for the fully deglycosylated mAb, however, remains completely separated from the second. At higher pH values of 5.5 and 6, the first transition for both the native and the partially deglycosylated IgG1 forms are completely merged into the second peak, while the first transition in the fully deglycosylated IgG form remains separated from the other thermal transition peaks at pH 5.5.

Using SYPRO orange as an extrinsic dye which shows increased fluorescence upon exposure to more apolar environments such as those associated with structural alterations in proteins, the thermal stability of the different IgG1 samples as a function of pH and temperature was followed (Figure 6). Among the three IgG1 mAb samples and pH values examined, a major transition at 70 ^{0}C was consistently observed except for the partially deglycosylated IgG1 at pH 4, in which the observed transition is very broad and is seen at a lower temperature (62 ^{0}C). Multiple additional transitions (prior to the main transition) are evident for the three IgG1 samples at pH 4.0. A destabilization effect due to carbohydrate removal is evident since both the partially and fully deglycosylated IgG1 forms start unfolding at ~28 ^{0}C compared to the native IgG at ~46 ^{0}C. At pH 4.5 and 5.0, an initial transition is noted at a lower temperature for the partially deglycosylated compared to the native IgG1 although they peak at about the same temperature. The presence of the multiple transitions for the fully deglycosylated IgG1 at pH

4.5 and 5.0, indicates more structurally disrupted states than the other mAb samples at lower temperatures. At pH 5.5 and 6.0, two of the IgG1 forms show a single major structural transition, with the fully deglycosylated form also manifesting a pre-transition at pH 5.5.

Using the results obtained from the four techniques described above, EPDs and radar charts were generated for the three IgG1 samples (Figure 7). Comparing the EPDs of the native (Figure 7A), the partially deglycosylated (Figure 7B), and the fully deglycosylated proteins (Figure 7C), the three EPDs share a common blue and green region. The blue region (based on separate evaluation of the data) signifies the region where the protein is in its stable, native-like state. The green color defines the region where the protein is in a structurally altered state. A third region appears in all the three EPDs, but with different colors and different intensities, corresponds to aggregation/precipitation of the protein. Comparing the blue (native structure) region across the three IgG1 glycoforms at pH 5.5 and 6.0, the native and the partially deglycosylated IgG1 samples have the same transition temperatures near 64 ^{0}C. The fully deglycosylated IgG1, however, starts its transition at lower a temperature (59 ^{0}C). At pH 5.0, the native and the partially deglycosylated IgG1 forms show a transition at 63 ^{0}C and 61 ^{0}C, respectively. For the fully deglycosylated IgG1 at pH 5.0, additional color elements are observed indicating the existence of a partially unfolded, conformationally disrupted state at this pH (see the ANS and

DSF data in Figures 4 and 6, respectively). At pH 4.0 and 4.5, the native IgG1 is less stable, with structural transitions at 50 and 55 ^{0}C, respectively. The partially deglycosylated IgG1 at pH 4 and 4.5 develops an additional light blue region, consistent with the existence of a partially unfolded state. (See the ANS data in Figure 4). The fully deglycosylated IgG1 at pH 4.5 shows a more structurally disrupted state compared to the other IgG1 forms, while an additional green region is observed for the fully deglycosylated IgG1 form at pH 4.0, indicating the existence of the extensively structurally altered state even at lower temperatures.

Radar charts were generated from the same data as shown on the right side of Figure 7. Spanning the same pH and temperature range examined with colored EPDs, similar regions were identified for the different IgG1 glycoforms indicating the existence of different conformational states (in the radar plots, structural transitions were identified by clustering analysis with k=3 as described in the methods section). The native-like, stable region for the untreated, control mAb (Figure 7A), the partially deglycosylated mab (Figure 7B), and the fully deglycosylated protein (Figure 7C) are depicted as dot-like entities (minimal structural transitions) and occupy 67, 52 and 40% of the radar chart's total area, respectively. Based on this simple analysis of the areas in the radar plots representative of native-like, stable form of the mAb, the effect of glycosylation

on IgG1 conformational stability is readily evident, with the decreased area qualitatively proportional to the enzymatic truncation of sugar moieties.

3.4 Discussion

In this study, a direct comparison of the structure and conformational stability of an IgG1 mAb and its truncated glycoforms was performed with a variety of biophysical techniques, over a wide range of solution conditions. Data was also analyzed with two vector based technologies. The different glycoforms were prepared by enzymatic treatments. Mass spectrometric analysis of the reduced IgG1 mAbs (Table 1) directly demonstrated that the partial and full deglycosylation was successful since the measured molecular weights of the heavy chain of the mAb glycoforms were in close proximity to the expected values. The native mAb contained the expected mixture of glycan structures for SP20 cells, in which the G2F/G1F, G1F/G1F and G2F/G0F glycosylation patterns are the dominant glycosylated forms as described elsewhere.[43] The partially deglycosylated mAb, produced by enzymatic treatment with Endo F2, contained a Fucose-GlcNac as a major glycan species structures consistent with the theoretical (average) mass. The presence of the fully deglycosylated protein, achieved by digesting with PNGase F, was evident from MS analysis (Table 1), where complete removal of the glycan and subsequent deamidation of the backbone Asn to Asp, was achieved as a result of the enzymatic reaction.

The destabilizing effects of removing the N-linked glycan in the C_H2 domain of the Fc region of IgGs has previously been demonstrated by selected techniques under certain conditions. In this regard, the ability of EPDs and radar charts to detect changes in conformational stability due to differences in post-translational modifications of a protein was examined in this work in a "model system" using three different glycoforms of an IgG1 mAb. Although this work covered a wider range of solution conditions, experimental techniques and data visualization approaches, some of the conditions examined here overlap with previous studies. The results with the IgG1 mAb of this work are consistent with previous reports with other IgG1 antibodies. For example, as a result of complete or partial removal of the C_H2 domain N linked glycan, destabilization of the C_H2 domain of an IgG1 has been shown by DSC. [22, 26, 30, 31, 33] In addition, an increase in fluorescence intensity spectra using intrinsic (Trp) and extrinsic (SYPRO orange dye) fluorescence spectroscopy was seen with full deglycosylation.[33] Differential scanning fluorimetry (DSF) has been used to evaluate conformational stability differences of an IgG1 in different formulation buffers.[23] The effect upon complete or partial removal of the N-linked glycan on the conformational stability of purified Fc proteins has also recently been evaluated using DSC,[21, 27, 28] as well as CD and extrinsic (ANS) fluorescence spectroscopy.[27] Results from DSC indicated a destabilization effect on the C_H2 domain of the Fc protein upon complete or partial deglycosylation, while results from CD and extrinsic

fluorescence indicated a significant destabilization effect under acidic conditions and less of an effect at neutral to basic pH.

The results of this work demonstrate a two-step methodology to evaluate differences in the conformational stability between several mAb glycoforms. First, "standard" EPD data analysis was used to screen mAb conformational stability using a variety of methods that probe different aspects of structure over a wide range of an environmental stresses (e.g., temperature and pH). Second, based on these initial results, an additional evaluation was conducted using the most sensitive experimental methods, with a focus on a narrower range of environmental conditions (near values associated with structural changes in the protein), using a combination of EPDs and radar charts for data visualization. For example, when comparing the untreated to the fully deglycosylated IgG1, a noticeable destabilization effect was first evaluated over a wide range of pH and temperature conditions by a variety of biophysical techniques (Figures 1 and 2). This initial evaluation showed the destabilization effects under mildly acidic conditions with some variability between the different analytical techniques in terms of their ability to detect structural changes as a result of deglycosylation. Based on these results, data were collected under "zoomed-in" conditions focusing on an optimal pH range (4.0-6.0 in 0.5 increments), where notable structural changes are detected, combined with 1.25 ^{0}C temperature steps to improve resolution (over the initially used 2.5 ^{0}C increments). We also

implemented the most sensitive analytical methods including ANS fluorescence spectroscopy, DSC, DSF and light scattering (LS). In addition, we added a partially deglycosylated mAb glycoform to better assess the sensitivity of this methodology. The "zoomed-in" EPDs and radar charts from these three IgG1 glycoforms (Figure 7) clearly reflect differences in the major structural variations between the three samples. Radar charts have the advantage of reflecting the individual technique(s) which reflect the structural change at an identifiable site in the diagram. For the three mAb glycoforms studied, radar charts clearly point to an ANS-DSF influence in detected structural changes associated with region II, with LS becoming a major tool for monitoring aggregation (Region III) at higher temperatures.

Although this work demonstrates the ability to compare conformational stability trends across mAb samples of known glycosylation content, the generation of EPDs and Radar charts for more formal evaluations such as regulatory comparability studies currently has practical limitations. For example, although visualization and rank ordering of structural transitions between samples is clearly useful for semi-qualitative comparisons of conformational stability, it still requires expert analysis by individual scientists of the individual biophysical data sets to confirm (and if necessary adjust) readouts from the initial clustering analysis. This is due to a combination of potential effects including noise in raw data, propagation of error when combining data sets across different instruments

and experiments, and limitations of clustering analysis.[51] Ongoing work in our laboratory is evaluating and addressing these topics including more advanced mathematical treatments to potentially allow for statistical comparisons and independence from a separate expert review. For example, comparative signature diagrams are an alternative approach recently described [53] to statistically compare differences in spectral readouts from different instruments when evaluating two protein samples across different temperatures and pH values.

In summary, this work combines data sets from multiple biophysical techniques that monitor different aspects of a protein's higher-order structural stability as function of environmental stress (e.g., secondary structure by CD, tertiary structure by fluorescence spectroscopy, quaternary structure and aggregation by light scattering). Data visualization by EPDs and Radar charts allows for convenient and rapid analysis of these large biophysical stability data sets. We also incorporated conformational stability data from DSC and DSF in EPD and Radar charts construction, for the first time, due to the sensitivity of these two methods in detecting more subtle structural stability differences between the different mAb glycoforms across different solution conditions. By assessing conformational stability as a function of environmental stress (pH, temperature), subtle differences in structural integrity may potentially be detected when these differences are not readily apparent when monitored using lower resolution methods under non-stressed conditions (analysis at low temperature at

neutral pH). Thus, evaluation of conformational stability differences may not only be an effective surrogate to monitor subtle differences in higher order structure between protein samples as part of formulation development, but also a useful complement to traditional accelerated stability data often used in analytical comparability studies.

Table 1: Mass spectrometry results of the heavy chain region of reduced samples of the IgG1 mAb. First column shows the masses of the PNGase F and Endo F2 treated IgG1 mAb obtained from MS analysis along with the masses measured for the two most abundant glycoforms (G0F and G1F) of the untreated mAb. The second, third and fourth columns show observed change in mass, predicted change in mass, and modification expected due to enzymatic treatment of the IgG1 mAb, respectively.

IgG1 Glycoform	***Heavy Chain (Da)***	***Δ mass observed (Da)***	***Δ mass predicted (Da)***	***Modification of Asn 297***
PNGase F treated	*49168.3**	-	-	*Deglycosylation, $N \rightarrow D$*
Endo F2 treated	*49516.8*	*+348.5*	*+348.3*	*+GlcNAc-Fucose*
Untreated:**				
G0F glycosylated	*50612.5*	*+1445*	*+1444.6*	*+G0F*
G1F glycosylated	*50774.7*	*+1607*	*+1606.5*	*+G1F*

*The theoretical mass of the nonglycosylated mAb heavy chain is 49167.3 Da.

**G0F, G1F are two main peaks used to follow deglycosylation (Supplemental figure 4)

Abbreviations: N: Asparagine, D: Aspartic acid, GlcNAc: N-acetylglucosamine, F: Fucose, G: Galactose, G0F: $GlcNAc_2Man_3GlcNAc_2Fuc$, G1F: $GalGlcNAc_2Man_3GlcNAc_2Fuc$.

Figure 1:

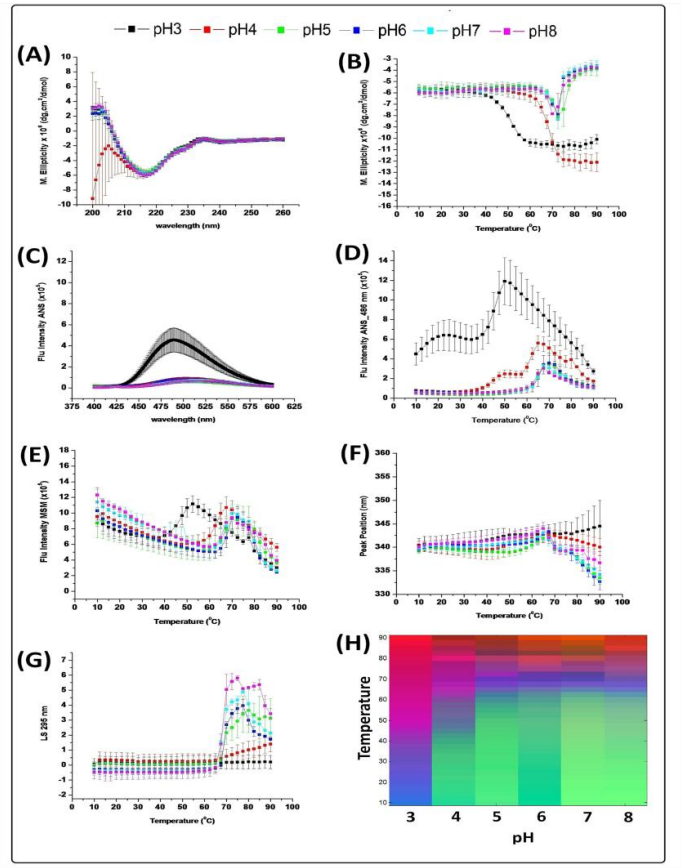

Biophysical characterization of the untreated (control) IgG1 mAb as a function of temperature and pH. (A) CD spectra at 10 ^{0}C, (B) CD intensity change at 217 nm with temperature, (C) ANS spectra at 10 ^{0}C, (D) ANS melting curve at 486 nm, (E) Fluorescence intensity vs. temperature, (F) Fluorescence peak position changes with temperatures, (G) Static light scattering intensity change with temperature, and (H) empirical phase diagram analysis of data. Data shown for n=3 measurements.

Figure 2:

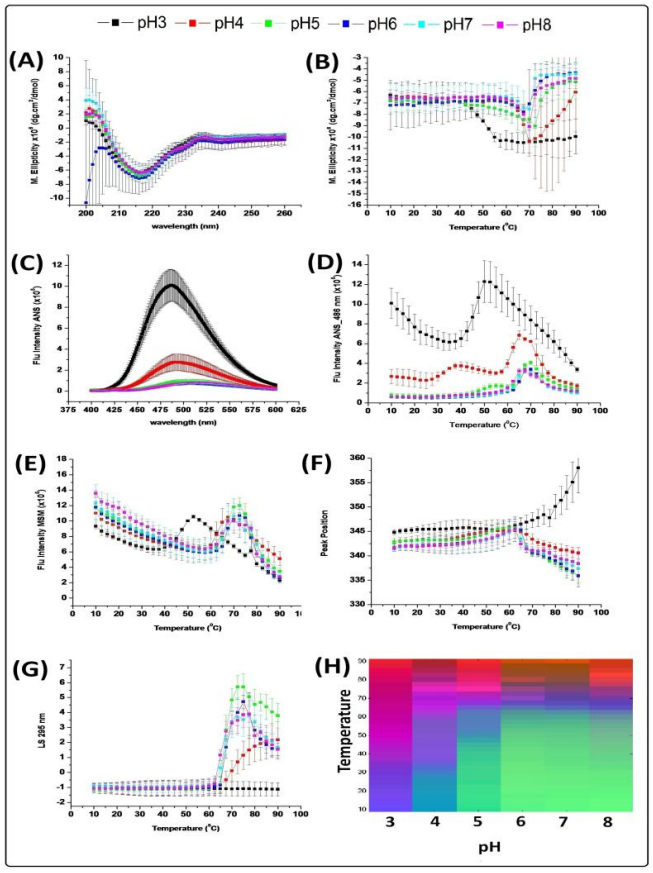

Biophysical characterization of PNGase treated, fully deglycosylated IgG1 mAb as a function of temperature and pH. (A) CD spectra at 10 ^{0}C, (B) CD intensity change at 217 nm with temperature, (C) ANS spectra at 10 ^{0}C, (D) ANS melting curve at 486 nm, (E) Fluorescence intensity vs. temperature, (F) Fluorescence peak position changes with temperatures, (G) Static light scattering intensity change with temperature, and (H) empirical phase diagram analysis of data. Data shown for n=3 measurements.

Figure 3:

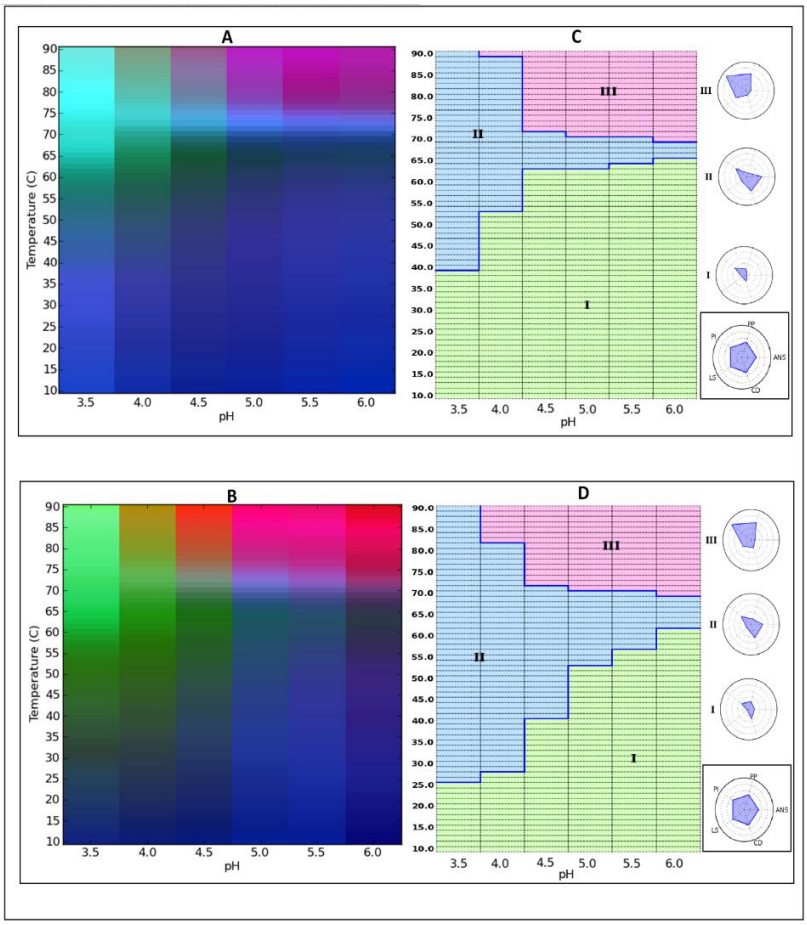

Empirical Phase Diagram (EPD) and Radar Chart analysis of the conformational stability of IgG1 mAb samples. (A) EPD of untreated (control) IgG1, (C) radar chart of untreated (control) IgG1, (B) EPD of fully deglycosylated IgG1, and (D) radar chart of fully deglycosylated IgG1. The temperature ramp was in 1.25°C increments.

Figure 4:

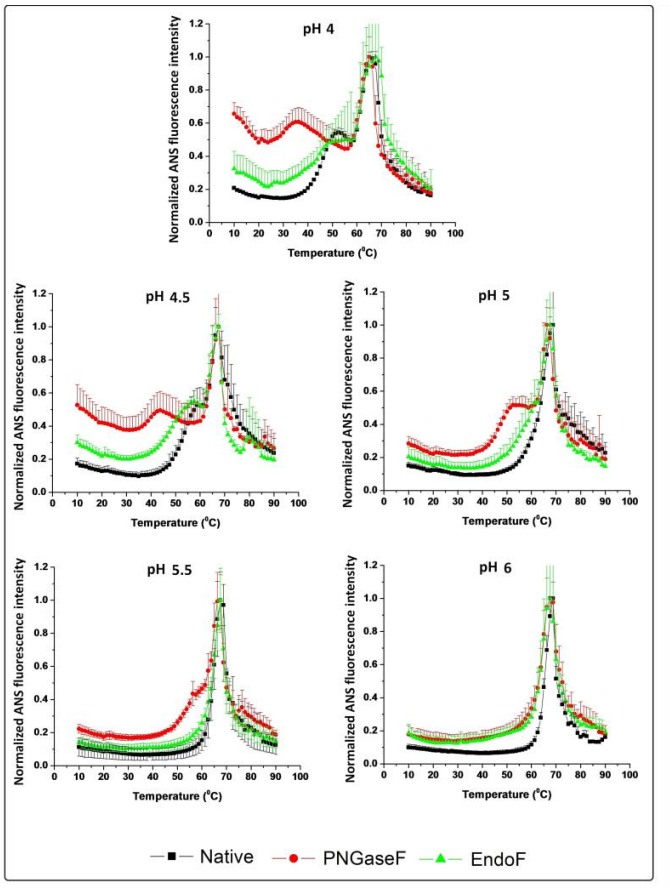

Normalized ANS fluorescence intensity change as a function of temperature in the presence of untreated (control) IgG1 (black line), partially deglycosylated IgG1 (green line), and fully deglycosylated IgG1 (red line) from pH 4 to 6. Normalized results were generated by fitting the data to be equal to 1 at the maxima and to 0 at the minima for incorporation into the EPDs and radar charts. Curves shown here are averages of three runs.

Figure 5:

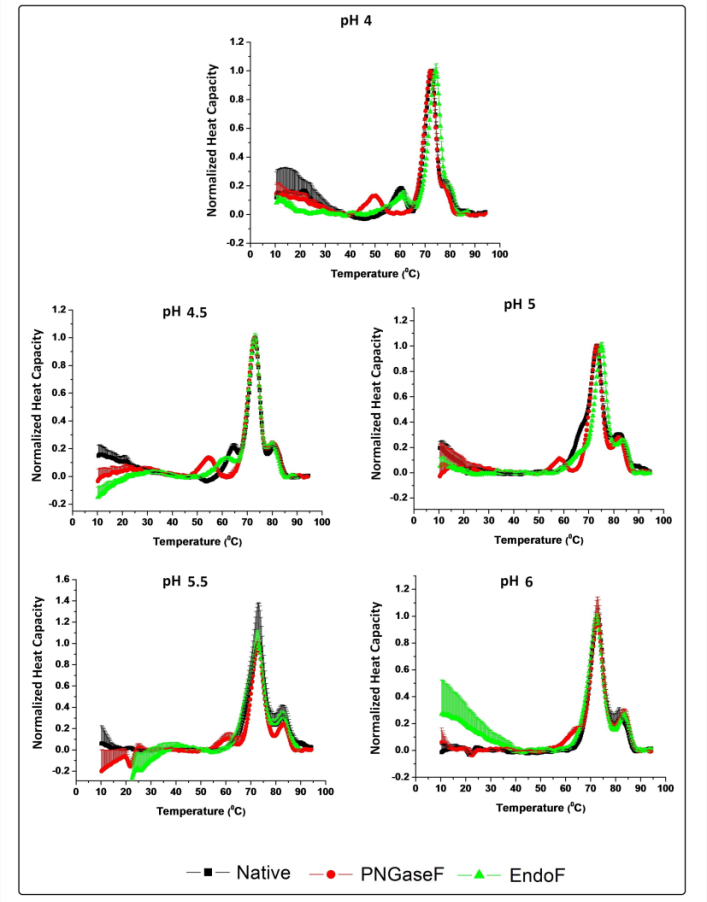

Differential scanning calorimetry (DSC) analysis of untreated (control) IgG1 (black line), partially deglycosylated IgG1 (green line), and fully deglycosylated IgG1 (red line) from pH 4 to 6. Normalized heat capacity changes were generated by fitting the data to be equal to 1 at the maxima and to 0 at the minima for incorporation into the EPDs and radar charts. Curves shown here are averages of three runs.

Figure 6:

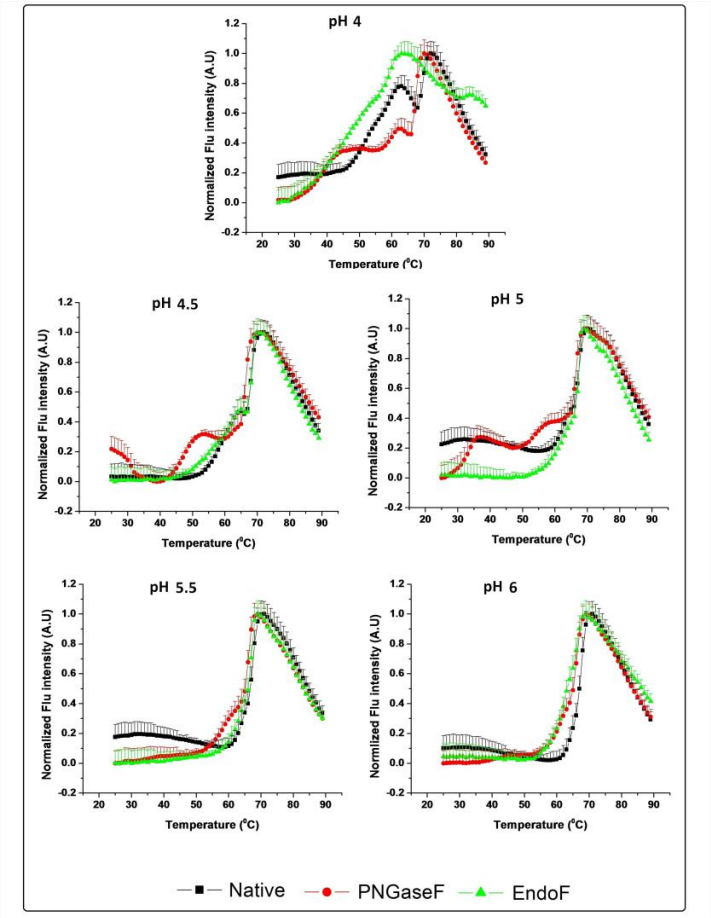

Differential scanning fluorimetry (DSF) analysis of untreated (control) IgG1 (black line), the partially deglycosylated IgG1 (green line), and the fully deglycosylated IgG1 (red line) from pH 4 to 6. Normalized results were generated by fitting the data to be equal to 1 at the maxima and to 0 at the minima for incorporation into the EPDs and radar charts. Curves shown here are averages of three runs.

Figure 7:

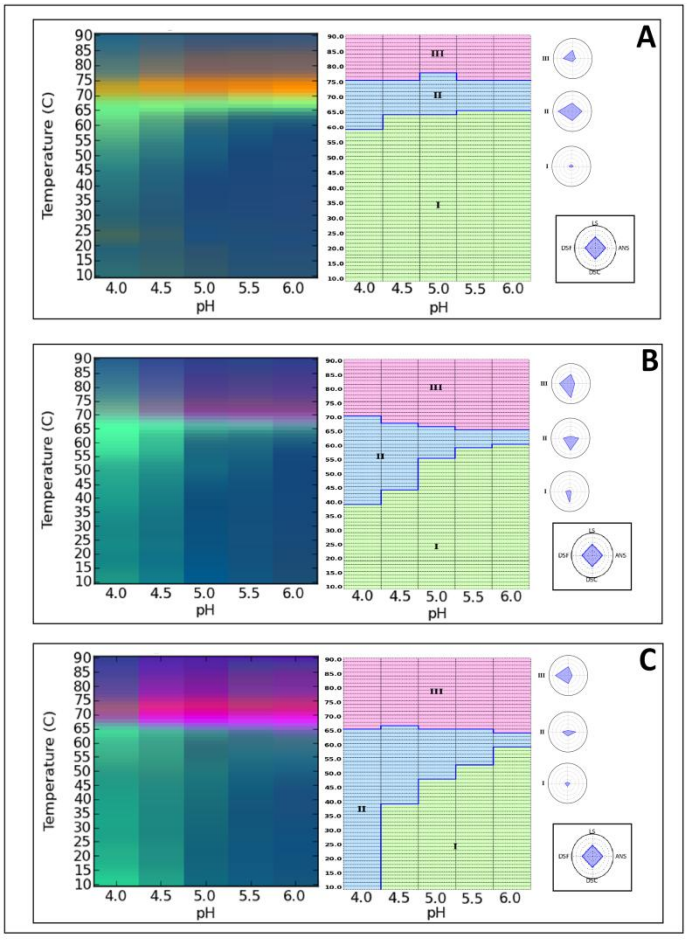

Empirical Phase Diagram (EPD) and Radar Chart analysis of the conformational stability of IgG1 mAb samples. Panel A shows the EPD (left) and the radar chart (right) for the untreated (control) IgG1. Panel B shows the EPD (left) and the radar chart (right) for the partially deglycosylated mAb due to Endo F2 treatment. Panel C shows the EPD (left) and the radar chart (right) for the fully deglycosylated mAb due to PNGase F treatment.

Supplemental Figure S1:

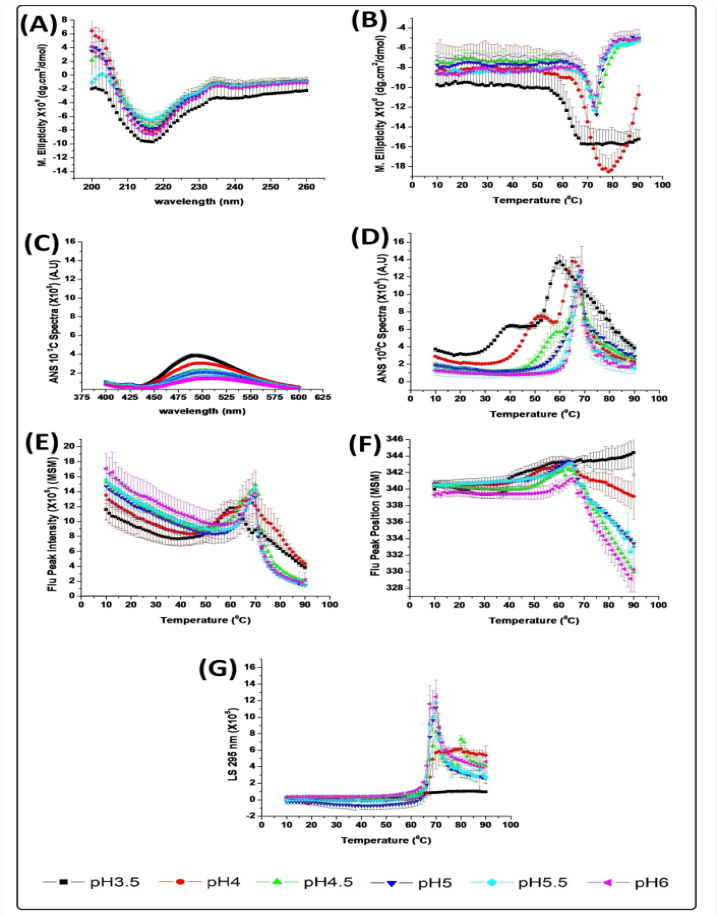

Biophysical characterization of untreated (control) IgG1 mAb showing (A) CD spectra at 10 ^{0}C, (B) CD intensity change at 217 nm with temperature, (C) ANS spectra at 10 ^{0}C, (D) ANS melting curve at 486 nm, (E) Fluorescence intensity and peak position changes with temperatures, and (G) Static light scattering intensity change with temperature. Temperature ramp was in 1.25°C increments. Curves shown here are averages of three runs.

Supplemental Figure S2:

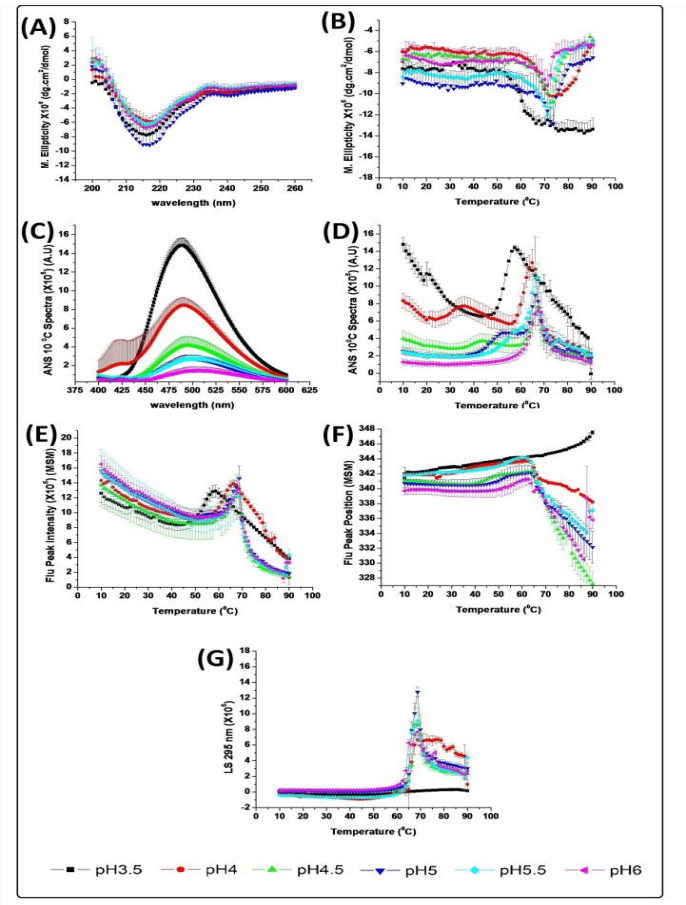

Biophysical characterization of fully deglycosylated IgG1 mAb showing (A) CD spectra at 10 ^{0}C, (B) CD intensity change at 217 nm with temperature, (C) ANS spectra at 10 ^{0}C, (D) ANS melting curve at 486 nm, (E) Fluorescence intensity and peak position changes with temperatures, and (G) Static light scattering intensity change with temperature. Temperature ramp was in 1.25°C increments. Curves shown here are averages of three runs.

Supplementary Figure S3:

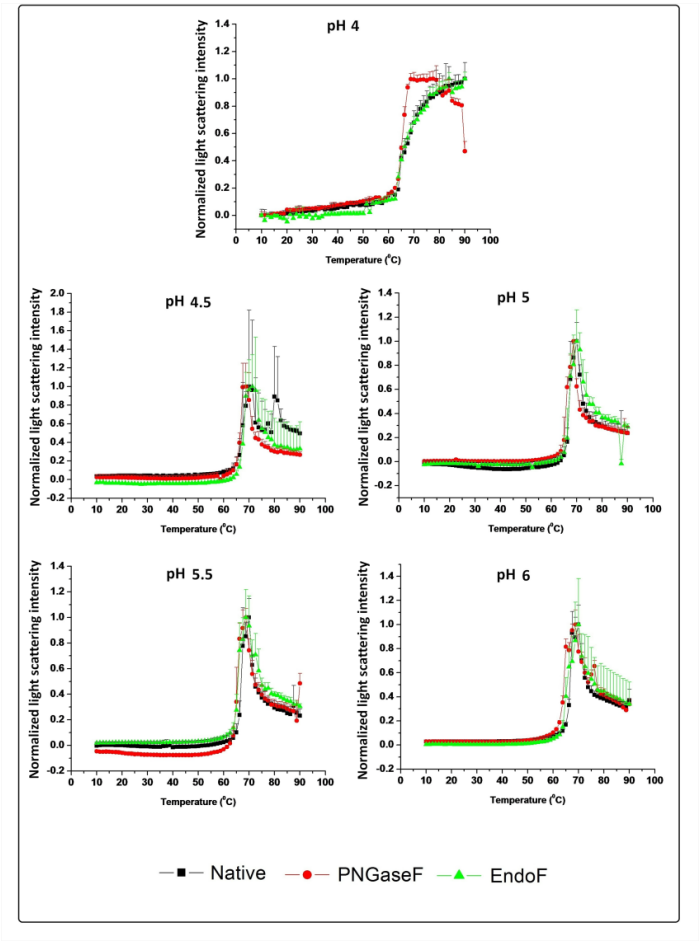

Static light scattering intensity changes as a function of temperature for the untreated (control) IgG1 (black line), the partially deglycosylated IgG1 (green line), and the fully deglycosylated IgG1 (red line) from pH 4 to 6. Normalized results were generated by fitting the data to be equal to 1 at the maxima and to 0 at the minima for incorporation into the EPDs and radar charts. Curves shown here are averages of three runs.

3.5 References

1) Reichert, J. M., Marketed therapeutic antibodies compendium. *mAbs* **2012,** *4* (3), 413-415.

2) Aaron L. Nelson, E. D., Janice M. Reichert, Development trends for human monoclonal antibody therapeutics. *Nature Reviews Drug Discovery* **2010,** *9*, 767-774.

3) Jefferis, R., The antibody paradigm: present and future development as a scaffold for biopharmaceutical drugs. *Biotechnology and Genetic Engineering Reviews* **2009,** *26* (1), 1-41.

4) Wang, W.; Singh, S.; Zeng, D. L.; King, K.; Nema, S., Antibody structure, instability, and formulation. *Journal of Pharmaceutical Sciences* **2007,** *96* (1), 1-26.

5) Jefferis, R., Isotype and glycoform selection for antibody therapeutics. *Archives of Biochemistry and Biophysics* **2012,** *526* (2), 159-166.

6) Arnold, J. N.; Wormald, M. R.; Sim, R. B.; Rudd, P. M.; Dwek, R. A., The Impact of Glycosylation on the Biological Function and Structure of Human Immunoglobulins. *Annual Review of Immunology* **2007,** *25* (1), 21-50.

7) Kanda, Y.; Yamada, T.; Mori, K.; Okazaki, A.; Inoue, M.; Kitajima-Miyama, K.; Kuni-Kamochi, R.; Nakano, R.; Yano, K.; Kakita, S.; Shitara, K.; Satoh, M., Comparison of biological activity among

nonfucosylated therapeutic IgG1 antibodies with three different N-linked Fc oligosaccharides: the high-mannose, hybrid, and complex types. *Glycobiology* **2007,** *17* (1), 104-118.

8) Jefferis, R., Glycosylation as a strategy to improve antibody-based therapeutics. *Nat Rev Drug Discov* **2009,** *8* (3), 226-234.

9) Jefferis, R.; Lund, J., Interaction sites on human IgG-Fc for FcγR: current models. *Immunology Letters* **2002,** *82* (1–2), 57-65.

10) Boyd, P. N.; Lines, A. C.; Patel, A. K., The effect of the removal of sialic acid, galactose and total carbohydrate on the functional activity of Campath-1H. *Molecular Immunology* **1995,** *32* (17-18), 1311-1318.

11) Radaev, S.; Sun, P. D., Recognition of IgG by Fcγ Receptor. *Journal of Biological Chemistry* **2001,** *276* (19), 16478-16483.

12) Yu, M.; Brown, D.; Reed, C.; Chung, S.; Lutman, J.; Stefanich, E.; Wong, A.; Stephan, J.-P.; Bayer, R., Production, characterization and pharmacokinetic properties of antibodies with N-linked Mannose-5 glycans. *mAbs* **2012,** *4* (4), 475-487.

13) Putnam, W. S.; Prabhu, S.; Zheng, Y.; Subramanyam, M.; Wang, Y.-M. C., Pharmacokinetic, pharmacodynamic and immunogenicity comparability assessment strategies for monoclonal antibodies. *Trends in Biotechnology* **2010,** *28* (10), 509-516.

14) Liu, L.; Stadheim, A.; Hamuro, L.; Pittman, T.; Wang, W.; Zha, D.; Hochman, J.; Prueksaritanont, T., Pharmacokinetics of IgG1 monoclonal antibodies produced in humanized Pichia pastoris with specific glycoforms: A comparative study with CHO produced materials. *Biologicals* **2011,** *39* (4), 205-210.

15) Alessandri, L.; Ouellette, D.; Acquah, A.; Rieser, M.; LeBlond, D.; Saltarelli, M.; Radziejewski, C.; Fujimori, T.; Correia, I., Increased serum clearance of oligomannose species present on a human IgG1 molecule. *mAbs* **2012,** *4* (4), 509-520.

16) Goetze, A. M.; Liu, Y. D.; Zhang, Z.; Shah, B.; Lee, E.; Bondarenko, P. V.; Flynn, G. C., High-mannose glycans on the Fc region of therapeutic IgG antibodies increase serum clearance in humans. *Glycobiology* **2011,** *21* (7), 949-959.

17) Bumbaca, D.; Boswell, C.; Fielder, P.; Khawli, L., Physiochemical and Biochemical Factors Influencing the Pharmacokinetics of Antibody Therapeutics. *The AAPS Journal* **2012,** *14* (3), 554-558.

18) Chen, X.; Liu, Y. D.; Flynn, G. C., The effect of Fc glycan forms on human IgG2 antibody clearance in humans. *Glycobiology* **2009,** *19* (3), 240-249.

19) Solá, R. J.; Griebenow, K., Effects of glycosylation on the stability of protein pharmaceuticals. *Journal of Pharmaceutical Sciences* **2009,** *98* (4), 1223-1245.

20) Krapp, S.; Mimura, Y.; Jefferis, R.; Huber, R.; Sondermann, P., Structural Analysis of Human IgG-Fc Glycoforms Reveals a Correlation Between Glycosylation and Structural Integrity. *Journal of Molecular Biology* **2003,** *325* (5), 979-989.

21) Mimura, Y.; Church, S.; Ghirlando, R.; Ashton, P. R.; Dong, S.; Goodall, M.; Lund, J.; Jefferis, R., The influence of glycosylation on the thermal stability and effector function expression of human IgG1-Fc: properties of a series of truncated glycoforms. *Molecular Immunology* **2000,** *37* (12-13), 697-706.

22) Ha, S.; Ou, Y.; Vlasak, J.; Li, Y.; Wang, S.; Vo, K.; Du, Y.; Mach, A.; Fang, Y.; Zhang, N., Isolation and characterization of IgG1 with asymmetrical Fc glycosylation. *Glycobiology* **2011,** *21* (8), 1087-1096.

23) He, F.; Hogan, S.; Latypov, R. F.; Narhi, L. O.; Razinkov, V. I., High throughput thermostability screening of monoclonal antibody formulations. *Journal of Pharmaceutical Sciences* **2010,** *99* (4), 1707-1720.

24) Wen J, Jiang Y, Narhi L. Effect of carbohydrate on thermal stability of antibodies. *Am Pharm Rev* **2008** 11:98–104.

25) Ha, S.; Wang, Y.; Rustandi, R. R., Biochemical and biophysical characterization of humanized IgG1 produced in Pichia pastoris. *mAbs* **2011,** *3* (5), 453-460.

26) Hari, S. B.; Lau, H.; Razinkov, V. I.; Chen, S.; Latypov, R. F., Acid-Induced Aggregation of Human Monoclonal IgG1 and IgG2: Molecular Mechanism and the Effect of Solution Composition. *Biochemistry* **2010,** *49* (43), 9328-9338.

27) Li, C. H.; Narhi, L. O.; Wen, J.; Dimitrova, M.; Wen, Z.-q.; Li, J.; Pollastrini, J.; Nguyen, X.; Tsuruda, T.; Jiang, Y., Effect of pH, Temperature, and Salt on the Stability of Escherichia coli- and Chinese Hamster Ovary Cell-Derived IgG1 Fc. *Biochemistry* **2012,** *51* (50), 10056-10065.

28) Latypov, R. F.; Hogan, S.; Lau, H.; Gadgil, H.; Liu, D., Elucidation of Acid-induced Unfolding and Aggregation of Human Immunoglobulin IgG1 and IgG2 Fc. *Journal of Biological Chemistry* **2012,** *287* (2), 1381-1396.

29) Lu, Y.; Westland, K.; Ma, Y.-h.; Gadgil, H., Evaluation of effects of Fc domain high-mannose glycan on antibody stability. *Journal of Pharmaceutical Sciences* **2012,** *101* (11), 4107-4117.

30) Liu, H.; Bulseco, G.-G.; Sun, J., Effect of posttranslational modifications on the thermal stability of a recombinant monoclonal antibody. *Immunology Letters* **2006,** *106* (2), 144-153.

31) Hristodorov, D.; Fischer, R.; Joerissen, H.; Müller-Tiemann, B.; Apeler, H.; Linden, L., Generation and Comparative Characterization of Glycosylated and Aglycosylated Human IgG1 Antibodies. *Molecular Biotechnology* **2013,** *53* (3), 326-335.

32) Ghirlando, R.; Lund, J.; Goodall, M.; Jefferis, R., Glycosylation of human IgG-Fc: influences on structure revealed by differential scanning micro-calorimetry. Immunology Letters **1999**, 68 (1), 47-52.

33) Kai Zheng, C. B. a. R. B., The impact of glycosylation on monoclonal antibody conformation and stability. *mAbs* **2011,** *3* (6), 568-576.

34) Raju, T. S.; Scallon, B. J., Glycosylation in the Fc domain of IgG increases resistance to proteolytic cleavage by papain. *Biochemical and Biophysical Research Communications* **2006,** *341* (3), 797-803.

35) Raju, T. S.; Scallon, B., Fc Glycans Terminated with N-Acetylglucosamine Residues Increase Antibody Resistance to Papain. *Biotechnology Progress* **2007,** *23* (4), 964-971.

36) Wu, S.-J.; Luo, J.; O'Neil, K. T.; Kang, J.; Lacy, E. R.; Canziani, G.; Baker, A.; Huang, M.; Tang, Q. M.; Raju, T. S.; Jacobs, S. A.; Teplyakov, A.; Gilliland, G. L.; Feng, Y., Structure-based engineering of a monoclonal antibody for improved solubility. *Protein Engineering Design and Selection* **2010,** *23* (8), 643-651.

37) Middaugh, C. R.; Litman, G. W., Atypical glycosylation of an IgG monoclonal cryoimmunoglobulin. *Journal of Biological Chemistry* **1987,** *262* (8), 3671-3.

38) Kayser, V.; Chennamsetty, N.; Voynov, V.; Forrer, K.; Helk, B.; Trout, B. L., Glycosylation influences on the aggregation propensity of

therapeutic monoclonal antibodies. *Biotechnology Journal* **2011,** *6* (1), 38-44.

39) Chennamsetty, N.; Helk, B.; Voynov, V.; Kayser, V.; Trout, B. L., Aggregation-Prone Motifs in Human Immunoglobulin G. *Journal of Molecular Biology* **2009,** *391* (2), 404-413.

40) Borrok, M. J.; Jung, S. T.; Kang, T. H.; Monzingo, A. F.; Georgiou, G., Revisiting the Role of Glycosylation in the Structure of Human IgG Fc. *ACS Chemical Biology* **2012,** *7* (9), 1596-1602.

41) Chirino, A. J.; Mire-Sluis, A., Characterizing biological products and assessing comparability following manufacturing changes. *Nat Biotech* **2004,** *22* (11), 1383-1391.

42) Schiestl, M.; Stangler, T.; Torella, C.; Cepeljnik, T.; Toll, H.; Grau, R., Acceptable changes in quality attributes of glycosylated biopharmaceuticals. *Nat Biotech* **2011,** *29* (4), 310-312.

43) Lubiniecki, A.; Volkin, D. B.; Federici, M.; Bond, M. D.; Nedved, M. L.; Hendricks, L.; Mehndiratta, P.; Bruner, M.; Burman, S.; DalMonte, P.; Kline, J.; Ni, A.; Panek, M. E.; Pikounis, B.; Powers, G.; Vafa, O.; Siegel, R., Comparability assessments of process and product changes made during development of two different monoclonal antibodies. *Biologicals* **2011,** *39* (1), 9-22.

44) Schenerman, M. A.; Hope, J. N.; Kletke, C.; Singh, J. K.; Kimura, R.; Tsao, E. I.; Folena-Wasserman, G., Comparability Testing of a

Humanized Monoclonal Antibody (Synagis®) to Support Cell Line Stability, Process Validation, and Scale-Up for Manufacturing. *Biologicals* **1999,** *27* (3), 203-215.

45) Jiang, X.-R.; Song, A.; Bergelson, S.; Arroll, T.; Parekh, B.; May, K.; Chung, S.; Strouse, R.; Mire-Sluis, A.; Schenerman, M., Advances in the assessment and control of the effector functions of therapeutic antibodies. *Nat Rev Drug Discov* **2011,** *10* (2), 101-111.

46) Federici, M.; Lubiniecki, A.; Manikwar, P.; Volkin, D. B., Analytical lessons learned from selected therapeutic protein drug comparability studies. *Biologicals* **2013,** *41* (3), 131-147.

47) Bhambhani, A.; Kissmann, J. M.; Joshi, S. B.; Volkin, D. B.; Kashi, R. S.; Middaugh, C. R., Formulation design and high-throughput excipient selection based on structural integrity and conformational stability of dilute and highly concentrated IgG1 monoclonal antibody solutions. *Journal of Pharmaceutical Sciences* **2012,** *101* (3), 1120-1135.

48) Cheng, W.; Joshi, S. B.; He, F.; Brems, D. N.; He, B.; Kerwin, B. A.; Volkin, D. B.; Middaugh, C. R., Comparison of high-throughput biophysical methods to identify stabilizing excipients for a model IgG2 monoclonal antibody: Conformational stability and kinetic aggregation measurements. *Journal of Pharmaceutical Sciences* **2012,** *101* (5), 1701-1720.

49) Hu, L.; Joshi, S. B.; Andra, K. K.; Thakkar, S. V.; Volkin, D. B.; Bann, J. G.; Middaugh, C. R., Comparison of the structural stability and dynamic

properties of recombinant anthrax protective antigen and its 2-fluorohistidine-labeled analogue. *Journal of Pharmaceutical Sciences* **2012,** *101* (11), 4118-4128.

50) Alsenaidy, M. A.; Wang, T.; Kim, J. H.; Joshi, S. B.; Lee, J.; Blaber, M.; Volkin, D. B.; Middaugh, C. R., An empirical phase diagram approach to investigate conformational stability of "second-generation" functional mutants of acidic fibroblast growth factor-1. *Protein Science* **2012,** *21* (3), 418-432.

51) Kim, J. H.; Iyer, V.; Joshi, S. B.; Volkin, D. B.; Middaugh, C. R., Improved data visualization techniques for analyzing macromolecule structural changes. *Protein Science* **2012,** *21* (10), 1540-1553.

52) Maddux, N. R.; Rosen, I. T.; Hu, L.; Olsen, C. M.; Volkin, D. B.; Middaugh, C. R., An improved methodology for multidimensional high-throughput preformulation characterization of protein conformational stability. *Journal of Pharmaceutical Sciences* **2012,** *101* (6), 2017-2024.

53) Iyer, V.; Maddux, N.; Hu, L.; Cheng, W.; Youssef, A. K.; Winter, G.; Joshi, S. B.; Volkin, D. B.; Middaugh, C. R., Comparative signature diagrams to evaluate biophysical data for differences in protein structure across various formulations. *Journal of Pharmaceutical Sciences* **2013,** *102* (1), 43-51.

54) Houde, D.; Arndt, J.; Domeier, W.; Berkowitz, S.; Engen, J. R., Characterization of IgG1 Conformation and Conformational Dynamics by

Hydrogen/Deuterium Exchange Mass Spectrometry. *Analytical Chemistry* **2009,** *81* (7), 2644-2651.

55) Houde, D.; Peng, Y.; Berkowitz, S. A.; Engen, J. R., Post-translational Modifications Differentially Affect IgG1 Conformation and Receptor Binding. *Molecular & Cellular Proteomics* **2010,** *9* (8), 1716-1728.

56) Gong, R.; Vu, B. K.; Feng, Y.; Prieto, D. A.; Dyba, M. A.; Walsh, J. D.; Prabakaran, P.; Veenstra, T. D.; Tarasov, S. G.; Ishima, R.; Dimitrov, D. S., Engineered Human Antibody Constant Domains with Increased Stability. *Journal of Biological Chemistry* **2009,** *284* (21), 14203-14210.

57) Wang, X.; Kumar, S.; Buck, P. M.; Singh, S. K., Impact of deglycosylation and thermal stress on conformational stability of a full length murine igG2a monoclonal antibody: Observations from molecular dynamics simulations. *Proteins: Structure, Function, and Bioinformatics* **2013,** *81* (3), 443-460.

58) Shi, S.; Liu, J.; Joshi, S. B.; Krasnoperov, V.; Gill, P.; Middaugh, C. R.; Volkin, D. B., Biophysical characterization and stabilization of the recombinant albumin fusion protein sEphB4–HSA. *Journal of Pharmaceutical Sciences* **2012,** *101* (6), 1969-1984.

59) Manikwar, P.; Majumdar, R.; Hickey, J. M.; Thakkar, S. V.; Samra, H. S.; Sathish, H. A.; Bishop, S. M.; Middaugh, C. R.; Weis, D. D.; Volkin, D. B., Correlating excipient effects on conformational and storage stability of an IgG1 monoclonal antibody with local dynamics as measured by

hydrogen/deuterium-exchange mass spectrometry. *Journal of Pharmaceutical Sciences* **2013**, 102 (7), 2136-5151.

60) Majumdar, R.; Manikwar, P.; Hickey, J. M.; Samra, H. S.; Sathish, H. A.; Bishop, S. M.; Middaugh, C. R.; Volkin, D. B.; Weis, D. D., Effects of Salts from the Hofmeister Series on the Conformational Stability, Aggregation Propensity, and Local Flexibility of an IgG1 Monoclonal Antibody. *Biochemistry* **2013,** *52* (19), 3376-3389.

Chapter 4

Global physical stability assessments of IgG1-Fc proteins: effects of glycosylation site occupancy and site 297 charge variations

4.1 Introduction

Monoclonal antibodies (mAbs) are well established as the leading class of protein-based drugs due to their high target specificity and long half lifes.[1, 2] The majority of mAbs developed to date are IgG1proteins, consisting of four polypeptide chains (two heavy and two light chains) that arrange into 12 Ig domains that form into a Y-shaped molecule with two antigen binding (Fab) regions and one crystallizable (Fc) region. The homodimeric, horseshoe shaped, Fc region contains two interacting C_H3 domains in the C-terminus end and two C_H2 domains in the N-terminus end of the molecule. The two C_H2 domains interact with each other through two buried N-linked glycosylation sites located at Asn 297 of each C_H2 domain.

Glycosylation of the Asn 297 residue is one of the most common post-translational modifications found within mAbs. In the past few years, we have seen rapid growth in our understanding of the role of glycosylation in with regard to both biological activity and pharmaceutical properties. Conformational changes of the C_H2 domain, as a result of fully or partially removing the glycan residues, have been found responsible for altering the functionality [3], stability [4-7] (chemical and physical) and pharmacokinetic profile [8] of various mAbs. Additionally, protease resistance (using papain) has been shown to be significantly lowered in deglycosylated mAbs.[9-10] These observations have been attributed to conformational differences due to the loss of both glycan-glycan and glycan-

protein backbone non-covalent interactions upon deglycosylation, this results in the deglycosylated mAb to adopt a more open conformational state.

Mass spectrometric analyses of glycopeptides from mAbs have revealed significant heterogeneity in terms of glycosylation patterns of both currently marketed mAbs and those under development, depending on a variety of factors including the antibody type, expression systems and cell culture conditions.[11-15] Among these glycoforms are the high mannose (HM) glycans consisting of 3 to 12 mannose units connected to two core GlcNAc units (N-acetyl glucosamine). In one study, an analysis of the glycan heterogeneity in Rituximab (a currently marketed drug for the treatment of non-Hodgkin's lymphoma) revealed that 1.7-5.4 % of the glycans present were a HM nature. [16] Mabs containing HM glycans are known to have faster clearance time compared to glycans having either GlcNAc, galactose or sialic acid units at the termini of the polysaccharide.[17, 18] The effect of having enriched or depleted levels of HM IgG1 within a heterogeneous mixture of IgG1 glycoforms was shown to not affect the physical stability of the mAb preparation.[19] Asymmetric mAb glycosylation (single arm glycosylation) has been reported for an IgG1 containing a single glycosylation in the Fab region.[20] This results in the IgG1 losing its divalent binding capacity to its antigen. Asymmetrically glycosylated IgG1 in the C_H2 domain was characterized by S Ha et. al. (2011) [21] with functional and stability differences between the

asymmetrically and the fully glycosylated IgG1 reported as a result of conformational changes in the C_H2 domain.

In this work, IgG1-Fc glycoforms containing well defined, homogeneous glycosylation patterns, produced from a *Pichia pastoris* yeast expression system followed by purification and specific enzymatic treatments, were utilized to more directly address the effect of glycosylation site occupancy and amino acid substitution (at Asn 297, the N-linked glycosylation site in C_H2 domain) on the structural integrity and conformational stability of an IgG1-Fc. The physical stability of this series of Fc glycoproteins was examined by high throughput biophysical analysis using multiple analytical techniques combined with data visualization tools (empirical phase diagrams or EPDs and radar charts). By using large physical stability data sets acquired from multiple high throughput low-resolution biophysical techniques as a function of environmental stresses (pH and temperature), differences in the structural integrity and conformational stability in this series of Fc glycoforms were detected. These stability trends, as a function of site occupancy and amino acid substitution in the Fc glycoforms, were not necessarily observed using the same biophysical techniques under non stressed conditions. As a result, evaluating the conformational stability differences between the different IgG1-Fc glycoproteins may serve as a surrogate to monitor differences in higher-order structure between IgG1-Fc samples, an

approach that could potentially be useful for analytical comparability studies.

4.2 Materials and Methods

4.2.1 Materials

Both the human IgG1-Fc sequence (comprising 446 amino acids with a theoretical molecular weight of 50132.92 Da) and a point mutant of the IgG1-Fc protein (with 446 amino acids and a theoretical molecular weight of 50160.96 Da) were prepared and expressed using a yeast expression system.[22] The nonglycosylated variant of the IgG1-Fc was made by mutating the N-linked glycosylation site at Asn 297 (EU numbering) to Gln 297, thus eliminating the Asn-X-Thr glycosylation site within the C_H2 domain. This was achieved through PCR site-directed mutagenesis, followed by transfecting the yeast with the mutated plasmid after sequencing it for verification as described elsewhere.[22] After expression, purification and concentration of the different IgG1-Fc glycoproteins (as described below), samples were dialyzed into the storage buffer (10 % sucrose, 20 mM histidine, pH 6.0) and frozen at -80 ^{0}C in aliquots of 0.5 mL. For the initial characterization of the IgG1-Fc proteins (SDS-PAGE, mass spectroscopy and SE-HPLC), samples were analyzed without further dialysis. For biophysical characterization (far-UV circular dichroism, intrinsic/extrinsic fluorescence spectroscopy and turbidity measurments), samples were dialyzed against 20 mM citrate phosphate buffer (pH 4.0-6.0, 0.5 increments) and adjusted

to an ionic strength of 0.15 with NaCl. Other chemicals and reagents not described below were obtained from Sigma–Aldrich (St. Louis, MO), Fisher Scientific (Pittsburg, PA), Invitrogen (Carlsbad, California) or Becton Dickinson and Company (Franklin Lakes, NJ).

4.2.2 Methods

4.2.2.1 Expression and purification of the IgG1-Fc proteins

IgG1-Fc proteins were cloned and then expressed using a methylotrophic *Pichia pastoris* yeast expression system as described previously.[22] Yeast were first grown at 25 ^{0}C for 72 hr in 2 mL of growth media composed of tissue culture media containing 1% yeast extract, 2% peptone, 5% glycerol and 100 µg/mL Zeocin (YPD/Zeocin culture media). This step was followed by inoculating the 2 mL culture into 50 mL of YPD/Zeocin culture media for another 72 hr at 25 ^{0}C. The 50 mL culture was then inoculated into a 1 L spinner flask containing YDP media, 0.00004% biotin and 0.004% histidine. The media was kept at 25 ^{0}C and aerated at a rate of 1 L/min through a sterilized glass sparger connected to 0.2 µm sterile filter. Twenty-five mLs of methanol were added in a drop wise fashion every 12 hr for a total period of 72 hr.

This 1 L of yeast containing culture media supernatant was harvested by centrifugation at 7000 rpm for 15 min at 4 ^{0}C followed by pH adjustment to 7.0 with 0.1 M NaOH or 0.1 M HCl , which was kept for ~7 hr at 4 ^{0}C. The

supernatant was then filtered and loaded onto a protein G column pre-equilibrated with 20 mM sodium phosphate that was adjusted to pH 7.0. Protein G column was packed in-house to make a 10 mL bed volume as described elsewhere.[23] The IgG1-Fc protein was then eluted using a 100 mM glycine solution adjusted to pH 2.7, and subsequently dialyzed against 20 mM sodium phosphate buffer adjusted to pH 7.0 at 4 ^{0}C overnight.

To separate the differentially glycosylated forms of the IgG1-Fc, two different purification methods were used. First, a cation exchange chromatography (CEX) method using ProPac WCX-10 semi-preparative (9 x 250 mm) column, (Dionex, Sunnyvale, CA) was developed. The column was equilibrated with Buffer A (20 mM sodium acetate pH 4.8) for 5 column volumes (CV). The protein G purified IgG1-Fc solution was then loaded onto the cation exchange column. Chromatographic separation was then performed in a linear gradient from 0 to 1M NaCl (10 CV) using Buffer B (20 mM sodium acetate pH 4.8, 1 M NaCl). Two mL fractions were collected throughout the gradient. Peaks were observed and collected corresponding to the diglycosylated and monoglycosylated IgG1-Fc proteins (which are primarily used in this study and represented ~80%, and 15% of the material, respectively) in addition to an aglycosylated IgG1-Fc form (~5% of the material). After analyzing column fractions with SDS-PAGE to confirm glycoprotein identity, the two collected IgG

Fc glycoforms were concentrated, dialyzed against 10% sucrose, 20 mM histidine pH 6.0 and frozen at -80 ^{0}C until further use.

A second, scaled-up purification process involved a hydrophobic interaction chromatography (HIC) method using a HiScreen fast flow phenyl sepharose column (4.7 mL bed volume and 7.7 X 100 mm bed dimensions, GE Healthcare) was adopted. The HIC column was equilibrated with Buffer A (20 mM sodium phosphate, 1M ammonium sulfate pH 7.0) for at least 5CV. The protein G purified IgG1-Fc solution was then loaded onto the HIC column. Chromatographic separation was then conducted in a linear gradient from 1.0 to 0 M ammonium sulfate (10 CV) using Buffer B (20 mM sodium phosphate, pH 7.0). Ten mL fractions were collected throughout the gradient. Two peaks were observed and collected corresponding to the diglycosylated and monoglycosylated glycoforms of the IgG1-Fc proteins. After analyzing column fractions with SDS-PAGE, the collected glycoforms were concentrated, dialyzed against storage buffer (10% sucrose, 20 mM histidine pH 6.0) and frozen at -80 ^{0}C until further use.

The nonglycosylated (QQ) IgG1-Fc mutant protein was expressed using a methylotrophic *Pichia pastoris* yeast expression system in a similar fashion to that described above. Yeast containing culture media supernatant was harvested by centrifugation at 7000 rpm for 15 min at 4 ^{0}C followed by a pH adjustment to 7.0 with 0.1 M NaOH or 0.1 M HCl. This product was kept for ~7 hr at 4 ^{0}C. The

supernatant was then loaded onto a protein G column and the nonglycosylated (QQ) IgG1-Fc protein was eluted using the same conditions as described above. Nonglycosylated (QQ) IgG1-Fc protein was also passed through phenyl sepharose column using the same conditions as described above. After analyzing column fractions with SDS-PAGE to confirm glycoprotein identity, the nonglycosylated (QQ) IgG1-Fc glycoform was concentrated, dialyzed against 10% sucrose, 20 mM histidine pH 6.0 and frozen at -80 ^{0}C until further use.

4.2.2.2 Deglycosylatation of Diglycosylated and Monoglycosylated IgG1-Fc proteins

The purified diglycosylated and monoglycosylated forms of the IgG1-Fc were deglycosylated using PNGase F enzyme (made in-house as described elsewhere).[24] Samples in storage buffer were thawed, treated with PNGase F in a protein to enzyme ratio of 500:1 (w/w) and incubated for 6 hr at 25 ^{0}C. .

4.2.2.3 Electrospray Ionization-Mass Spectrometry

IgG1-Fc proteins were analyzed by electrospray ionization mass spectrometry (ESI-MS). ESI spectra of reduced protein samples (15 mM dithiothreitol, pH 7.0, room temperature) were acquired on a SYNAPT G2 hybrid quadrupole / ion mobility / Tof mass spectrometer (Waters Corp., Milford, MA). The instrument was operated in a sensitivity mode with all lenses optimized on the MH+ ion obtained from Enkephalin. The sample cone voltage was 30eV.

Argon was admitted to the trap cell that was operated at 4eV for maximum transmission. Spectra were acquired at 9091 Hz pusher frequency covering the mass range from 100 to 3000 u and accumulating data for 1.5 seconds per cycle. Time to mass calibration was made with Nal cluster ions acquired under the same conditions. Samples were desalted on a reverse phase C4 column, 1 cm, 1 mm I.D. (Vydac, Midland, Canada, 300 A pore size. The 5 µm particles were packed by Micro-Tech Scientific) using a NanoAcquity chromatographic system (Waters Corp., Milford, MA). The solvents used were A (99.9% H_2O, 0.1% formic acid) and B (99.9% acetonitrile, 0.1% formic acid). A short gradient was developed from 1 to 70% B in 4 min with a flow rate of 20 µl/min. Masslynx 4.1 software was used to collect the data. The MaxEnt 1routine was used for processing data to convert peaks of multiply charged protein ions into uncharged deconvoluted protein spectra.

4.2.2.4 Sodium Dodecyl Sulfate-Polyacrylamide Gel Electrophoresis (SDS-PAGE)

Samples were made by mixing 20 µg of the protein with 10µl of Sodium dodecyl sulfate. Five µl of dithiotheritol (50 mM) was added for sample reduction. Samples were then incubated at 80 ^{0}C for 2 min and loaded onto a NuPAGE 4-12 % Bis-tris gel (Invitrogen, Carlsbad, California) using 20x MES as a running buffer. The running time was 65 min at 160V. After the run, gels were rinsed with water, stained with Coomassie blue for an hour and then destained

using 10 % methanol, 10 % glacial acetic acid solution. Protein molecular weight standards (BIO-RAD, Hercules, CA) were loaded for molecular weight estimation. Bands densitometry measurements were performed using the imageJ program (NIH). Briefly, individual gel lanes were highlighted for analysis in which high band intensity corresponds to high peak area from which the purity of each sample was calculated as described in detail elsewhere.[25, 26]

4.2.2.5 Western Blot analysis

After protein separation by SDS-PAGE, gels under reducing and non-reducing conditions were transferred onto a polyvinylidene fluoride (PVDF) membrane (Bio-RAD, Hercules, CA) using 25 mM Tris, 192 mM glycine, 20 % (v/v) methanol buffer (pH 8.3). Non-specific binding was blocked using 5 % nonfat milk dissolved in Tris-buffered saline (pH 7.5) for 3 hr at 4 ^{0}C followed by the addition of an anti-IgG-Fc specific secondary antibody that was alkaline phosphatase labeled (Thermo scientific, Waltham, MA). The mixture was incubated overnight at 4 ^{0}C followed by washing the PVDF membranes with Tris-buffered saline containing 0.05 % Tween 20. Protein bands were visualized by NBT/BCIP substrates (Thermo scientific, Waltham, MA) which yield an intense black/purple precipitate when reacted with alkaline phosphatase.

4.2.2.6 Size-Exclusion High-Performance liquid Chromatography (SE-HPLC)

Experiments were performed using a Shimadzu high-performance liquid chromatography system equipped with a photodiode array detector and a temperature controlled autosampler. A Tosoh TSK-Gel Bioassist $G3SW_{xL}$ column (7.8 mm ID x 30.0 cm L) and a corresponding guard column (TOSOH Biosciences, King of Prussia, Pennsylvania) were used for Fc protein characterization. Initially, the SEC column was equilibrated for at least 10 CV with the running buffer (200 mM sodium phosphate, pH 6.8) and under the running conditions (30 ^{0}C column temperature and 0.7 mL/min flow rate). Gel filtration molecular weight standards (Bio-Rad, Hercules, CA) were used for column calibration. Protein samples at a concentration of 0.5 mg/ml were injected in a volume of 35 µL, and a 30 min run time was used. Peaks quantification was carried out using instrument software.

4.2.2.7 Far-UV Circular Dichroism Spectroscopy

Far-UV CD spectra ranging from 260 to 200 nm were collected, with a resolution and bandwidth of 1 nm, using a Chirascan specrtopolarimeter (Applied Photophysics, Surrey, United Kingdom) equipped with four cell holder and peltier type temperature controller. For all measurements, 200 µl of a protein concentration of 0.2 mg/ml was placed into a 0.1 cm path length quartz cuvette.

Proteins were run in triplicate and corresponding buffer blanks were run and subtracted from each sample.

4.2.2.8 Intrinsic (Trp) Fluorescence Spectroscopy

Intrinsic (Trp) fluorescence was measured using a Photon Technology International (PTI) Quantum master fluorometer (New Brunswick, New Jersey) equipped with a four position cuvette holder and a turreted peltier temperature controller. A protein sample (200 µl) of 0.2 mg/ml in 0.2 cm path length quartz cuvette was used. Samples were excited at 295 nm with emission spectra collected from 310 to 400 nm at a resolution of 1 nm, collection rate of 1 nm/sec, and an integration time of 1 sec. Temperature was raised in increments of 1.25 ^{0}C from 10 to 90^{0}C. The slit widths used for both excitation and emission were 6 nm. Fluorescence peak position changes were determined by a center of spectral mass "MSM" method using Origin™ 7.0 software. This method shifts the actual peak position approximately 10 nm, but produces more reproducible values of the wavelength maximum. Proteins samples were run in triplicate and corresponding buffer blanks were run and subtracted from each sample spectrum.

4.2.2.9 Differential Scanning Fluorimetry (DSF)

DSF measurements were performed using MX3005P QPCR system (Agilent Technologies). A protein concentration of 0.2 mg/ml in a total sample volume of 100 µl was used. SYPRO™ orange dye purchased from Invitrogen, Inc. (Carlsbad, CA) supplied in a concentrated form (5000x) dissolved in DMSO

was diluted to 40x and then added to the protein samples to achieve 1x dye concentration for measurements. Using FAM filter sets, the mixture was excited at 492 nm and the emission intensity change at 516 nm was followed. The temperature was raised from 25 to 90 ^{0}C using 60 ^{0}C/hr as a heating rate and 1 ^{0}C as a step size. Data were transferred to Excel software (Microsoft, Redmond, WA) for data analysis. Proteins samples were run in triplicate and corresponding buffer blanks were run and subtracted from each sample.

4.2.2.10 Turbidity measurments

Temperature induced protein aggregation was followed using a Cary 100 UV-Visible spectrophotometer (Varian Inc, Palo Alto, California) equipped with a 12 cell holder with peltier type temperature controller. A protein concentration of 0.2 mg/ml in a total volume of 200 µl was used in 1 cm path length quartz cells. For all measurements, a wavelength of 350 nm was used to monitor light scattering (optical density) and the temperature was raised in increments of 1.25 ^{0}C from 10 to 90 ^{0}C. Proteins samples were run in triplicate and corresponding buffer blanks were run and subtracted from each sample.

4.2.2.11 Construction of Empirical Phase Diagrams (EPDs) and Radar Charts

The three-index Empirical Phase Diagram and Radar Chart data visualization methods were used to describe biophysical stability characteristics of the various Fc proteins. Detailed descriptions of the construction of both three-

index EPDs and radar plots are published elsewhere.[27] In this work, three biophysical data sets were used for data visualization: Sypro Orange fluorescence, Trp peak position fluorescence, and optical density at 350 nm. These three techniques were chosen for EPD construction because they displayed clear thermal transitions; in contrast, circular dichroism thermal stability data did not show clear transitions (data not shown). For the three index EPDs, the Sypro Orange fluorescence stability data were mapped to the color red, Trp fluorescence peak position stability data to the color green, and optical density stability data to the color blue. The combination of these RGB values produced a single color at each point in pH and temperature coordinates. For each technique and protein, the minimum value was mapped to the loss of the color component, and the maximum value was mapped to the full color intensity. The resulting color map was generated: The color black indicates minimum values of all three techniques, which can be interpreted as the structure closest to the native state (least amount of structural change). The green or red color appears within the three index EPD as the Trp fluorescence peak positions changes (displays red shift) or Sypro Orange binding increases, respectively. The blue appears when high turbidity is measured by optical density values at 350 nm. To determine common regions within the three index EPD, a k-Means clustering algorithm is first applied to each EPD to identify boundries of similarly color regions. The resulting clusters can scatter as small blocks of colors, especially over the structurally altered regions.

Then, using visual assessments and comparisons to the raw physical stability profiles for each instrument, only certain commonly observed clusters were selected. Radar charts were generated to display similar characteristics (changes in readouts from each of the three biophysical instruments) for each of these commonly observed clusters. The same three analytical techniques and min-max range were used for preparing radar charts. The minimum value was mapped to the center of the radar chart, while the maximum value was mapped onto the outer circumference. All values within the cluster were averaged from multiple runs and values were connected to yield a final polygon to represent a specific structural state.

4.3 Results

4.3.1 Initial characterization of the different IgG1-Fc glycoforms

A pictorial presentation of the five different types of IgG-Fc proteins (diglycosylated, monoglycosylated and three different non-glycosylated forms) examined in this study is presented in Figure 1. High mannose (HM) IgG1-Fc glycoforms were expressed in yeast and purified using a combination of Protein G and either cation exchange or hydrophobic interaction chromatography. First, an IgG1-Fc bearing HM glycans at both C_H2 domains (~80 % of the amount purified) designated diglycosylated IgG1-Fc was identified. Second, an IgG1-Fc containing HM glycan at a single C_H2 domain (~15 % of the amount purified)

labeled monoglycosylated IgG1-Fc was found. In addition, IgG1-Fc proteins with variations in amino acid residues at site 297 of the C_H2 domain were prepared. IgG1-Fc with Asp/Asp and Asp/Asn residues were made by treating the diglycosylated and monoglycosylated IgG1-Fc proteins with the enzyme PNGase F. PNGase F cleaves the glycan residue(s) and converts Asn to Asp, adding one or two negative charges to the IgG1-Fc molecules. Finally, a N297Q IgG1-Fc mutant, with Asn/Asn substituted with Gln/Gln through site directed mutagenesis, was also expressed and purified (Figure 1).

To confirm the correct masses for each of the purified IgG1-Fc glycoproteins, mass spectrometric analysis of reduced samples was performed (Table 1 and supplementary Figure S1). The nonglycosylated (QQ) Fc mutant had a mass of 25,077 Da, in close agreement (+ 3 Da) with the mass predicted from the sequence. MS analysis of diglycosylated IgG1-Fc protein revealed a mass of 26,766 Da reflecting a predominant Man $_8$ glycosylation form, in close agreement to the predicted mass (26,769.5 Da). Additional, peaks with additional one, two, three and four mannoses were also present indicating glycoforms with 9, 10, 11 and 12 mannoses, respectively, but in lower abundance (see supplemental Figure S1). The monoglycosylated IgG1-Fc protein had two distinct peaks with masses of 25,062 and 26,766 Da in agreement with nonglycosylated and Man $_8$ glycosylated arms of the glycoprotein. A heavier peak reflecting the presence of Man $_9$ IgG1-Fc glycoform was detected as well (see supplemental Figure S1).

Upon PNGase F enzymatic treatment of the diglycosylated and monoglycosylated IgG1-Fc samples, a mass of 25,063 Da was observed for each protein indicating fully deglycosylated Fc proteins.

SDS-PAGE gel analysis for the IgG1-Fc samples under reducing conditions is shown in Figure 2A. The diglycosylated Fc protein showed a single band at around 28 kDa. Slightly lower MW of around ~ 26 kDa were observed, as expected, for both the nonglycosylated DD (PNGase treated) and nonglycosylated mutant (QQ) Fc proteins (in lanes 2, 3 and 5, respectively). Monoglycosylated Fc protein (lane 3) had two bands at ~28 and ~26 kDa confirming the presence of glycosylated and nonglycosylated IgG1-Fc arms. Upon PNGase F treatment of the monoglycosylated Fc, the glycosylated arm (previously seen at ~28 kDa) disappears and a major band is seen instead ~26 kDa. Both monoglycosylated (with and without PNGase treatment) have a second band at ~39 kDa. The purity of the IgG1-Fc protein samples (under denaturing conditions) was determined by densitometric analysis of reduced SDS-PAGE gels (Table 2). Diglycosylated, nonglycosylated DD and the nonglycosylated mutant (QQ) were determined to have ~97 % purity. The monoglycosylated Fc protein (and the corresponding nonglycosylated DN form derived from PNGase treatment of the monoglycosylated Fc) showed somewhat lower purity values of ~84% (see discussion section). Size exclusion high performance liquid chromatography (SE-HPLC) was then used to evaluate purity (under non-denaturing conditions) to

determine if aggregates were present in IgG1-Fcs samples after purification (Figure 2B shows representative SEC chromatograms). The purity of the IgG1-Fc samples was determined, as shown in Table 2, and results indicate the Fc protein samples are primarily monomeric (91.1-96.6%) with some aggregates present across the IgG1-Fc samples (1.8-8.2%). The remaining area can be accounted for by the presence of small amounts of fragments at 0.2-2.0% (data not shown). The monoglycosylated Fc proteins contained ~3.4-4.0% aggregates and showed either similar or somewhat lower aggregate levels compared to the diglycosylated and nonglycosylated Fc samples (see Table 2).

4.3.2 Structural integrity at ambient temperature conditions

The overall secondary structure of the five IgG1-Fc proteins was evaluated at 10 ^{0}C by far-UV circular dichroism (CD) analysis from 260 to 205 nm under at various pH conditions (Figure 3). The CD spectrum of the diglycosylated and nonglycosylated mutant (QQ) IgG1-Fc proteins show a clear minimum at 217 nm that is apparent under all pH conditions tested indicating a β-sheet rich structure, as expected from immunoglobulin folded domains. The same overall β-sheet rich secondary structure is seen for the nonglycosylated DD at pH 4.0-4.5, whereas, at pH 5.0, 5.5 and 6.0 a constant decrease in CD signal is observed indicating some alteration in the protein secondary structure under these pH conditions. For the monoglycosylated IgG1-Fc protein, a different CD spectrum is observed

compared to the other Fc protein samples with a positive hump present at 212 nm that increases in intensity as the solution pH increases. This could potentially be attributed to an increasing influence from type I β-turns. When the monoglycosylated IgG1-Fc protein was deglycosylated using PNGase F (nonglycosylated DN), more native-like structural features in the CD spectra were detected, in the form of a minimum at 217 nm, across all pH conditions examined. These results indicate the monoglycosylated Fc protein is in a structurally perturbed state, and that upon deglycosylation, the effect is at least partially reversible with the regaining of native-like secondary structure seen by CD (monoglycosylated vs. DN nonglycosylated forms of the Fc protein in Figure 3). The CD spectra intensity signals as a function of increasing temperature were monitored. Due to data noisy data, however, as well as the lack of intensity change as a function of temperature for many of the Fc proteins (e.g., monoglycosylated as well its deglycosylated form), the CD thermal melting curves were not further employed in this study (data not shown).

The structural integrity of the overall tertiary structure of the five IgG1-Fc proteins was then evaluated using intrinsic (Trp) fluorescence spectroscopy (Figure 4). Diglycosylated and nonglycosylated mutant (QQ) IgG1-Fc proteins manifest fluorescence spectra at pH 4.0, with relatively high peak intensities, and λ_{max} values of 333.8 and 332.1 nm, respectively. As the pH is raised, the λ_{max} starts shifting to lower wavelengths (with λ_{max} values of 329.6 and 330.6 nm

accompanied by relatively lower peak intensity), indicating the average Trp residues in a more apolar environment, and presumably more folded state. For the nonglycosylated DD IgG1-Fc protein, the λ_{max} does not shift to lower wavelength as the solution pH is raised, remaiing at ~333 nm, suggesting that deglycosylated protein remains in the same structure, presumably an effect due to deglycosylation and amino acid substitution (Asn to Asp at site 297). Monoglycosylated IgG1-Fc protein, however, shows a small red shift in λ_{max} as a function of increasing solution pH, indicating potentially less stability at pH 6.0 (vs. pH 4.0), whereas the nonglycosylated DN behaves more like the diglycosylated and QQ nonglycosylated mutants it does show a noticeable blue shift in λ_{max} as the pH is raised from pH 4.0 to 6.0 (~334 to ~330 nm). These intrinsic fluorescence spectroscopy results, similar to the CD results above, indicate that monoglycosylated Fc protein is in a structurally perturbed state, and that upon deglycosylation, the effect is at least partially reversible (see the data for monoglycosylated vs. DN nonglycosylated forms of the Fc protein in Figure 4 at pH 4.0 vs. pH 6.0).

4.3.3 Physical stability of IgG1-Fc proteins as a function of pH and temperature

The conformational stability of the tertiary structure of the five IgG1-Fc proteins was evaluated using a combination of intrinsic (Trp) fluorescence and extrinsic fluorescence (i.e., differential scanning fluorimetry, DSF) spectroscopy

(see Figure 5 A and B). Figure 5 shows the average results from three replicates while the same physical stability data are shown in Supplemental Figure S3 A and B with corresponding standard deviation error bars from triplicate measurements. The conformational stability of the five Fc proteins was first evaluated by following changes in λ_{max} as a function of increasing temperature (Figure 5A). It should be noted that the λ_{max} values in Figure 5A are shifted by about 10-15 nm compared to the actual values (see Figure 4), due to the use of a spectral central of mass method as described in the methods section. Diglycosylated and nonglycosylated mutant (QQ) both had relatively low λ_{max} peak positions at the starting temperature across the pH conditions tested (~339-340 nm using the MSM method) with higher thermal stability being observed for the diglycosylated IgG1-Fc protein. The nonglycosylated DD IgG1-Fc protein, with λ_{max} peak positions of ~340 nm, showed a subtle, steady increase in peak position as temperature was raised followed by a more dramatic increase in peak position. The monoglycosylated and nonglycosylated DN forms had λ_{max} peak positions of ~340-341 nm with little to no detectable shift in peak position as the temperature increases, except for the monoglycosylated Fc protein at pH 6.0 where a transition curve is detected (Figure 5A). In DSF analysis, SYPRO orange dye was used as a probe for detecting structurally disrupted proteins, seen in the form of increased fluorescence intensity upon exposure to apolar environments due to structural alternations and/or aggregate formation (See Figure 5B). Diglycosylated IgG1-Fc

was the most thermally stable protein manifesting two thermal transitions (presumably sequential unfolding events of the C_H2 and C_H3 domains). This was seen across most of the pH conditions tested (except at pH 4.0) with an observed increase in thermal stability as a function of increasing pH. Additionally, fluorescence peak intensity at the starting temperature in the range of pH 5.0-6.0 is decreased compared to the values at the lower pH conditions. For the monoglycosylated Fc protein at pH conditions between 4.0 and 5.5, and nonglycosylated DN protein at pH between 4.0 and 5.0, single thermal transition, consistent with a more structurally disrupted C_H2 domain. Two thermal transitions were seen for the nonglycosylated mutant (QQ) and the nonglycosylated DD Fc proteins under most of the pH conditions tested, except at pH of 4.0 and 4.5, again consistent with the presence of a more structurally altered C_H2 domain under lower pH conditions compared to higher pH.

Temperature induced aggregation was evaluated by monitoring optical density changes at 350 nm as a function of increasing temperature and pH (Figure 5C). Differences between the IgG1-Fc proteins were observed in terms of the onset temperature of aggregation as well as the profile of the optical density transitions. Diglycosylated IgG1-Fc protein did not show detectable thermal transitions in optical density across all pH conditions tested. The monoglycosylated Fc protein, on the other hand displayed a single transition in optical density at pH 4.0, 4.5 and 6.0 starting at 21, 33, and 76 ^{0}C, respectively,

whereas, at pH 5.0 and 5.5, two transitions were detected with the first transitions starting at 45 and 79 ^{0}C and the second at 52 and 75 ^{0}C, respectively. For the nonglycosylated mutant (QQ), a single thermal event of increasing optical density was detected at ~79 ^{0}C at pH 5.0-6.0, with no thermal transitions noted at lower pH values of pH 4.0 and 4.5. Similarly, the nonglycosylated DD Fc protein showed no detectable thermal transition at pH 4.0, a single thermal transition in optical density starting at 78 ^{0}C at pH 4.5, and at 82 ^{0}C for pH 5.0, 5.5 and 6.0. In contrast, the nonglycosylated DN Fc protein manifested two optical density thermal transitions under all pH conditions examined with increasing thermal stability being observed as a function of increasing pH. At pH 4.0, the nonglycosylated DN protein showed an increase in optical density starting from 10 ^{0}C followed by a second major increase at 69 ^{0}C. At pH 4.5, 5.0 and 5.5, an initial increase in optical density was detected at 40, 46 and 52 ^{0}C, followed by a second increase at 75, 78 and 74 ^{0}C, respectively. Two adjacent transitions in optical density were seen at pH 6.0, with the first transition initiating at 57 ^{0}C followed by a second transition at 74 ^{0}C.

4.3.4 Conformational stability evaluations using various data visualization techniques

Using the physical stability data acquired from differential scanning fluorimetry, intrinsic fluorescence spectroscopy (peak position), and turbidity measurments, three index EPDs (see Supplemental Figures S4-S8) and radar

charts (see Supplemental Figure S4-S8 and Supplementary Figure S9) were constructed for each of the individual IgG-Fc proteins. These supplemental figures show the contributions from each of the individual biophysical instruments to the observed changes in conformational integrity as a function of pH and temperature. For ease of comparison, a summary figure was constructed showing the overall results from each of the five individual IgG-Fc proteins merged into one display (Figure 6). The five color plots in Figure 6 highlight five regions with similar structural characteristics designated regions A-E, as observed in the three-index EPDs for the five different IgG1-Fc proteins with various glycosylation occupancy (diglycosylated, monoglycosylated) as well as the nonglycosylated forms of the Fc protein containing amino acid variations (QQ, DD and DN) in the C_H2 domain. In addition, as shown in the legend box in Figure 6, radar plots were prepared to better define the five different conformational regions (regions A through E) that can be observed in each of the five Fc proteins under the various pH and temperature conditions.

Region A represents a state in which the protein exists in its most native-like conformation. As shown in the radar chart legend in Figure 6, there are minimal changes in signals for each of the three biophysical techniques (intrinsic Trp and extrinsic SYPRO orange fluorescence spectroscopy as well as turbidity at OD 350nm), which results in a black color for region A as shown in the EPDs for the five Fc proteins in Figure 6. For region B, there are small changes in the

signals from the biophysical instruments, which represents protein with a slightly altered conformation (minor increases in SYPRO orange fluorescence intensity and Trp fluorescence peak position) which manifest as a dark green color in the EPDs shown in Figure 6. Regions C and D represents more altered conformational states with either a substantial increase in SYPRO orange fluorescence intensity (Region C as a dark red color) or notable changes in Trp fluorescence peak position (Region D as a green color). Finally, Region E represents an aggregated state of the Fc protein with increased signal in optical density at 350 nm (see also the radar chart) as shown as a blue color in Figure 6.

A comparison of the IgG1-Fc proteins with variations in glycosylation occupancy (see the vertical direction in the three color plots on left side of Figure 6) shows different degrees of structural integrity and conformational stability. At low temperatures, the diglycosylated Fc protein at pH 5.5 and 6.0 is present in a native-like structural state (black color, region A). A structural transition to a structurally altered state (dark red, region C) starts as Fc diglycosylated Fc protein reaches temperatures around 48 ^{0}C in this pH range. At lower temperatures in the pH range of 4.5 and 5.0, the diglycosylated Fc protein is present in a slightly altered conformation (dark green, region B), where it transitions to a more extensive altered structures at temperatures of 38 and 44 ^{0}C, respectively. At pH 4.0 at all temperatures, the diglycosylated protein is present in this more structurally altered structural state. Diglycosylated protein did not show any

detectable aggregation by optical density measurements, thus no region E was observed in the EPD for the fully glycosylated Fc protein.

The nonglycosylated Fc mutant (QQ) at lower temperatures and at pH 5.5 and 6.0 also shows a native like region (black color, region A). Thermal transition temperatures to the structurally altered region C (dark red color), however, initiate at lower temperatures (35 and 44 ^{0}C, respectively) compared to the diglycosylated protein (Figure 6). Additionally, the nonglycosylated mutant (QQ) at pH 4.5 and 5.0 exists at a more extensive structurally altered conformational region, unlike the diglycosylated protein which shows a more native-like conformation in this pH range (B region, dark green). In addition, Region E (blue color), representing the Fc protein at an aggregated state is detected for the nonglycosylated mutant (QQ) at elevated temperatures in the pH range of 5.0 to 6.0.

In comparison to the di- and non- glycosylated forms, the monoglycosylated Fc protein at low temperatures from pH 4.5 to 6.0, exists in a structurally altered Region D (green color) as shown in Figure 6. Thus, no native like state (Region A, black color) can be detected. A region representing aggregated protein (region E, blue color) is also seen at high temperature for the monoglycosylated Fc. The monoglycosylated Fc protein was the least stable compared to the diglycosylated and nonglycosylated (QQ) Fc proteins with no stable region A being detected and lower temperature thermal transitions noted depending on the pH and biophysical readout.

A comparison of the three different nonglycosylated IgG1-Fc proteins with variations in the amino acid residue in site 297 (also see Figure 6) also shows different degrees of structural integrity and conformational stability. The nonglycosylated DD and nonglycosylated DN Fc proteins, containing two and one Asp 297, respectively, were created by PNGase F enzymatic treatment of the corresponding di- and mono- glycosylated Fc molecules (See Figure 1). The nonglycosylated mutant (QQ) with two Gln residues was also prepared and evaluated as a nonglycosylated Fc protein containing a nuncharged amino acid residue at the 297 site. As shown in Figure 6, the nonglycosylated DD IgG1-Fc protein at a pH between 5.0 and 6.0 exists in an altered state (region D, green color). A small region of aggregated protein (region E, blue color) is detected at higher temperature. The nonglycosylated DN Fc protein shows an enhanced structural integrity at pH 6.0, compared to the nonglycosylated DD form where a more native like conformation (region B, dark green) is detected. A structurally altered state (region D, green) is observed for the nonglycosylated DN protein at pH 5.0 and 5.5 (similar to that seen for the nonglycosylated DD form). A relatively large region of aggregated protein (region E, blue color) is present at high temperature for the nonglycosylated DN protein, indicating that this form is most prone to aggregation upon heating. Finally, the nonglycosylated mutant (QQ), as already discussed above, defines a region where the proteins exists in a native-like conformation at pH 5.5 and 6.0 that is not seen for the nonglycosylated

DD or DN species. In summary, the presence of a charged amino acid residue at site 297 in the C_H2 domain (through the conversion of Asn to Asp as a result of the PNGase F enzymatic treatment) had a measurable influence on the IgG-1 Fc conformational stability. Comparing the nonglycosylated DD to the nonglycosylated mutant (QQ), a stability advantage was detected for the nonglycosylated mutant (QQ) with a stable, native like region A being detected and higher temperature thermal transitions noted depending on the pH and the method of detection employed.

4.4 Discussion

Comparability exercises are routinely performed in the biopharmaceutical industry as a result of manufacturing process changes (e.g., cell culture or purification steps) or alteration in final product presentation (e.g., formulation composition or different packaging material) for protein based drugs under development or currently marketed.[28, 29] In these studies, the critical quality attributes of the pre and post-change protein-drug are evaluated in a head-to-head fashion to better understand the effect (if any) of the process or product changes on key comparability elements such physiochemical integrity, storage stability, functionality, immunogenicity and pharmacokinetics. With regard to physiochemical characterization, numerous advances have been made in terms of characterization of a protein's primary structure and post translational

modifications through multiple chromatographic (size exclusion, reverse phase and ion exchange HPLC) and electrophoretic (capillary isoelectric focusing and capillary sodium dodecyl sulfate) methods typically applied with mass spectrometric detection (intact molecular weight, peptide maps, and oligosaccharides maps). Challenges regarding the development of analytical techniques for the structural determination of higher order structures still remain, however, resulting in the requirement for functional potency assays to ensure biological activity as a surrogate to demonstrate the protein is properly folded. Although multiple high-resolution analytical techniques have been used for the characterization of the higher order structures of proteins, ranging from nuclear magnetic resonance (NMR)[30], X-ray crystallography [31], small angle x-ray scattering (SAXS) [32] and hydrogen-deuterium exchange mass spectrometry (HDX-MS),[33-36] multiple practical drawbacks such as the requirement of isotope labeling, generation of protein crystals, interference of excipients, and/or the complicated and time consuming nature of these approaches have limited their use in biocomparability studies.

Alternatively, comparing the physical stability profile of proteins using lower resolution techniques may be useful complement to higher sensitivity analytical methods such as NMR and hydrogen-deuterium exchange mass spectrometry to examine subtle differences in protein structure in formulated drug product dosage forms. The effect of variations introduced into the glycan structure

of an IgG1mAb, through enzymatic glycan truncation, protein structural integrity was recently evaluated in our laboratory by this alternative approach using more readily available biophysical instruments (e.g., fluorescence spectroscopy, light scattering and differential scanning calorimetry).[37] By using a combination of lower resolution biophysical techniques to study the physical stability of mAb glycoforms over a specific pH and temperature range (at 0.5 pH intervals from 4-6 and 1.25 ^{0}C temperature increments from 25-90^{0}C), combined with recently developed data visualization tools, structural and conformational stability differences between the different IgG1glycoforms were demonstrated. In this study, a comprehensive evaluation of the overall structural integrity and conformational stability of five different IgG1-Fc glycoproteins using multiple biophysical methods across a wide range of pH and temperature conditions is undertaken and comparisons are made between their corresponding global physical stability profiles (three index EPDs and radar charts).

First, initial characterization of the five well-defined glycoforms of IgG1-Fc (Figure 1) was carried out using a combination of mass spectrometry (MS), sodium dodecyl sulfate polyacrylamide gel (SDS-PAGE), size exclusion high performance chromatography (SE-HPLC) and spectral characterization (CD and fluorescence spectroscopy) to evaluate mass (degree of glycosylation), purity and overall structural integrity prior to initiating physical stability studies. The five proteins had measured masses in close agreement to their expected masses due to

their glycosylation status (Table 1 and supplementary Figure S1). The five proteins were shown to have relatively high purity (~91-97%), in primarily monomeric forms as seen from SE-HPLC analysis (Table 2 and Figure 2A) with some relatively low levels of aggregation and fragmentation, under non-denaturing conditions. Purity under denaturing conditions was analyzed by SDS-PAGE under reduced conditions and showed values ranging from ~97-99% for the diglycosylated Fc derived proteins and ~84% for the monglycosylated Fc derived proteins (Table 2 and Figure 2B). One of the minor impurity bands was accounted for by the presence of residual PNGase remaining from the enzymatically treated Fc samples (see Figure 2B; lane 7). The gels were further analyzed by non-reduced SDS-PAGE and Western Blot analysis (see Supplemental Figure S2). All five samples showed the expected migration for the major bands (i.e. Fc protein) in non-reduced gel. The migration of the second minor protein band (~39 kDa) found in the monoglycosylated derived proteins was not affected by PNGase enzymatic treatment or by reduction with DTT (and did not react with the anti-human IgG-Fc antibody by western blot analysis). This impurity could not be further removed despite Protein G affinity purifications combined with cation exchange or HIC columns. These differences in the purification behavior between di vs. mono- glycosylated IgG-Fc proteins are the subject of ongoing work in our laboratories. Similar levels of ~80% purity were recently reported for a monoglycosylated IgG1 mAb.[21] In summary, since the

impurity was a relatively minor band on SDS-PAGE, was not readily observed by SEC analysis, the monoglycosylated derived Fc proteins were determined to be sufficiently pure for subsequent biophysical analysis performed in this work.

The secondary and tertiary structure of the five proteins using circular dichroism (CD) and intrinsic Trp fluorescence spectroscopy was then evaluated (Figures 3 and 4, respectively). The diglycosylated and nonglycosylated mutant (QQ) were both present in a more native-like structure, especially at pH 5-6 (as determined by λ_{max} values and CD minima near 217 nm). Monoglycosylated Fc at all pH conditions tested was structurally disturbed as indicated by the altered CD spectra shape and the red shifted λ_{max} values. Interestingly, upon deglycosylation of the monoglycosylated Fc (creating the nonglycosylated DN form), the Fc protein showed some recovery of native like secondary structure, more similar to the CD spectra of the diglycosylated Fc form with increasing solution pH. This observation further supports the hypothesis that lower purity level of the monoglycosylated Fc does not the interpretability of the measurement of structure.

The physical stability of the five IgG1-Fc proteins were then evaluated as a function of pH and temperature using a combination of biophysical techniques including extrinsic and intrinsic fluorescence spectroscopy (i.e., DSF with Sypro Orange and Trp fluorescence peak position) and optical density (turbidity) measurements to evaluate the influence of varying glycosylation levels and amino

acid residues substitutions (site 297). IgG1-Fc proteins with varying glycosylation occupancy levels showed differences in their conformational and colloidal stability with the diglycosylated IgG1-Fc being the most stable protein followed by the nonglycosylated mutant (QQ). Perhaps surprisengly the monoglycosylated IgG1-Fc manfiested the lowest relative physical stability (Figure 5). In terms of the effect of amino acid substitution and negative charge introduction at site 297 in the C_H2 domain, the nonglycosylated QQ, DN and DD forms of the IgG-Fc were evaluated using the same biophysical techniques. Compared to the nonglycosylated DD and DN, the nonglycosylated mutant (QQ) demonstrated increased conformational stability (Figure 5).

Using the physical stability data sets acquired from DSF, fluorescence peak position and optical density measurements as a function of pH and temperature, data visualization methods were employed to further examine subtle conformational stability differences between the five different IgG1-Fc proteins. To the best of our knowledge, the effect of glycosylation site occupancy on IgG Fc physical stability has only been reported in one limited study by Ha et. al. (2011), which evaluated the thermal stability of an asymmetrically glycosylated (single arm glycosylated) IgG1 using one method (differential scanning calorimetry) at one pH value (pH 6.0).[21] The C_H2 domain of the fully glycosylated IgG1 was thermally more stable than the C_H2 domain of the

asymmetrically glycosylated IgG1 by ~1 ^{0}C, with no detectable change in transition temperatures involving the other IgG1 domains.

For the IgG Fc glycoforms evaluated in this work, three index EPDs and radar charts (Figure 6) for the IgG1-Fc with different glycosylation site occupancy were prepared (Figure 6) and were able to detect similar structural state among the three IgG1-Fc proteins with different conformational stabilities. Region A (Black color), where the proteins exist in a more native-like conformation as determined by these three biophysical methods, was only detected for the diglycosylated and nonglycosylated QQ at pH 5.5 and 6.0. In addition, a higher transition temperature to an altered conformational form (region C) was observed for the diglycosylated protein in this pH range. Diglycosylated protein at lower temperatures and pH conditions (4.5 and 5.0) was present in a slightly altered conformational state (region B), a conformational state that the nonglycosylated QQ protein doesn't seem to access, reflecting the important role glycosylation may play in stabilization of the C_H2 domain in acidic environments[7]. Due to fluorescence λ_{max} peak position values shifting to higher wavelengths relative to the diglycosylated and nonglycosylated QQ, the monoglycosylated Fc protein at pH 5.5 and 6.0 was determined to be present in an altered conformational state (region D). The monoglycosylated Fc protein was then deglycosylated, and showed recovery of native like structure under these conditions.

Conformational stability differences between the nonglycosylated IgG1-Fc proteins with variations in amino acid substitutions at site 297 (QQ, DN and DD) were detected as well. Nonglycosylated QQ was the only Fc protein that existed at a native-like conformation (region A) at low temperatures at pH 5.5 and 6.0, whereas, nonglycosylated DN and DD both existed in a slightly and more extensively altered forms (regions B and D) suggesting the important role charge may play in the conformational stability of the C_H2 domain of these Fc proteins and potentially in mAbs in general.[38-40]

In summary, by assessing large data sets concerning conformational stability as a function of environmental stress (pH, temperature), subtle differences in IgG1-Fc glycoform structural integrity were detected. These differences were not readily apparent under non-stressed conditions (i.e. lower temperatures at more neutral pH). Thus, the use of conformational stability data combined with advanced data visualization methods may be an effective surrogate to monitor subtle differences in higher order structure due to post-translational modifications such as glycosylation and amino acid substitution/mutation. During analytical comparability studies of protein drugs within their pharmaceutical dosage forms, it is essential to gather higher order structural information without altering formulation conditions (such as protein concentration, pH, ionic strength, excipients, etc.). Biophysical analysis of conformational stability using lower resolution techniques in a high throughput setup, combined with EPD/radar chart

analysis for data visualization, may be a useful complement to higher sensitivity analytical methods such as NMR and hydrogen-deuterium exchange mass spectrometry to examine subtle differences in protein higher order structure in formulated drug product dosage forms.

Table 1: Mass spectrometry analysis of reduced monomeric forms of the purified IgG-Fc proteins. The Molecular weight column shows the masses of the reduced non-glycosylated IgG1-Fc obtained from MS analysis along with the masses measured for the most abundant glycoforms (man_8-$GlcNAc_2$) of the glycosylated Fc. The values for calculated change in mass, and predicted change in mass are also shown. Based on these results, the modification expected due to enzymatic treatment and/or glycan variation of the IgG1-Fc proteins is then presented.

	IgG1-Fc proteins	Molecular Weight (Da)	Δ Mass observed (Da)	Δ Mass predicted (Da)	Reduced Fc fragment Modifications [a]	
					Arm 1	***Arm 2***
Non-glycosylated IgG1-Fc	**Mutant (QQ)**	*25,077*	*+11*	*+14*	*N → Q*	*N → Q*
	Mono-glycosylated + PNGase F (DN)	*25,063* [b]	*-3*	*+1*	*Deglycosylation N → D*	*N*
	Di-glycosylated + PNGase F (DD)	*25,063* [b]	*-3*	*+1*	*Deglycosylation N → D*	*Deglycosylation N → D*
Glycosylated IgG1-Fc	**Mono-glycosylated** [c]	*26,766 / 25,062* [b]	*+ 1,700/ - 4*	*+ 1,703.5/ 0*	*+Man_8-$GlcNAc_2$*	*N*
	Di-glycosylated [c]	*26,766*	*+ 1,700*	*+ 1,703.5*	*+ Man_8-$GlcNAc_2$*	*+ Man_8-$GlcNAc_2$*

[a] D, aspartic acid; N, asparagine; Q, glutamine; GlcNAc, N-acetylglucosamine; Man, Mannose. [b] The theoretical mass of the reduced, non-glycosylated IgG1-Fc protein is 25,066.39 Da. [c] Man $_{8-12}$-$GlcNAc_2$ glycoforms were observed during MS analysis for the di-glycosylated IgG1-Fc. Man $_{8-9}$ $GlcNAc_2$ glycoforms were observed for the mono-glycosylated IgG1-Fc.

Table 2: Purity values for the different glycosylated and nonglycosylated IgG1-Fc proteins determined under denaturing (reduced SDS-PAGE) and non-denaturing (SE-HPLC) conditions.

	IgG1-Fc proteins	Purity		
		SDS-PAGE [a]	SE-HPLC [b]	
			Monomer [c]	Aggregate [c]
Non-glycosylated IgG1-Fc	**Mutant (QQ)**	*99 %*	*96.6 %*	*1.8 %*
	Monoglycosylated + PNGase F (DN)	*84 %*	*93.7 %*	*4.0 %*
	Diglycosylated + PNGase F (DD)	*99 %*	*91.1 %*	*8.2 %*
Glycosylated IgG1-Fc	**Mono-glycosylated**	*84 %*	*95.3 %*	*3.4 %*
	Di-glycosylated	*97%*	*91.8 %*	*7.8 %*

[a] SDS-PAGE purity was determined from densitometry measurements of the reduced gel in figure 2.

[b] SE-HPLC % measurements are an average of three runs. Fragments observed were between 0.2 and 2 %.

[c] Standard deviation observed for the monomer and aggregation peaks was ~ 1.0% and 0.6 %, respectively.

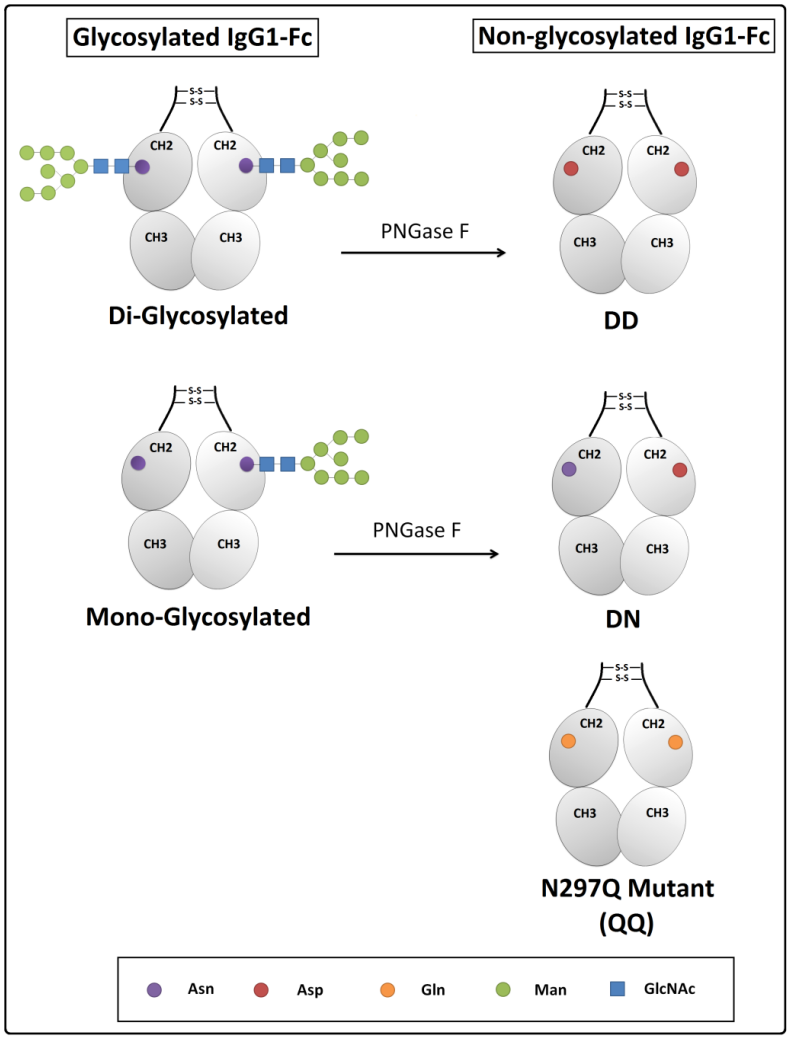

Figure 1: Summary of the five different IgG1-Fc proteins examined in this study. The left side shows the two glycosylated forms of the Fc protein (diglycosylated and monoglycosylated), while, the right side shows the three different nonglycosylated IgG1-Fc protein variants (two from PNGase treatment of glycoforms and one point mutant). Identity of amino acid residue at site 297 in the C_H2 domain (Asn, Asp, Gln) and the nature of glycoforms (Man, mannose and GlcNAc, N-acetylglucosamine) are indicated in the figure.

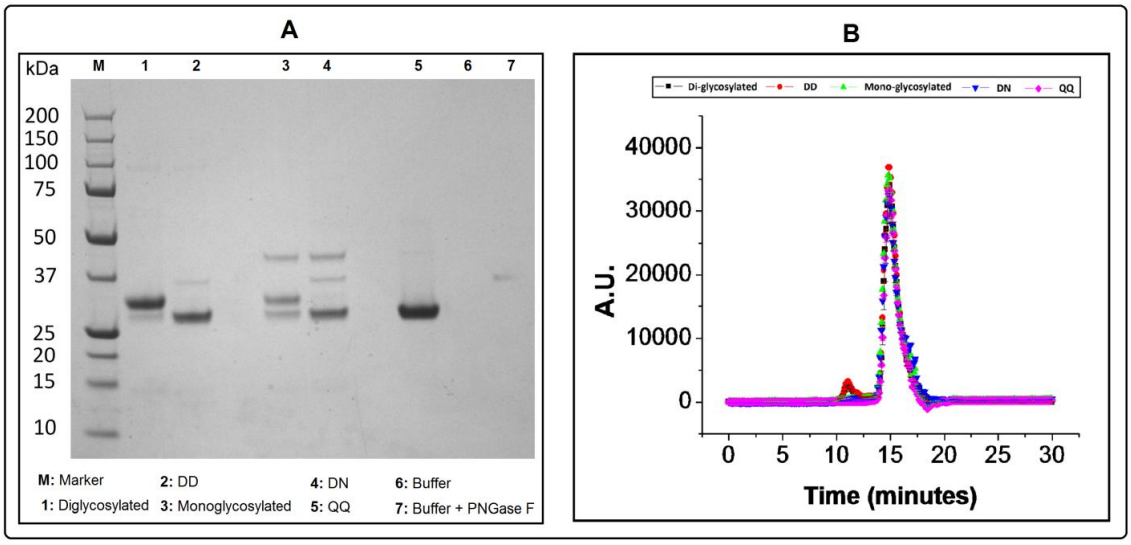

Figure 2: Purity of IgG1-Fc proteins under denaturing and non-denaturing conditions. (A) SDS-PAGE gels of IgG1-Fc samples under reduced conditions, (B) representative SE-HPLC chromatograms.

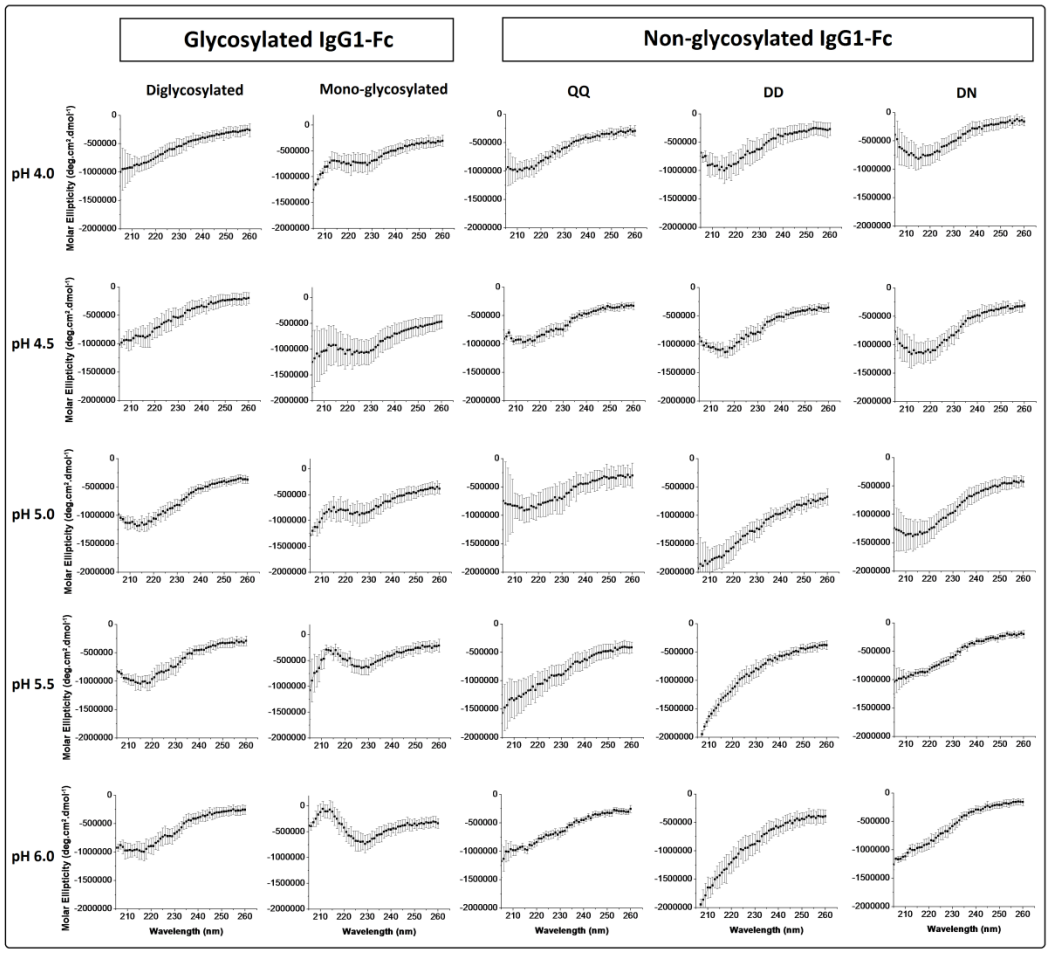

Figure 3: Far-UV CD spectra from 205-260 nm at 10 ^{0}C for the two different Fc glycoforms (di- and mono glycosylated) and three different nonglycosylated IgG1-Fc samples (QQ, DD, NN) across pH range of 4.0-6.0. See Figure 1 for a pictorial summary of the five Fc proteins examined.

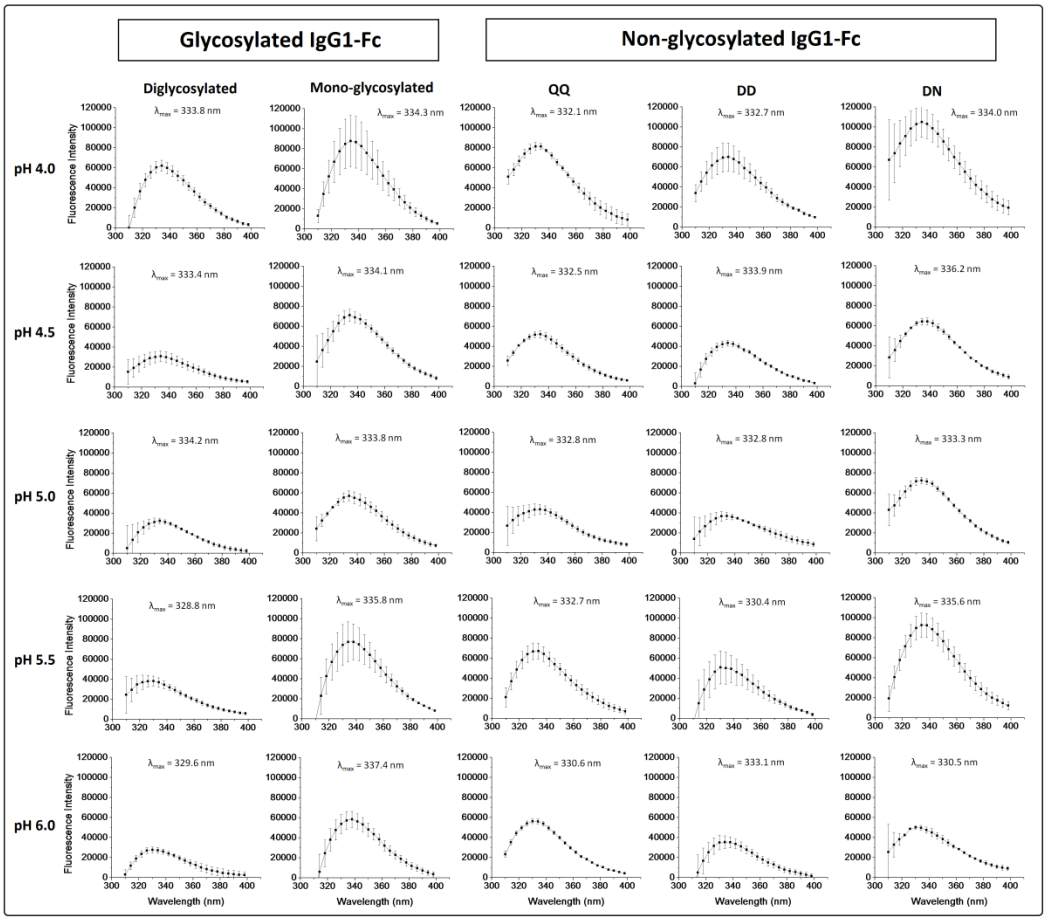

Figure 4: Intrinsic (Trp) fluorescence spectra at 10 ^{0}C for the two different glycosylated (di- and mono glycosylated) and three different nonglycosylated forms (QQ, DD, NN) of the IgG1-Fc across the pH range of 4.0- 6.0. The λ_{max} values are also shown for each protein at each pH condition. See Figure 1 for pictorial summary of the five Fc proteins examined.

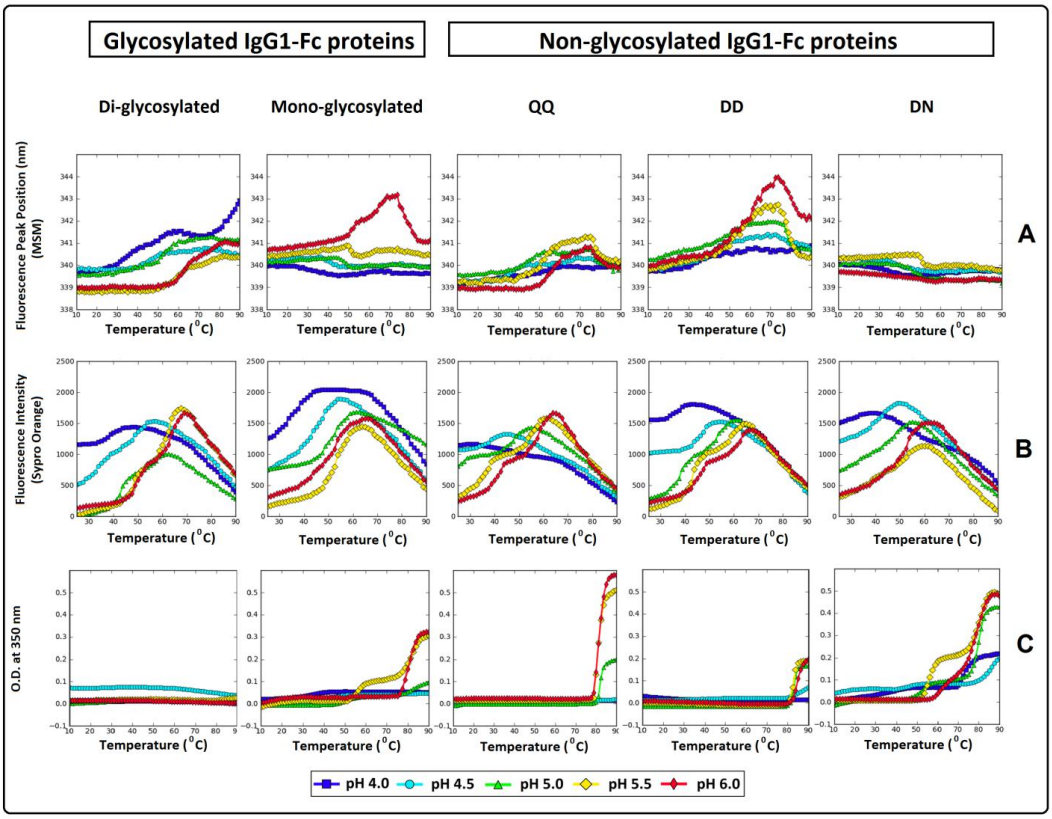

Figure 5: Thermal melting curves for the two different glycosylated (di- and mono glycosylated) and three different nonglycosylated forms (QQ, DD, NN) of the IgG1-Fc across the pH range of 4.0-6.0. Biophysical measurements include (A) Intrinsic Trp fluorescence, (B) Extrinsic Sypro Orange fluorescence spectroscopy and (C) optical density at 350 nm. See Figure 1 for pictorial summary of the five Fc proteins examined.

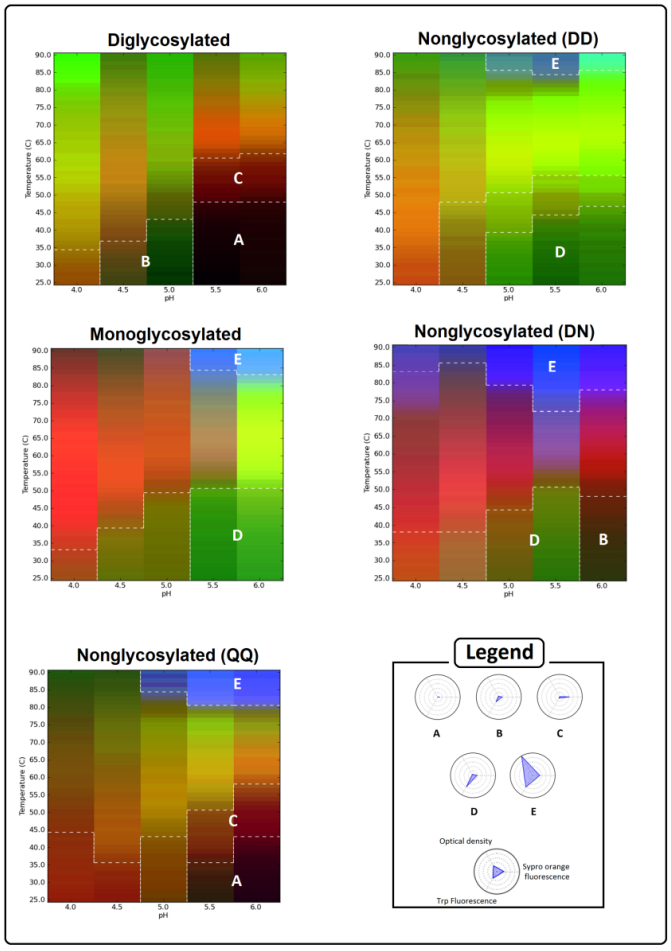

Figure 6: Three index EPDs for the two different glycosylated (di- and mono glycosylated) and three different nonglycosylated forms (QQ, DD, NN) forms of the IgG1-Fc.The legend box contains radar plots defining the five different conformational stability regions observed in the five different Fc proteins. Region A (Black) and B (Dark green) represent region where the protein exist in a native-like and slightly altered structures, respectively. Regions C (Dark red) and D (Green) represent regions where the Fc proteins exist at an altered structural state as seen from an increase in SYPRO orange and Trp fluorescence signals, respectively. Region E (Blue) represents a region where the Fc proteins are in an aggregated state as seen by an increased optical density signal.

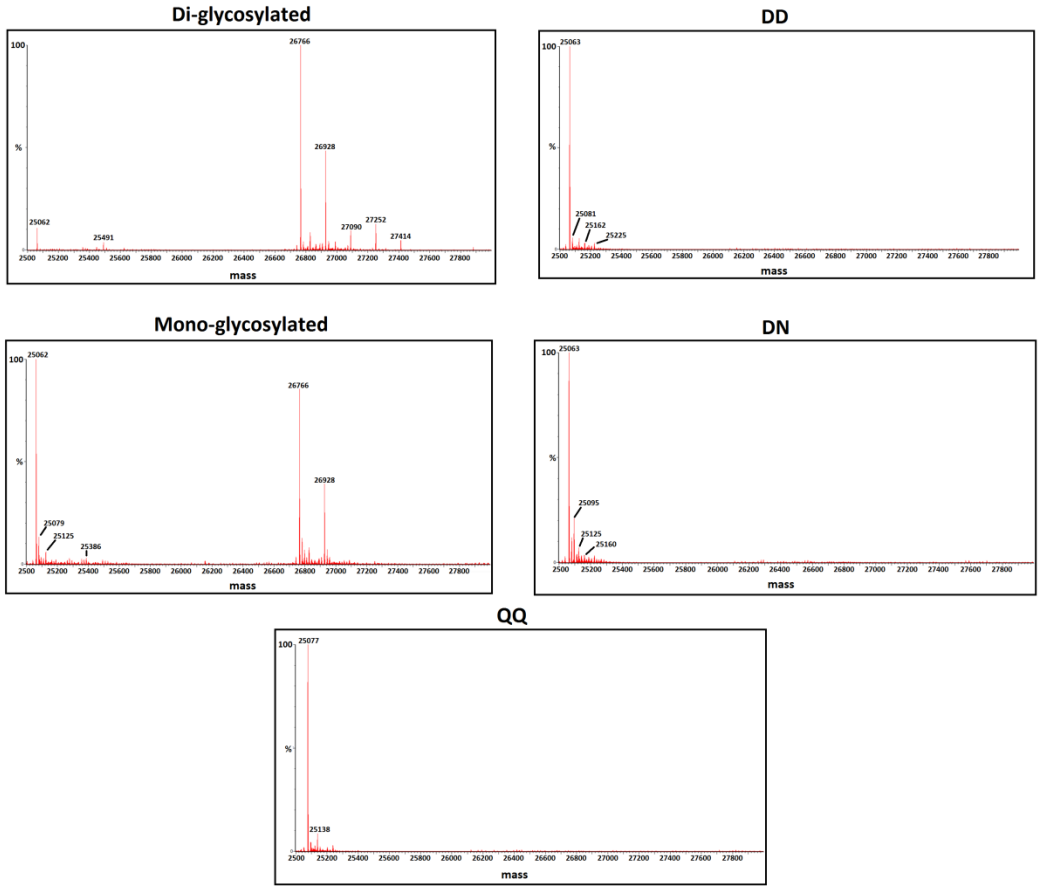

Supplementary Figure S1: Mass spectrometry data acquired for the reduced forms of the different IgG1-Fc proteins. See Table 1 for nomenclature describing the different IgG1-Fc proteins and summary of results.

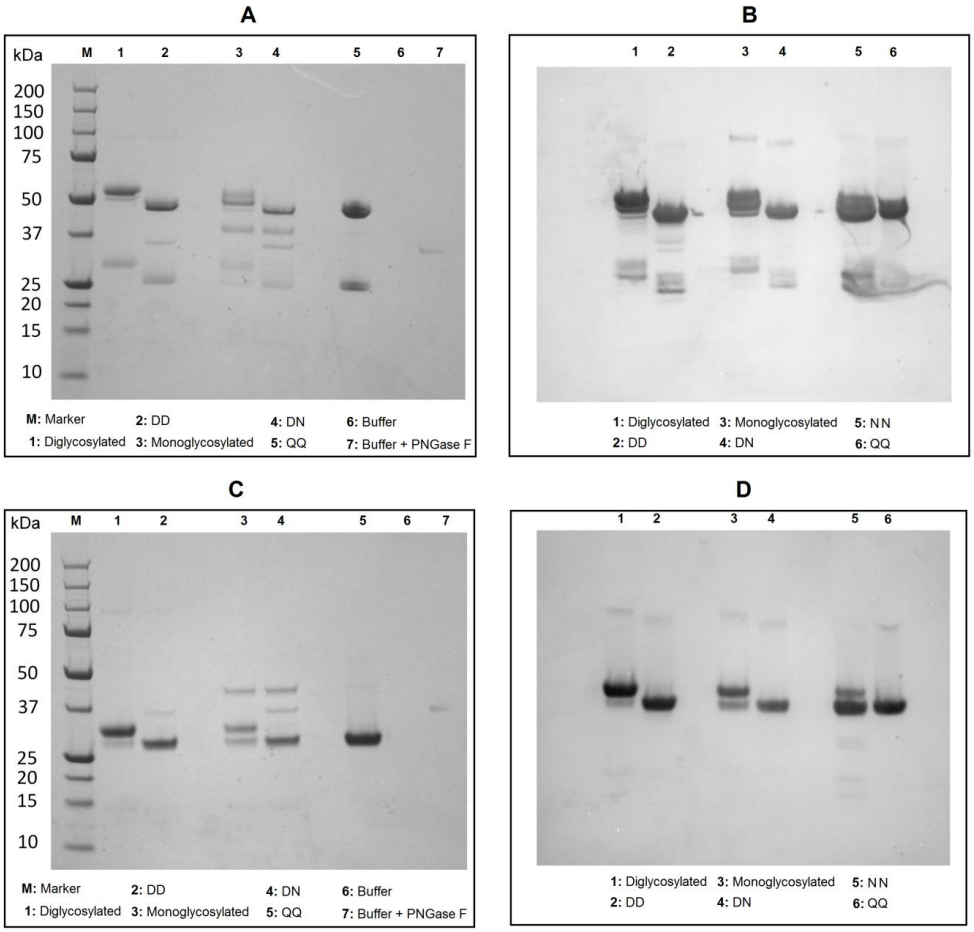

Supplementary Figure S2: SDS PAGE (A) and Western Blot (B) analysis of non-reduced IgG1-Fc samples and SDS PAGE (C) and Western Blot (D) analysis of reduced IgG1-Fc samples. See Figure 2A for nomenclature describing the different IgG1-Fc proteins and results of the reduced SDS-PAGE gel.

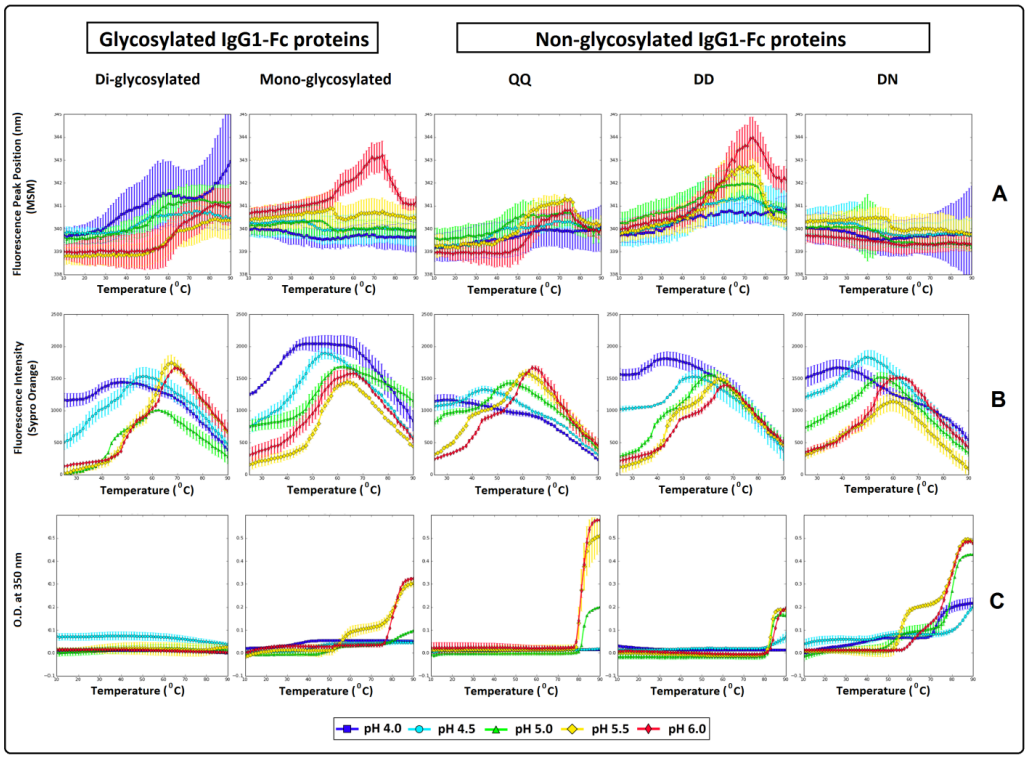

Supplementary Figure S3: Thermal melting curves with standard deviation error bars (n=3) for the two different glycosylated (di- and mono glycosylated) and three different nonglycosylated forms (QQ, DD, NN) forms of the IgG1-Fc as measured by (A) intrinsic Trp fluorescence, (B) extrinsic Sypro orange fluorescence (DSF), and (C) turbidity at 350 nm.

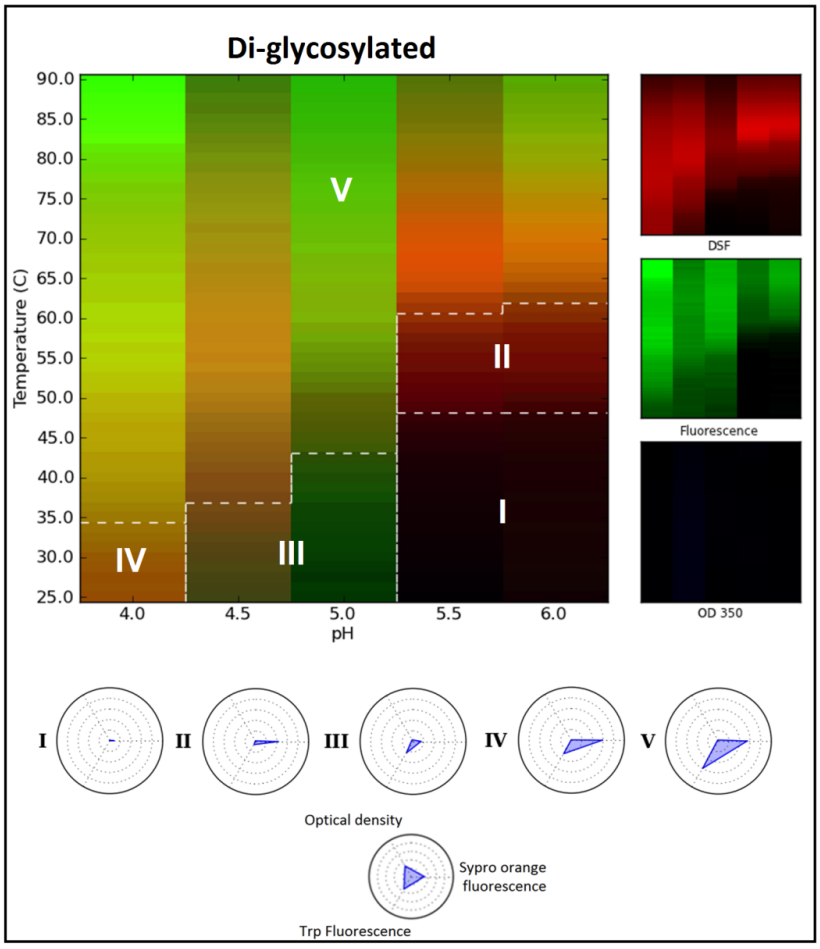

Supplementary Figure S4: Three index EPDs and radar chart results for the diglycosylated IgG1-Fc protein. On the upper left side, the influence of each technique (DSF in red, Trp fluorescence peak position in green and optical density in blue as shown in upper right figures) is visualized resulting in black color representing no detectable change on the Fc protein structure. On the bottom, the individual radar charts show contribution from each of the same instruments (see legend at the bottom), and in roman numerals states are shown mapping the different conformational regions as seen in the three index EPD.

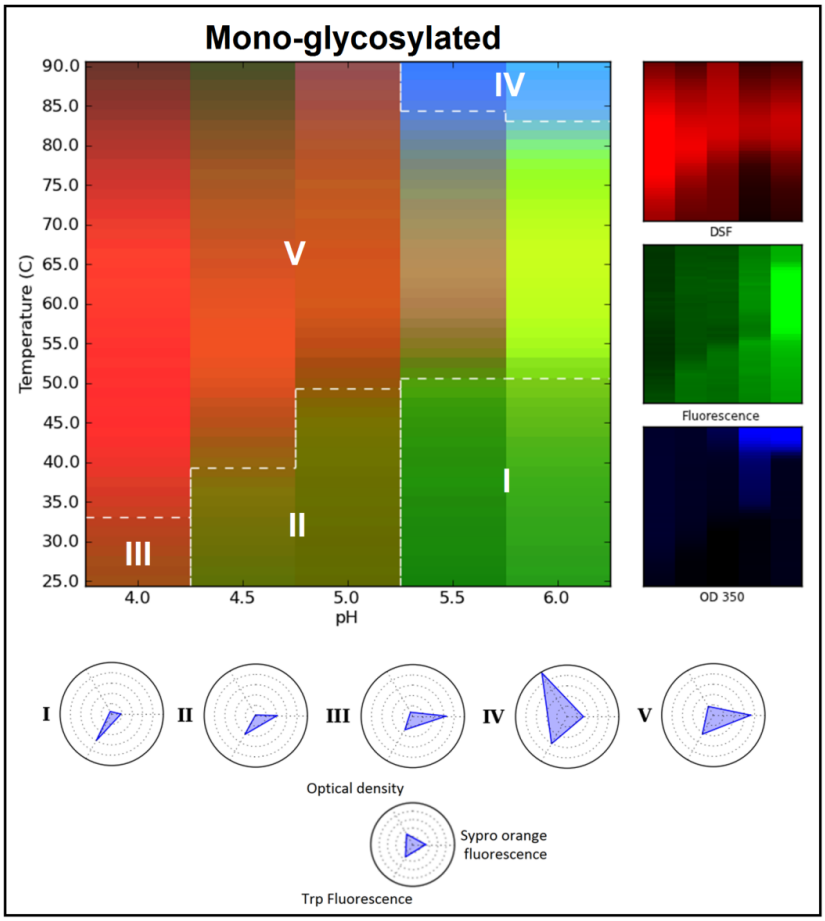

Supplementary Figure S5: Three index EPD and radar chart results for the monoglycosylated IgG1-Fc protein. On the upper left side, the influence of each technique (DSF in red, Trp fluorescence peak position in green and optical density in blue as shown in upper right figures) is visualized resulting in black color representing no detectable change on the Fc protein structure. On the bottom, the individual radar charts show contribution from each of the same instruments (see legend at the bottom), and in roman numerals are shown mapping the different conformational regions as seen in the three index EPD.

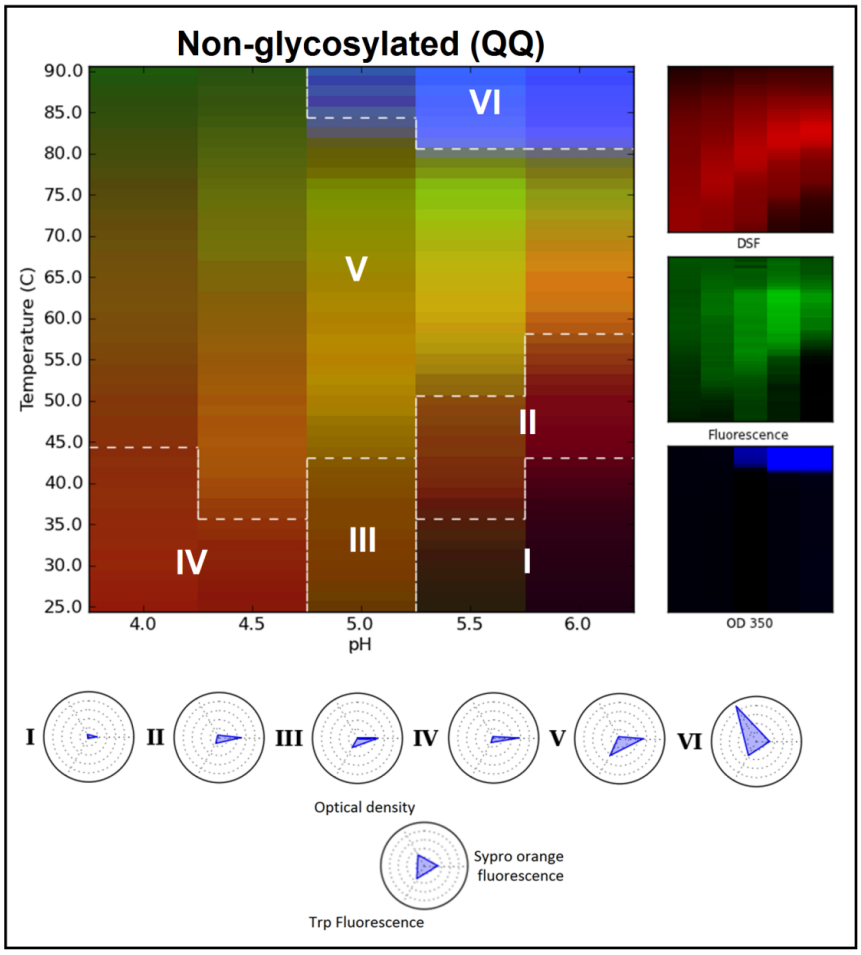

Supplementary Figure S6: Three EPD and radar chart results for the nonglycosylated mutant (QQ) IgG1-Fc protein. On the upper left side, the influence of each technique (DSF in red, Trp fluorescence peak position in green and optical density in blue as shown in upper right figures) is visualized resulting in black color representing no detectable change on the Fc protein structure. On the bottom, the individual radar charts show contribution from each of the same instruments (see legend at the bottom), and in roman numerals are shown mapping the different conformational regions as seen in the three index EPD.

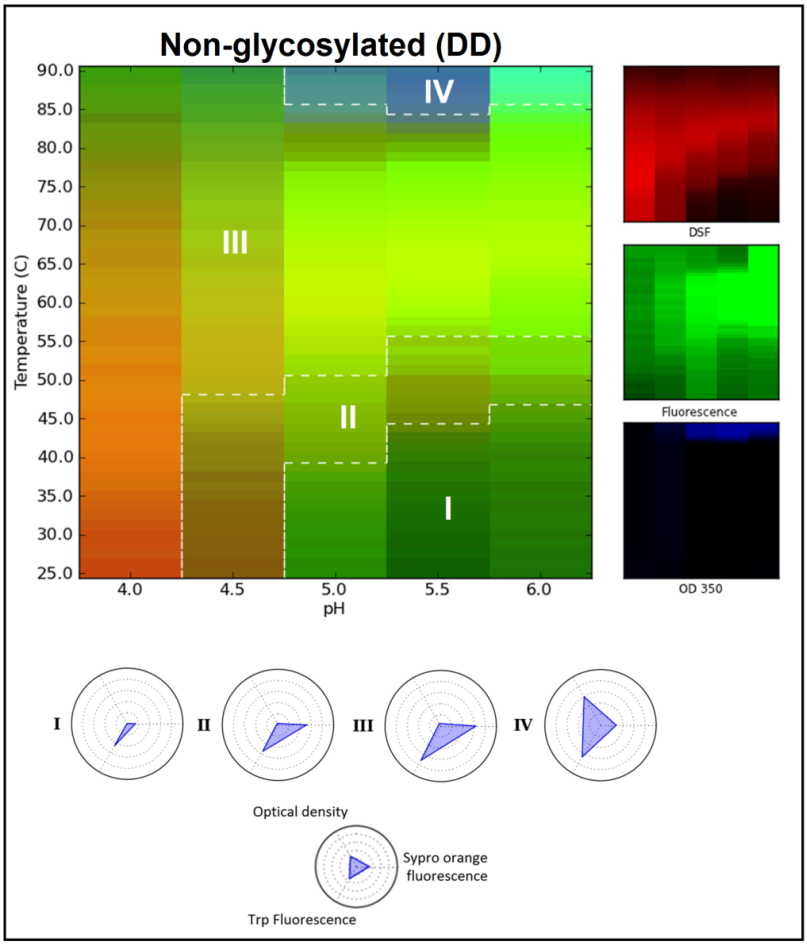

Supplementary Figure S7: Three index EPD and radar chart results for the nonglycosylated (DD) IgG1-Fc protein. On the upper left side, the influence of each technique (DSF in red, Trp fluorescence peak position in green and optical density in blue as shown in upper right figures) is visualized resulting in black color representing no detectable change on the Fc protein structure. On the bottom, the individual radar charts show contribution from each of the same instruments (see legend in the bottom), and in roman numerals are shown mapping the different conformational regions as seen in the three index EPD.

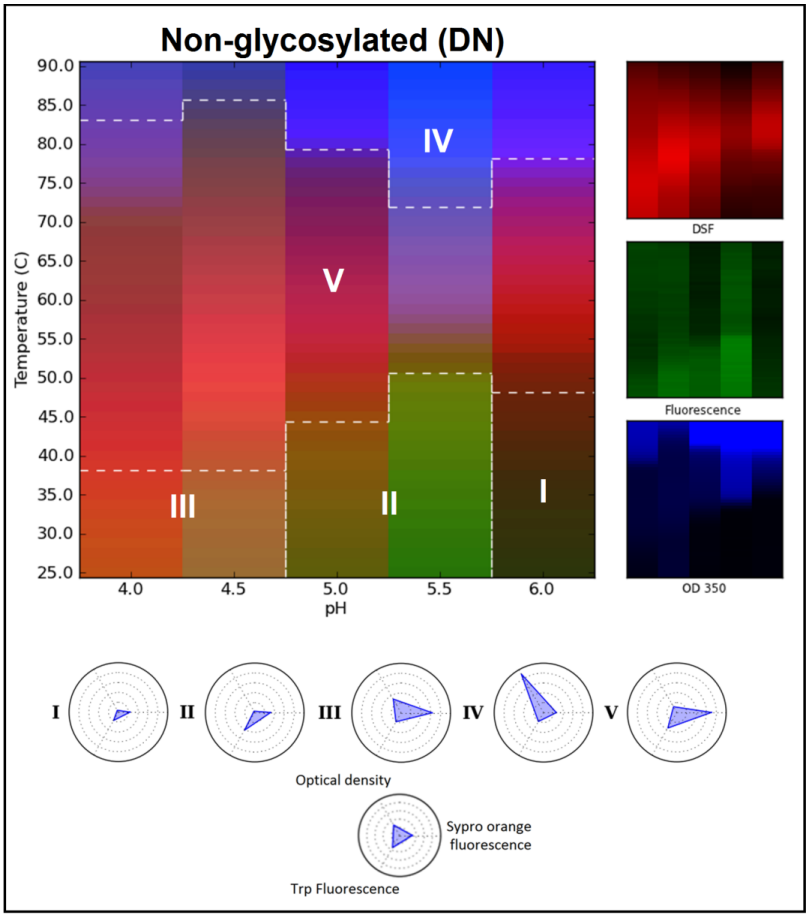

Supplementary Figure S8: Three index EPD and radar chart results for the nonglycosylated (DN) IgG1-Fc protein. On the upper left side, the influence of each technique (DSF in red, Trp fluorescence peak position in green and optical density in blue as shown in upper right figures) is visualized resulting in black color representing no detectable change on the Fc protein structure. On the bottom, the individual radar charts show contribution from each of the same instruments (see legend in the bottom), and in roman numerals are shown mapping the different conformational regions as seen in the three index EPD.

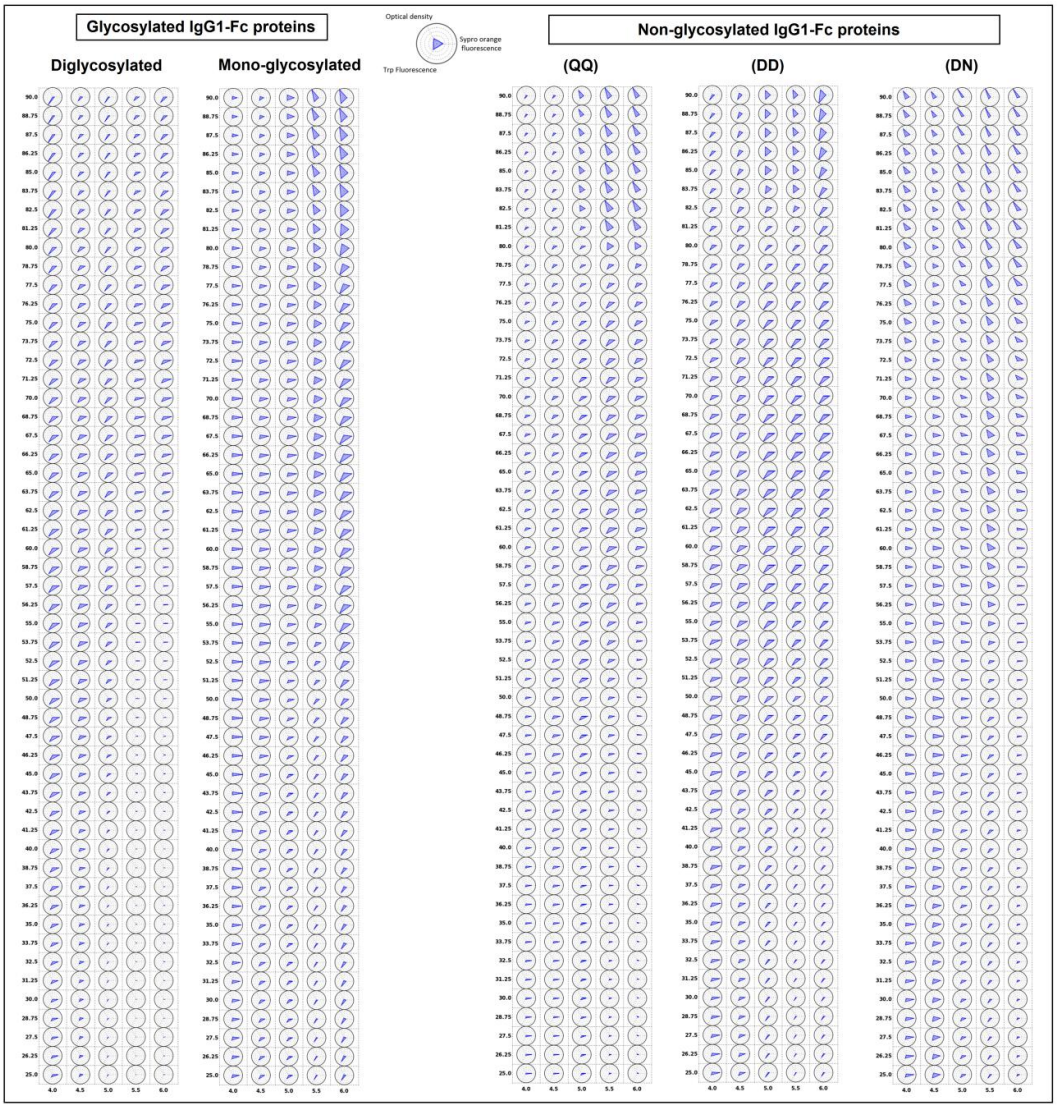

Supplementary Figure S9: Summary Radar plot showing the individual radar chart results at each temperature and pH condition tested for the two different glycosylated (di- and mono glycosylated) and three different nonglycosylated forms (QQ, DD, NN) of the IgG1-Fc. The legend summarizes contribution from each biophysical instrument.

4.5 References

1- Aggarwal, S. R., What's fueling the biotech engine—2011 to 2012. *Nature Biotechnology* **2012,** *30,* 1191–1197

2- Reichert, J. M., Antibodies to watch in 2013: Mid-year update. *mAbs* **2013,** *5* (4), 0-1.

3- Arnold, J. N.; Wormald, M. R.; Sim, R. B.; Rudd, P. M.; Dwek, R. A., The Impact of Glycosylation on the Biological Function and Structure of Human Immunoglobulins. *Annual Review of Immunology* **2007,** *25* (1), 21-50.

4- Li, C. H.; Narhi, L. O.; Wen, J.; Dimitrova, M.; Wen, Z.-Q.; Li, J.; Pollastrini, J.; Nguyen, X. C.; Tsuruda, T.; Jiang, Y., The Effect of pH, temperature and salt on the stability of E. coli and CHO derived IgG1 Fc. *Biochemistry* **2012**.

5- Kayser, V.; Chennamsetty, N.; Voynov, V.; Forrer, K.; Helk, B.; Trout, B. L., Glycosylation influences on the aggregation propensity of therapeutic monoclonal antibodies. *Biotechnology Journal* **2011,** *6* (1), 38-44.

6- Wang, W.; Antonsen, K.; Wang, Y. J.; Wang, D. Q., pH dependent effect of glycosylation on protein stability. *European Journal of Pharmaceutical Sciences* **2008,** *33* (2), 120-127.

7- Latypov, R. F.; Hogan, S.; Lau, H.; Gadgil, H.; Liu, D., Elucidation of Acid-induced Unfolding and Aggregation of Human Immunoglobulin IgG1 and IgG2 Fc. *Journal of Biological Chemistry* **2012,** *287* (2), 1381-1396.

8- Liu, L.; Stadheim, A.; Hamuro, L.; Pittman, T.; Wang, W.; Zha, D.; Hochman, J.; Prueksaritanont, T., Pharmacokinetics of IgG1 monoclonal antibodies produced in humanized Pichia pastoris with specific glycoforms: A comparative study with CHO produced materials. *Biologicals* **2011,** *39* (4), 205-210.

9- Raju, T. S.; Scallon, B. J., Glycosylation in the Fc domain of IgG increases resistance to proteolytic cleavage by papain. *Biochemical and Biophysical Research Communications* **2006,** *341* (3), 797-803.

10- Raju, T. S.; Briggs, J. B.; Chamow, S. M.; Winkler, M. E.; Jones, A. J. S., Glycoengineering of Therapeutic Glycoproteins: In Vitro Galactosylation and Sialylation of Glycoproteins with Terminal N-Acetylglucosamine and Galactose Residues. *Biochemistry* **2001,** *40* (30), 8868-8876.

11- Leymarie, N.; Zaia, J., Effective Use of Mass Spectrometry for Glycan and Glycopeptide Structural Analysis. *Analytical Chemistry* **2012,** *84* (7), 3040-3048.

12- Zauner, G.; Selman, M. H. J.; Bondt, A.; Rombouts, Y.; Blank, D.; Deelder, A. M.; Wuhrer, M., Glycoproteomic analysis of antibodies. Molecular & Cellular Proteomics 2013.

13- Sinha, S.; Pipes, G.; Topp, E. M.; Bondarenko, P. V.; Treuheit, M. J.; Gadgil, H. S., Comparison of LC and LC/MS Methods for Quantifying N-Glycosylation in Recombinant IgGs. *Journal of the American Society for Mass Spectrometry* **2008,** *19* (11), 1643-1654.

14- Wuhrer, M., Glycomics using mass spectrometry. *Glycoconjugate Journal* **2013,** *30* (1), 11-22.

15- Baković, M. P.; Selman, M. H. J.; Hoffmann, M.; Rudan, I.; Campbell, H.; Deelder, A. M.; Lauc, G.; Wuhrer, M., High-Throughput IgG Fc N-Glycosylation Profiling by Mass Spectrometry of Glycopeptides. *Journal of Proteome Research* **2013,** *12* (2), 821-831.

16- Visser, J.; Feuerstein, I.; Stangler, T.; Schmiederer, T.; Fritsch, C.; Schiestl, M., Physicochemical and Functional Comparability Between the Proposed Biosimilar Rituximab GP2013 and Originator Rituximab. *BioDrugs* **2013**, 1-13.

17- Putnam, W. S.; Prabhu, S.; Zheng, Y.; Subramanyam, M.; Wang, Y.-M. C., Pharmacokinetic, pharmacodynamic and immunogenicity comparability assessment strategies for monoclonal antibodies. *Trends in Biotechnology* **2010,** *28* (10), 509-516.

18- Goetze, A. M.; Liu, Y. D.; Zhang, Z.; Shah, B.; Lee, E.; Bondarenko, P. V.; Flynn, G. C., High-mannose glycans on the Fc region of therapeutic IgG antibodies increase serum clearance in humans. *Glycobiology* **2011,** *21* (7), 949-959.

19- Lu, Y.; Westland, K.; Ma, Y.-h.; Gadgil, H., Evaluation of effects of Fc domain high-mannose glycan on antibody stability. *Journal of Pharmaceutical Sciences* **2012,** *101* (11), 4107-4117.

20- Labeta MO, Margni RA, Leoni J, Binaghi RA. Structure of asymmetric
non-precipitating antibody: Presence of a carbohydrate residue in only one Fab region of the molecule. Immunology. 1986. 57:311–317.

21- Ha, S.; Ou, Y.; Vlasak, J.; Li, Y.; Wang, S.; Vo, K.; Du, Y.; Mach, A.; Fang, Y.; Zhang, N., Isolation and Characterization of IgG1 with Asymmetrical Fc Glycosylation. *Glycobiology* **2011**.

22- Xiao, J.; Chen, R.; Pawlicki, M. A.; Tolbert, T. J., Targeting a Homogeneously Glycosylated Antibody Fc To Bind Cancer Cells Using a Synthetic Receptor Ligand. Journal of the American Chemical Society 2009, 131 (38), 13616-13618.

23- Porath, J., General methods and coupling procedures. In Methods in Enzymology, Nathan P. Kaplan, N. P. C. W. B. J.; Meir, W., Eds. Academic Press: 1974; Vol. Volume 34, pp 13-30.

24- Loo, T.; Patchett, M. L.; Norris, G. E.; Lott, J. S., Using Secretion to Solve a Solubility Problem: High-Yield Expression in Escherichia coli and Purification of the Bacterial Glycoamidase PNGase F. Protein Expression and Purification 2002, 24 (1), 90-98.

25- Rasband, W.S., ImageJ, U. S. National Institutes of Health, Bethesda, Maryland, USA, http://imagej.nih.gov/ij/, 1997-2012.

26- Caroline A. Schneider, W. S. R. K. W. E., NIH Image to ImageJ: 25 years of image analysis. Nature Methods 2012, 9, 671–675.

27- Kim, J. H.; Iyer, V.; Joshi, S. B.; Volkin, D. B.; Middaugh, C. R., Improved data visualization techniques for analyzing macromolecule structural changes. *Protein Science* **2012,** *21* (10), 1540-1553.

28- Federici, M.; Lubiniecki, A.; Manikwar, P.; Volkin, D. B., Analytical lessons learned from selected therapeutic protein drug comparability studies. *Biologicals* **2012,** *40*.

29- Lubiniecki, A.; Volkin, D. B.; Federici, M.; Bond, M. D.; Nedved, M. L.; Hendricks, L.; Mehndiratta, P.; Bruner, M.; Burman, S.; DalMonte, P.; Kline, J.; Ni, A.; Panek, M. E.; Pikounis, B.; Powers, G.; Vafa, O.; Siegel, R., Comparability assessments of process and product changes made during development of two different monoclonal antibodies. *Biologicals* **2011,** *39* (1), 9-22.

30- Amezcua, C. A.; Szabo, C. M., Assessment of higher order structure comparability in therapeutic proteins using nuclear magnetic resonance spectroscopy. *Journal of Pharmaceutical Sciences* **2013,** *102* (6), 1724-1733.

31- Berkowitz, S. A.; Engen, J. R.; Mazzeo, J. R.; Jones, G. B., Analytical tools for characterizing biopharmaceuticals and the implications for biosimilars. *Nat Rev Drug Discov* **2012,** *11* (7), 527-540.

32- Borrok, M. J.; Jung, S. T.; Kang, T. H.; Monzingo, A. F.; Georgiou, G., Revisiting the Role of Glycosylation in the Structure of Human IgG Fc. *ACS Chemical Biology* **2012,** *7* (9), 1596-1602.

33- Houde, D.; Arndt, J.; Domeier, W.; Berkowitz, S.; Engen, J. R., Characterization of IgG1 Conformation and Conformational Dynamics by Hydrogen/Deuterium Exchange Mass Spectrometry. *Analytical Chemistry* **2009,** *81* (7), 2644-2651.

34- Houde, D.; Peng, Y.; Berkowitz, S. A.; Engen, J. R., Post-translational Modifications Differentially Affect IgG1 Conformation and Receptor Binding. *Molecular & Cellular Proteomics* **2010,** *9* (8), 1716-1728.

35- Manikwar, P.; Majumdar, R.; Hickey, J. M.; Thakkar, S. V.; Samra, H. S.; Sathish, H. A.; Bishop, S. M.; Middaugh, C. R.; Weis, D. D.; Volkin, D. B., Correlating excipient effects on conformational and storage stability

of an IgG1 monoclonal antibody with local dynamics as measured by hydrogen/deuterium-exchange mass spectrometry. *Journal of Pharmaceutical Sciences* **2013,** *102* (7), 2136-2151.

36- Majumdar, R.; Manikwar, P.; Hickey, J. M.; Samra, H. S.; Sathish, H. A.; Bishop, S. M.; Middaugh, C. R.; Volkin, D. B.; Weis, D. D., Effects of Salts from the Hofmeister Series on the Conformational Stability, Aggregation Propensity, and Local Flexibility of an IgG1 Monoclonal Antibody. *Biochemistry* **2013,** *52* (19), 3376-3389.

37- Alsenaidy, M. A.; Kim, J. H.; Majumdar, R.; Weis, D. D.; Joshi, S. B.; Tolbert, T. J.; Middaugh, C. R.; Volkin, D. B., High-Throughput Biophysical Analysis and Data Visualization of Conformational Stability of an IgG1 Monoclonal Antibody After Deglycosylation. *Journal of Pharmaceutical Sciences* **2013,** *102* (11), 3942-3956.

38- Khawli, L. A.; Goswami, S.; Hutchinson, R.; Kwong, Z. W.; Yang, J.; Wang, X.; Yao, Z.; Sreedhara, A.; Cano, T.; Tesar, D. B.; Nijem, I.; Allison, D. E.; Wong, P. Y.; Kao, Y.-H.; Quan, C.; Joshi, A.; Harris, R. J.; Motchnik, P., Charge variants in IgG1: Isolation, characterization, in vitro binding properties and pharmacokinetics in rats. mAbs 2010, 2 (6), 613-624.

39- Vlasak, J.; Bussat, M. C.; Wang, S.; Wagner-Rousset, E.; Schaefer, M.; Klinguer-Hamour, C.; Kirchmeier, M.; Corvaïa, N.; Ionescu, R.; Beck, A., Identification and characterization of asparagine deamidation in the light chain CDR1 of a humanized IgG1 antibody. Analytical Biochemistry 2009, 392 (2), 145-154.

40- Yadav, S.; Laue, T. M.; Kalonia, D. S.; Singh, S. N.; Shire, S. J., The Influence of Charge Distribution on Self-Association and Viscosity Behavior of Monoclonal Antibody Solutions. Molecular Pharmaceutics 2012, 9 (4), 791-802.

Chapter 5

Summary, conclusions and future work

5.1 Summary and conclusions

Since the introduction of recombinant DNA technology in the late 1970's, an increasing number of protein-based therapeutics has been approved by regulatory agencies with approximately 200 therapeutic proteins currently available to address a wide variety of medical conditions. The size and complexity of protein drugs, however, increases their susceptibility to chemical or structural modifications due to process and product changes, which could have a negative impact on the shelf-life stability, potency or immunogenicity profile. Thus, a thorough evaluation and characterization of the structural integrity and conformational stability of therapeutic proteins is an essential task for the successful development of a biopharmaceutical product.

In recent statements by Dr. Steven Kozlowski, [1] the director of the office of biotechnology products in the FDA, describing some of the current difficulties encountered in characterizing therapeutic proteins during clinical development, he stated: "*New or enhanced analytical technologies and measurement systems and standards that can more accurately and precisely assess the higher order structure and attachments of biologics would provide additional assurance of the quality of biologics*" as well as "*Improved analytical methods would enable quicker and more confident assessments of the potential effects of changes in the manufacturing process, equipment, or raw materials*". In these statements, the need to develop better analytical methodologies to more accurately characterize a

protein therapeutic's higher order structural integrity as part of comparability exercises was expressed by Dr. Kozlowski, providing a summary of the current analytical challenge that needs to be met in the future to ensure the successful introduction of new manufacturing processes including biosimilars.

Although NMR, X-ray crystallography, cryo EM and H/D exchange mass spectrometry are powerful, higher resolution analytical techniques that can provide structural details about a protein's folded structure and dynamics, there remains many practical limitations in their wide spread use (e.g., large molecular weight of proteins, presence of formulation components, cost and analytical complexity) as part of formulation development and comparability studies. With that being said, the need for new and novel approaches to better monitor the higher order structural integrity of proteins in pharmaceutical dosage forms during comparability studies is of great interest.

Lower resolution biophysical techniques such as circular dichroism (to monitor overall secondary structure of proteins), intrinsic/extrinsic fluorescence spectroscopy (to monitor tertiary structure of proteins), differential scanning calorimetry (to monitor protein thermal stability), as well as static light scattering and turbidity assays (to monitor protein aggregation) are more commonly used techniques to evaluate the higher-order structural integrity and conformational stability of protein-based drugs during development. No one single analytical technique, however, provides sufficient information to establish the overall

higher-order structural integrity of such complex macromolecules as proteins. Therefore, the use of more than one lower resolution biophysical technique is generally needed for better characterization. The multidimensional nature of physical stability data gathered from multiple biophysical techniques, especially when used in a high throughput mode allowing for analysis of multiple solution conditions, makes analysis and visualization of larger data sets problematic. Advanced data visualization methods such as empirical phase diagrams (EPDs) and radar charts were used in this dissertation to summarize experimental biophysical data acquired from high throughput experiments and visualize the macromolecule's physical stability behavior across a wide range of environmental stress and solution conditions.

High throughput biophysical analysis of proteins, combined with analysis of the large data sets of their physical stability using various advanced data visualization techniques (EPDs and radar charts), was evaluated in this dissertation as a way to compare the structural integrity of different versions of the same protein to each other (as would be done in comparability studies). Using varying mutants and glycoforms of different proteins (with different molecular weights, hydrodynamic sizes, post-translational modifications, and inherent thermodynamic stability), the structural differences in the form of known "major alterations" (i.e., different point mutations) or "minor alterations" (i.e., different post translational modifications) were specifically introduced into three different

proteins: FGF-1 (chapter 2), IgG1 mAb (chapter 3), and IgG1-Fc protein (chapter 4). The various forms of these different proteins were extensively characterized in terms of physical stability properties using multiple low-resolution biophysical techniques to monitor different aspects of the higher-order structural across a wide range of pH and temperature conditions. These large data sets of biophysical data were then used to construct EPDs and radar charts for data visualization and structural comparisons between the different variants of the different proteins.

In the second chapter, the conformational stability profile of wild type recombinant FGF-1 (a protein which requires binding to heparin for its mitogenic activity and physicochemical stability) with and without heparin was compared to physical stability profile of 10 different FGF-1 mutants. The overall goal was to evaluate the extent to which the heparin dependence of FGF-1 solution stability could be reduced or eliminated. Comparisons were made in terms of structural integrity and conformational stability across varying values of solution pH and temperature using multiple biophysical techniques through the use of data visualization employing empirical phase diagrams. Results indicated that four of the FGF-1 mutants (K12V/C117V, C83T/C117V/ L44F/F132W, A66C, K12V/C117V/P134V) without heparin displayed high physiochemical stability and similar bioactivity to the FGF-1 WT in the presence of heparin. These FGF-1 mutants were highlighted as potentially good candidates for future therapeutic applications from a pharmaceutical stability and biological potency point of view.

In the third chapter, the structural integrity and conformational stability of an IgG1 monoclonal antibody (mAb), after partial or complete enzymatic removal of the N-linked Fc glycan, were compared with the untreated mAb over a wide range, as well as a narrower range, of temperatures and solution pH, again using multiple biophysical techniques with data visualization employing both EPDs and radar charts. Subtle-to-larger stability differences between the different glycoforms were observed. Differential scanning calorimetry and differential scanning fluorimetry showed an improved ability to detect differences in the physical stability of these mAb glycoforms and were utilized in a final round of physical stability comparisons. On the basis of these results, a two-step methodology was demonstrated in which conformational stability of a mAb glycoform is first screened using a wide variety of instruments and environmental stresses, followed by a second evaluation with optimally sensitive experimental conditions, analytical techniques, and data visualization methods. With this approach, glycosylation influences on the structural integrity and conformational stability of an IgG1 mAb was characterized and better defined. Fully glycosylated mAb was shown to have significantly improved stability over the partially and fully deglycosylated forms, especially in terms of the conformational stability of the C_H2 domain where the N-linked glycosylation site resides.

In the fourth chapter, a variety of IgG1-Fc proteins with different glycosylation site occupancies (diglycosylated, monoglycosylated and

nonglycosylated QQ) and different amino acid residues with charge differences (nonglycosylated DD, nonglycosylated DN and nonglycosylated QQ in the C_H2 domain) were produced and purified. These Fc glycoforms were first characterized using multiple electrophoretic, chromatographic and biophysical techniques, followed by extensive biophysical characterization of physical stability under stressed conditions. As seen from the results presented in the third chapter, glycosylation site occupancy played a significant role in the Fc protein's structural integrity and conformational stability. Diglycosylated Fc protein was shown to be structurally more stable than the nonglycosylated QQ Fc protein, with thermal transition temperatures from the native-like to a structurally altered conformational states occurring at higher temperatures for the diglycosylated protein across different pH values. These results further confirmed the destabilizing effect of deglycosylation on Fc protein's physical stability. To our surprise, the monoglycosylated Fc protein was inherently unstable compared to the other two proteins, where it existed in structurally altered conformational state even under ambient environmental conditions of temperature and solution pH. Comparisons of the non-glycosylated Fc proteins containing amino acids with different charges at the N-linked glycosylation site within the C_H2 domain, were performed as described in this chapter as well. Nonglycosylated DD (with two Asps), nonglycosylated DN (with one Asp), generated from the PNGase F enzymatic treatment of the diglycosylated and monoglycosylated IgG1-Fc

proteins, respectively, were compared to the uncharged, nonglycosylated QQ (with two Glns) in terms of their structural integrity and conformational stability. Nonglycosylated DD Fc protein (with two negative charged amino acid residues in the C_H2 domain) was found to be conformationally unstable across the pH and temperature conditions tested compared to the uncharged nonglycosylated QQ Fc protein (which exists in a native-like structural state at lower temperatures and at neutral pH conditions). Nonglycosylated DN Fc protein (containing one charged amino acid residue) illustrated an intermediate physical stability, with a slightly altered conformational state being detected at low temperatures at pH 6.0, whereas, it existed at a altered structural state at lower pH conditions.

In summary, using this approach, differences in conformational stability of various FGF-1 mutants, IgG mAb glycoforms, and IgG1-Fc glycoforms were detected under environmental stress conditions that could not necessarily detect differences in structural integrity using the same biophysical techniques under ambient conditions (i.e., no stress). Thus, an evaluation of conformational stability differences may serve as an effective surrogate to monitor differences in higher-order structure between protein samples during physiochemical comparability studies.

5.2 Future work

Despite the successful use of EPDs and radar charts to enhance of understanding of the structural integrity and conformational stability of different

forms of the same protein many analytical challenges still remain. For example, improving our understanding of the precision of EPD phase transitions using clustering methodologies remains as a major challenge for using EPDs and radar charts for comparability applications. Other challenges include successfully incorporating additional biophysical techniques to better identify different conformational aspects of the protein's structures as well as better understanding the relationship of these stressed stability data with long term storage stability would be of great interest.

In terms of improved analytical precision, although both major and subtle differences in the structural integrity and conformational stability between the different versions of three different proteins were readily detected using EPDs and radar charts methodologies, better defining the precision of the phase transition stands as a challenge that needs to be addressed. During structural comparisons between two or more proteins, it is of great importance to establish if the differences observed between proteins are greater than the differences between multiple measurements of the same protein. This challenge could be addressed in the future through the introduction of mathematical models that could incorporate the observed variability during data collection into the EPDs and radar charts displays. Such incorporation of precision would enhance the conclusions made regarding similarity or dissimilarity between proteins during evaluations of their physiochemical stability as part of analytical comparability studies.

In terms of new analytical techniques, over the past few years, higher-resolution methods such as, hydrogen/deuterium exchange mass spectrometry (H/DX-MS) has evolved into a versatile technique for investigating structural, dynamic and pharmaceutical stability aspects of proteins, a methodology that is currently being employed for such investigations in our laboratory.[2, 3] Evaluating both global conformational stability (from EPDs and radar charts) and local dynamic information (from H/DX-MS) of proteins for more complete understanding of the possible correlation between protein stability and flexibility is of a great interest. Such an understanding should not only improve comparisons of stability as part of comparability assessments, but may also enable the more rational design and optimization of protein formulation conditions (e.g., selection of stabilizing excipients).

Finally, during the formulation development of biopharmaceutical products, long term stability studies are conducted under the intended storage conditions to evaluate protein's physical and chemical stability over time. Studies assessing the possible use of EPDs and radar charts, which provide a summary of conformational stability data under accelerated conditions, as a predicative tool for long term stability of proteins could be evaluated in future work. If proven to be predicative, EPDs and radar chart profiles of protein physical stability could compliment accelerated stability studies more commonly utilized as part of comparability assessments.

5.3 References

1- US Food and Drug Administration. Potential need for measurement standards to facilitate R&D of biologic drugs: statement of Steven Kozlowski, M.D. before the U.S. House of Representatives. FDA website [online], http://www.fda.gov/NewsEvents/Testimony/ ucm183596.htm (2009).

2- Majumdar, R.; Manikwar, P.; Hickey, J. M.; Samra, H. S.; Sathish, H. A.; Bishop, S. M.; Middaugh, C. R.; Volkin, D. B.; Weis, D. D., Effects of Salts from the Hofmeister Series on Conformational Stability, Aggregation Propensity, and Local Flexibility of an IgG1 Monoclonal Antibody. Biochemistry 2013.

3- Manikwar, P.; Majumdar, R.; Hickey, J. M.; Thakkar, S. V.; Samra, H. S.; Sathish, H. A.; Bishop, S. M.; Middaugh, C. R.; Weis, D. D.; Volkin, D. B., Correlating excipient effects on conformational and storage stability of an IgG1 monoclonal antibody with local dynamics as measured by hydrogen/deuterium-exchange mass spectrometry. Journal of Pharmaceutical Sciences 2013, 102 (7), 2136-2151.